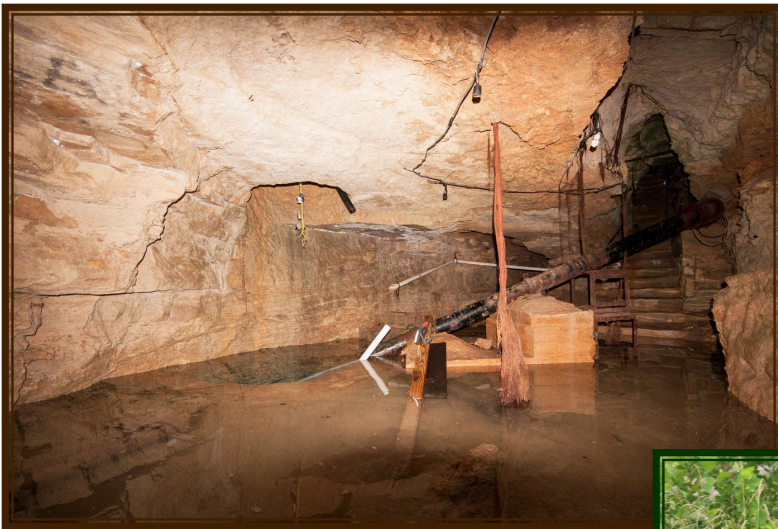


# ***An Investigation into the Recharge Pathways and Mechanisms In the Northern Segment of the Edwards Aquifer, Bell County, Texas (Phase I, Phase II & Phase III)***



*A final research report submitted to the  
Bell County Adaptive Management Coalition  
(December, 2015)*

*A final research report submitted to the  
Bell County Adaptive Management Coalition  
(December, 2016)*



*A final research report submitted to the  
Bell County Adaptive Management Coalition  
(December, 2017)*



**Submitted By:**

Stephanie S. Wong, graduate student

Dr. Joe C. Yelderman Jr., Ph.D., P.G.

Baylor University, Department of Geology



# Bell County Adaptive Management Coalition

By: Tim Brown

Bell County Commissioner – Precinct 2

## Historical Perspective of the Coalition/Stakeholders:

We organized a stakeholders group a couple of years ago when the issue of endangered species first came up, specifically regarding the proposed listing of the Eurycea salamanders that live in the springs.

The group consists of Bell County, the Village of Salado, Salado Water Supply Corporation and Clearwater Underground Water Conservation District as well as some private property contributors. We have raised and spent a substantial amount of money on a variety of studies ranging from biological research focused directly on the target species to geo-hydrologic research designed to enhance our understanding of the structure and function of our portion of the Edwards BFZ aquifer.

We have forged very productive partnerships with U.S. Fish & Wildlife, Texas Parks & Wildlife, U.S. Geological Survey, Baylor University, and a number of private property owners to facilitate ongoing research. The benefits so far include the decision to list the Salado salamanders as threatened, rather than endangered, and substantially expanding what we know about the structure of the aquifer there in close proximity to the springs.

Our goal is to continue the efforts to maintain the assurance that conditions do warrant a more onerous burden of an endangered listing and, ultimately, to broaden our understanding of the geo-hydrology of the entire system so we can eventually develop the necessary regulatory tools to accommodate growth and development and at the same time protect the system.

It's a long-range strategy that has been very successful so far. The problems are that it involves a commitment to a vision that may be difficult for some people to grasp and harder for some to support politically. Funding by the Coalition is handled by the Bell County Auditor's Office on an annual basis. Partners of the Coalition submit commitments to the Auditor once the annual memorandum of agreement is signed by all parties.

**Phase I**

# An Investigation into the Recharge Pathways and Mechanisms In the Northern Segment of the Edwards Aquifer, Bell County, Texas



*A final research report submitted to the Clearwater Underground Water Conservation District, Bell County, Texas  
(December, 2015)*

Submitted By:  
Stephanie S. Wong, graduate student  
Dr. Joe C. Yelderman Jr., Ph.D., P.G.  
Baylor University, Department of Geology



## Executive Summary

Efforts to learn more about the hydrologic processes in the Northern Segment of the Edwards Balcones Fault Zone aquifer revealed several important discoveries that will aid water management and direct future research needs. These discoveries are listed below with interpretations regarding their potential significance.

1. a. Synoptic water levels measured in 2013 included more wells than ever measured before (39) and revealed little change from 2010 synoptic levels. Overall aquifer levels, individual well levels, and general flow patterns remained similar to those previously measured.  
b. The synoptic water level data indicate that the aquifer weathered the epic drought of 2011 without any significant water level changes.
2. a. The presently known spring orifices in downtown Salado, Texas, east of Interstate Highway 35, appear to all be part of an integrated fracture system as documented by dye tracer tests.  
b. The connectivity of these springs through the fracture system implies that aquatic organisms such as the Salado Salamander should hypothetically be able to move about among the springs.
3. a. Two spring discharge points not previously described in the literature by Brune (1975) were documented through observation and dye tracer tests. These springs have been designated "Side Spring and Rock Spring".  
b. Finding dye in Side Spring which occurs in the area where Little Bubbly Spring (also called Little Boiling Spring) normally discharges during high aquifer levels indicates connectivity to the fracture system in this area even though Little Bubbly was not discharging during the dye tests. Finding dye in Rock Spring during the dye tracer tests indicates groundwater on the north side of Salado Creek may be connected through fractures to the springs on the south side.
4. a. The dye tracer test conducted in 2015 confirmed the flow directions and connectivity data from the 2013 tracer test under higher flow conditions and revealed groundwater flow velocities of approximately 350 feet/hour or almost 6 feet/minute.  
b. The fact that the same springs were all connected under both high and low flow conditions is important and indicates a well-developed fracture system with strong connectivity. The high groundwater flow velocities in the immediate area of the springs are important to consider in management decisions.
5. a. Specific conductance (SC) and temperature (T) measurements in cross sections of Big Boiling Spring as well as upstream and downstream of the confluence between Big Boiling Spring discharge and Salado Creek confirm the mixing patterns of groundwater and surface water from Big Boiling Spring and also confirm Rock Spring as a groundwater discharge point.  
b. The cross section data are important to quantify groundwater/surface water mixing, aid in habitat assessments, and aid in sample location selection.
6. a. Natural radon confirmed the location of Rock Spring and the groundwater/surface water mixing model of the SC and T cross sections.  
b. Natural radon appears to work as an indicator of groundwater discharge into surface water and can be used to quantify groundwater/surface water interactions near streams.
7. a. Nitrogen data from field and laboratory analysis showed values that are interpreted to be slightly above expected background levels but no nitrate values were observed to be over the drinking water limit. There were no strong trends but some of the higher values were found in the more developed areas.  
b. The nitrogen data warrant further investigation and monitoring.

8.
  - a. Weather stations have been placed at three strategic locations within the aquifer outcrop and the Salado Creek watershed.
  - b. Data from these weather stations will be useful in analyzing the rainfall and recharge response to specific springs.
  
9.
  - a. Data collected with multi-parameter dataloggers in the cave well and several springs indicated rapid groundwater responses to large rainfall events. The data also show slight water quality changes.
  - b. The multi-parameter datalogger data further refined the fracture system at the springs by indicating a slightly slower response to recharge at Doc Benedict Spring than adjacent Anderson Spring. The responses to recharge captured by the dataloggers also provide important timing information to aid in the development of future monitoring strategies.
  
10.
  - a. A cutthroat flume and several V-notched weirs were constructed and employed to collect flow measurements at some of the smaller discharge points such as Little Bubbly and Side springs.
  - b. The flume and weir assessments were useful in locating potential sites and selecting appropriate measuring devices.
  
11.
  - a. Progress using LiDAR data to detect recharge features has been slow and time consuming but is progressing slowly.
  - b. The LiDAR data still look promising for determining areas of important recharge potential.

# Contents

Executive Summary .....	ii
Contents .....	iv
Project Overview .....	1
- Project area	
- Project Timeline	
Groundwater flow .....	4
- Synoptic groundwater level (Summer 2013)	
- Tracer tests (July 2013, April 2015)	
Water Chemistry .....	15
- Cross sections	
- Natural radon	
- North bank groundwater discharge	
- Aquifer water chemistry (DNP)	
Aquifer response to recharge .....	26
- Weather Stations and rain gauges	
- Multi-parameter monitoring (OTT CTD, Solinst Levelloggers)	
- Flumes and weirs	
Recharge features characterization .....	33
- LiDAR	
Summary & Project Conclusions .....	34
Project experience/Concluding thoughts .....	35
References .....	36
Appendix .....	37

## Project Overview

A body of research was undertaken by Baylor University (“Baylor”) to gain a deeper understanding of the Northern Segment of the Edwards Balcones Fault Zone (BFZ) Aquifer (“the Northern Segment”). Specifically, knowledge of how much recharge occurs and the pathways that recharge takes to the aquifer will greatly assist groundwater resource management. An enhanced scientific understanding of the Northern Segment will provide insight to the Clearwater Underground Water Conservation District (CUWCD) and community stakeholders, as well as support collaboration between the district and community in future decision-making processes.

Activities under this body of work focused on instrumentation, knowledge building, field tests and feasibility studies. Due to the timing of the FWS permitting process and prevailing hydrologic conditions, the body of research has evolved through the course of the project. Keeping in mind the overarching-goals of the study to improve understanding of recharge and groundwater flow in the Northern Segment, and through consultation between Baylor and CUWCD, research activities evolved and expanded to include several aspects not in the original proposal. Specifically, project components were added to investigate water chemistry of the Northern Edwards: surface and groundwater were analyzed repeatedly for natural radon, and wells were sampled for various chemical parameters including dissolved nitrates and phosphates.

After brief descriptions of project objectives, study area, and timeline, this report addresses topics of groundwater flow, water chemistry, aquifer response to recharge, and recharge features characterization. Each section describes the rationale for a given work, methods and instrumentation employed, and results. Project expenditures are summarized. Lastly, this report ends with a discussion of possible future work.

### Project area

This body of research was conducted in the outcrop portion of the Northern Segment in Bell County (Figure 1). Focus was placed on the Salado Springs complex in downtown Salado due to ease of access, as well as their importance as critical habitat for the Salado salamander and a measure of CUWCD’s DFC (Figure 2). Some sampling was also done in the down-dip portion of the aquifer for comparison.

There are three formations that comprise the Northern Segment of the Edwards Balcones Fault Zone aquifer. They are in ascending order; the Comanche Peak Formation, the Edwards Formation and the Georgetown Formation. All of these units are sedimentary rocks, Cretaceous in age, and comprised mainly of carbonate (limestones). The Edwards and Comanche Peak formations are part of the Fredricksburg Group and the Georgetown is part of the Washita Group. They are fairly well connected hydraulically and considered as one hydrostratigraphic unit referred to as the Edwards aquifer; specifically the Northern Segment of the Edwards Balcones Fault Zone aquifer. The underlying confining unit is the uppermost member of the Walnut formation, the Keys Valley member. It is comprised of carbonaceous clay material and referred to as a marl. The overlying confining unit is the Del Rio Formation (sometimes referred to as the Grayson Formation). The Del Rio is a carbonaceous clay-rich unit and often referred to as the Del Rio Clay. Upper Cretaceous units overlying the Del Rio Formation that crop out in the Salado Creek basin include the Buda Formation, Eagle Ford Group and the Austin Chalk. None of these are considered aquifers in this area. Figure 2 shows a map of the geologic units in the Salado Creek basin and environs.

### Project timeline

The general timeline for this investigation into the Northern Segment is shown in Figure 3. In 2011, CUWCD connected with Dr. Joe Yelderman at Baylor University to conduct preliminary research and gather known knowledge on the Northern Segment. In 2012, the Salado Salamander (*Eurycea chisolmensis*) which is endemic to Salado Springs was proposed to be listed as endangered, further highlighting the need for an increased understanding of the Northern Segment in general and Salado Springs specifically. A formal contract was proposed to the CUWCD board in 2013 outlining this present body of research. In February of 2014, the Salado Salamander was officially listed by the U.S. Fish and Wildlife Service as threatened (Department of the Interior, 2014). Because of

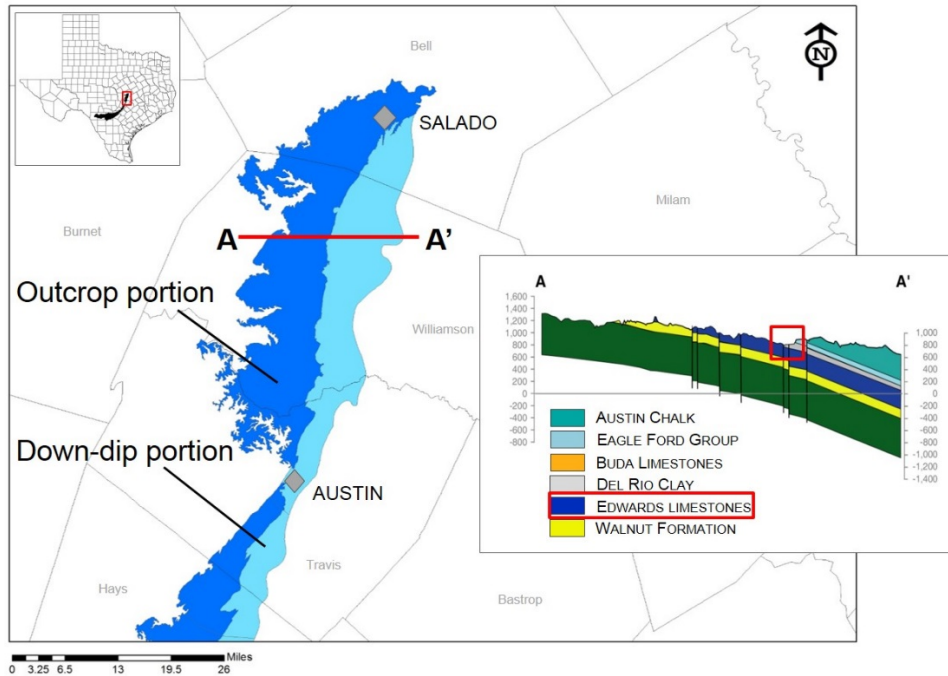


Figure 1: This study was conducted in Northern Segment of the Edwards Balcones Fault Zone aquifer in Bell County.

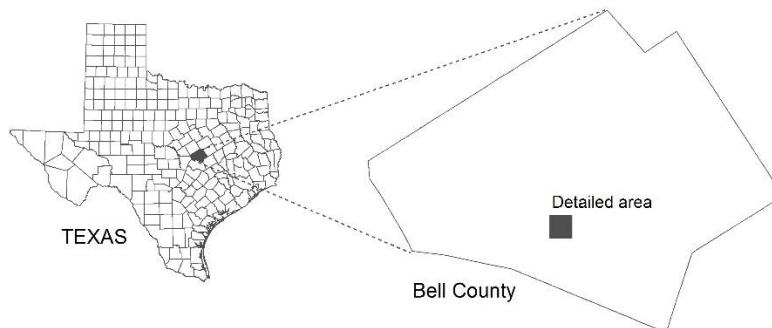
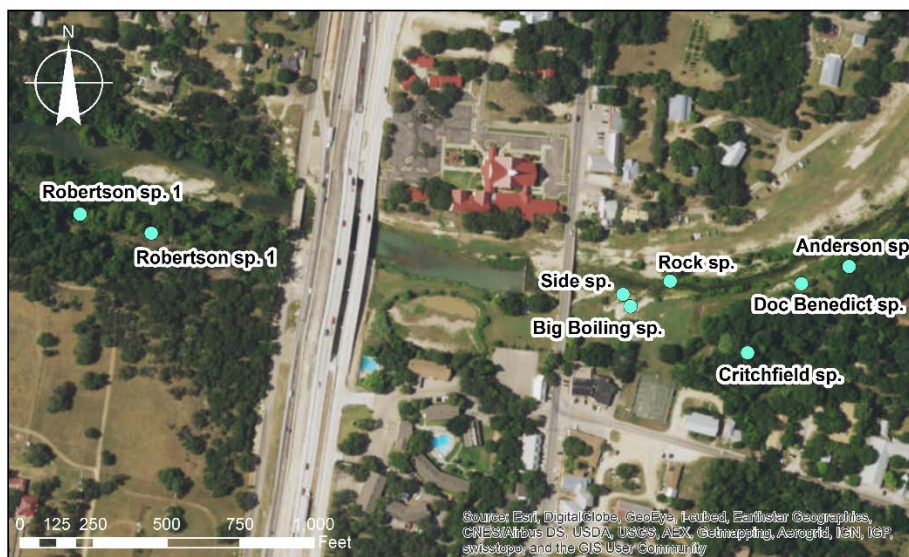


Figure 2: Location of springs in the Salado Springs complex, which was a focus area for this body of research due to ease of access and the springs' importance as a management parameter for CUWCD.

The listing, the Salado Springs complex became officially designated as critical habitat and a research permit was required to conduct tracer tests and install piezometers to study groundwater flow patterns in the complex. Ms. Stephanie Wong spearheaded the permit application process on behalf of CUWCD, and a five-year research permit was awarded to CUWCD in February 2015.

Although this report serves as a final summary of the research efforts completed under the 2013 contract between Baylor and CUWCD, there is still much to learn about the Northern Segment system. Collaborative efforts, monitoring, and data gathering are on-going.

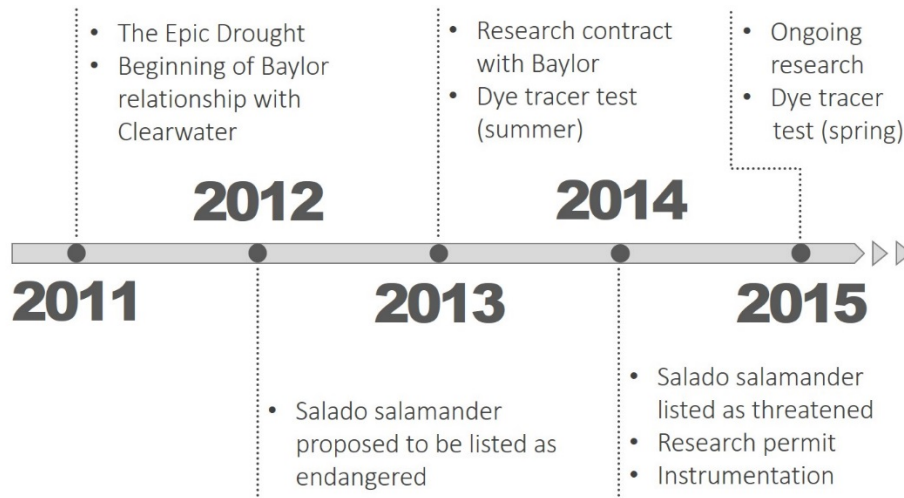


Figure 3: Timeline for the Northern Segment research project. Key events for each year are listed.

## Groundwater Flow

### Synoptic Groundwater Level

In the summer of 2013, CUWCD spearheaded an effort to capture a synoptic water level in the Northern Segment. Synoptic water levels provide data that can be used to ascertain groundwater flow directions and periodic synoptic water level measurements provide a basis for assessing changes in flow directions and changes in the overall aquifer water volume. Two teams (Dirk Aaron and Joe Yelderman; and Todd Strait and Stephanie Wong) measured thirty-nine wells over two days in July 2013, resulting in a large and well-distributed data set over the outcrop and down-dip portions of the Northern Segment. Water levels were feet-to-water measurements obtained using the sonic water level meter. The water levels were converted to water elevations, hand-contoured, and then digitized for presentation (Figure 4). The predominant flow direction in the Northern Segment is southeast, from the outcrop to the down-dip portion of the aquifer. Flow is also deflected towards the northeast around Salado Springs. No cone of depression is evident in the Northern Segment at the contour interval used in Figure 4.

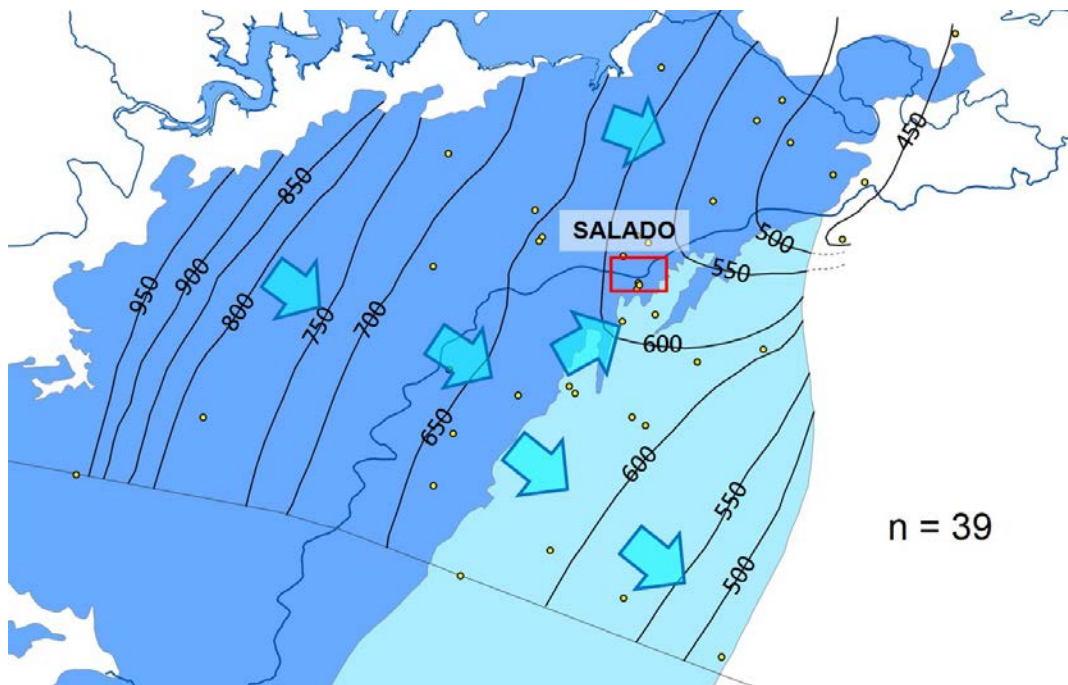


Figure 4: Synoptic surface of groundwater elevations in the Northern Segment.

Wells that were measured in 2013 and 2010 (the previous synoptic water level measurement) were plotted to compare water level change through time (Figure 5). Seven wells were measured in both 2010 and 2013. The assessment of the water levels in the well pairs showed little change. Two wells were identical, two wells showed a slight decline and two wells showed a slight rise. The 2013 water level in the seventh well pair was not usable but overall the water level data indicate there has not been a water level change to any great degree even though the time between 2010 and 2013 included the epic drought of 2011. The steady water levels indicate sustainable usage during this time period and imply effective groundwater management within the area.

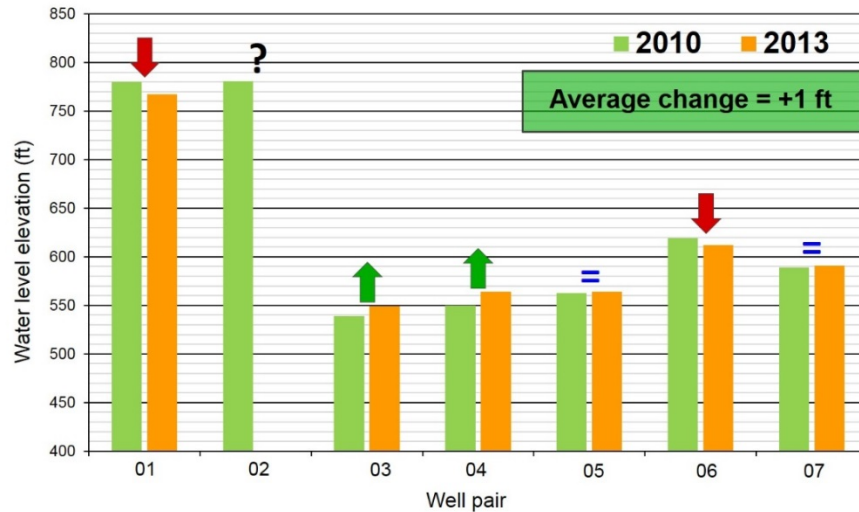


Figure 5: Water levels measured in 2010 and again in 2013 for seven Edwards aquifer well pairs in Bell County.

### Dye Tracer Tests

Groundwater tracing techniques are a direct method of determining point-to-point groundwater travel times and flow directions in karst aquifers. Most tracer testing involves introducing nontoxic, fluorescent, dyes at injection points, such as caves, sinkholes, or wells. After injection, charcoal receptors and water samples are used to passively and actively collect water at wells and springs within the monitored area, and are analyzed for the presence of dyes. The dye tracer tests completed as part of this body of research was preceded by research by Mahler et al. (1998) who conducted a tracer test with particles. Clay particles were tagged with lanthanide cations (trivalent elements with periodic numbers 57 through 71). These were injected into the Stagecoach Inn Cave Well and detected at Big Boiling Spring, confirming a groundwater flow path between the cave and the springs.

#### *Methodology overview*

For this study, tracer tests using a single injection point and one fluorescent dye were conducted to investigate relatively short groundwater flow paths between the Stagecoach Inn Cave Well and springs in the Salado Springs complex (Figure 1). Tracer tests tested the hypothesis that fractures like the one observable in the Stagecoach Inn cave support specific groundwater flow paths directly to specific springs and do not affect other springs in the area. All spring outlets, as well as other groundwater and surface water sites, were monitored along Salado Creek (Figure 6). Both passive and active sampling was employed to detect the presence or absence of dye at each monitor site. The first tracer test took place in the summer of 2013. At 8:30 am on July 31, 2013, one slug of 128 g of uranine dye was introduced into the Stagecoach Inn Cave Well. Detection sites were sampled until 8 pm of the same day. Charcoal receptors were collected and replaced at 8 pm, collected and replaced again at 9 am on August 1, 2013, and then collected on August 7, 2013. A second tracer test took place in the spring of 2015, under higher flow conditions. At 8:45 am on April 18, 2015, 74 g of uranine dye were introduced into the Stagecoach Inn Cave Well. Detection sites were sampled until 7 pm of the same day. Charcoal receptors were collected and replaced at 7 pm, collected and replaced again at 3 pm on April 19, 2015, and then collected on April 27, 2015.



Figure 6: Conceptual overview of Salado Springs dye trace tests.

*Dye*

Sodium fluorescein, commonly called, “uranine”, was selected for this study because of its nontoxicity, cost effectiveness, and ease of detection (Table 1). The dye used is fluorescent and used as colorants in medicine, foods, cosmetics, and industrial applications.

Table 1. Chemical characteristics of sodium fluorescein (uranine).

Common Name .....	Uranine (sodium fluorescein)
Color Index .....	Acid Yellow
Generic Name Molecular Weight CAS Number .....	73 376.27 518-47-8
Excitation Wavelength (nm) .....	493

Eosin was chosen as a secondary dye to complement and confirm the uranine trace during the summer 2013 tracer test. Because of the similarity of results to those of the uranine trace as well as research permit restrictions; eosin was not used for the spring 2015 tracer test.

*Injection Point*

For the Salado Springs tracer tests, the Stagecoach Inn Cave Well was selected for the injection point because it appears to represent a direct pathway to Big Boiling Spring, supported through previous published research as well as local anecdotal accounts. Tracer tests originating in karst features such as caves, sinkholes, or sinking streams (perennial) are expected to be more successful in reaching an aquifer flow path in a timely manner than those originating from other injection points. The straight-line distance between the cave and Big Boiling Spring is 747 ft. The straight-line distance between the cave and Anderson Spring, the most downstream spring in the complex, is 1258 ft.

### *Monitoring sites*

A series of groundwater and surface water monitoring sites were selected, including all the named springs in the Salado Springs complex: Robertson Spring, Big Boiling Spring, Little Bubbly Spring, Critchfield Spring, Doc Benedict Spring, and Anderson Spring.

In the summer 2013 tracer test, all the named springs were monitored except Little Bubbly which was not flowing. Critchfield Spring was also not visibly flowing, but the spring pool contained standing water. Three upstream sites, where dye was not expected, were monitored as control points. These included Robertson Spring which was not flowing (but had standing water), immediately above the low-water dam between Main Street and Interstate Highway 35, and underneath the Main Street Bridge in Salado Creek. Additional to the named springs, a gravel seep associated with Big Boiling and Little Bubbly springs (“Side Spring”) was monitored. Stream sites that were downstream of springs had potential to experience dye. Monitored sites included the Big Boiling Spring run, the north bank across from Big Boiling Spring, the south bank downstream from Big Boiling Spring, the south bank at the USGS flow gage site, and the north bank in Pace Park across from the USGS flow gage (Figure 6).

A slightly refined suite of monitoring sights was chosen for the spring 2015 tracer test (Figure 6). All the named springs were flowing and were monitored except Little Bubbly. Control sites included two outlets of Robertson Spring (Robertson Spring was flowing during this test), Salado Creek upstream of Robertson Spring, immediately above the low-water dam between Main Street and Interstate Highway 35, and Salado Creek between the Main Street Bridge and Side Spring. In addition to the named springs of the complex, Side Spring and a groundwater discharge point on the north bank (“Rock Spring”) were monitored. The USGS flow gage and Pace Park were again used as surface water monitoring sites.

### *Sampling*

Sampling for presence of dye included both passive (charcoal receptors) and active (automated and manual grab sampling) methods. For both tracer tests, charcoal receptors sometimes known as “bugs” were placed at all monitoring sites at least a week before each test to assess background concentrations of the tracer material and then also placed at each site during the test. For the summer 2013 test, water samples were collected at Big Boiling Spring frequently (every ten minutes) throughout the test using an ISCO automated sampler, while occasional grab samples (every two hours) were collected at the other sites. For the spring 2015 test, automated samplers were not available. Instead, at least one field assistant was assigned to manually sample each monitoring site. Big Boiling, Anderson, and Rock springs were sampled at 15 minute intervals; while Side Spring and all sites downstream of Big Boiling Spring were sampled at 1 hour intervals. Grab samples were also collected every time a charcoal receptor was collected. A control blank and field blank were collected every field day as quality control.

### *Lab preparation*

An elution process was performed to analyze the level of dye picked up by the activated charcoal indicators. The packets of charcoal were air-dried and opened, and enough charcoal to fill the bottom of a plastic two-ounce Solo cup was removed from the packet. Fifteen milliliters of eluent, made up of a solution of 95% isopropyl alcohol and 5% potassium hydroxide, was added to the charcoal (Figure 7A). After an hour of elution time, the eluate was poured into 10 ml glass vials for analysis.

Water samples collected from Big Boiling Spring using an ISCO automatic were transferred to 10 ml glass vials for analysis. Manually-collected grab samples were collected using the same 10 ml glass vials.

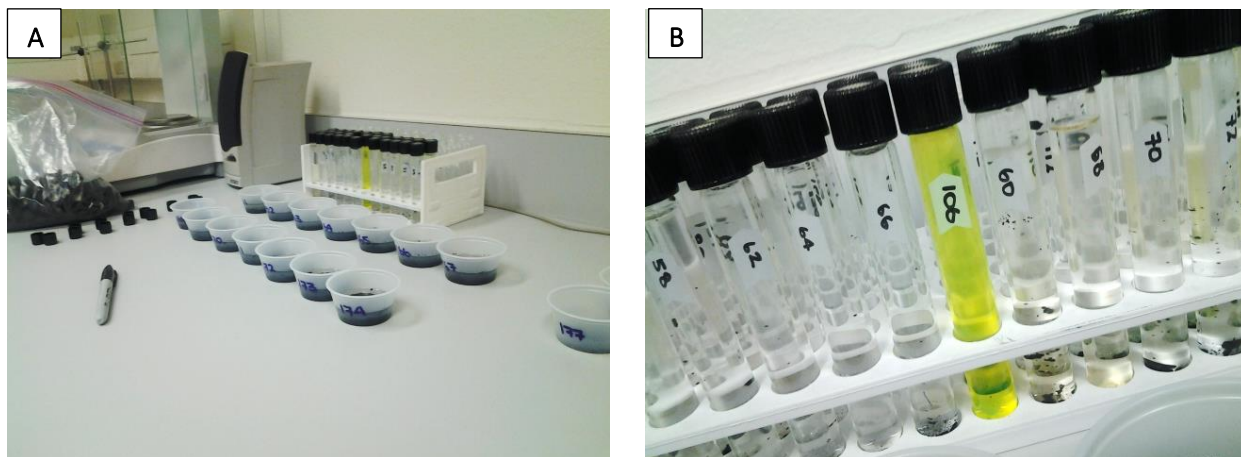


Figure 7. A) Set-up for eluting dye from the charcoal detectors; B) Samples that contained visible dye were at too high of a concentration for analysis. These samples were diluted for analysis, and then normalized back to 100% for comparison.

#### *Sample analysis*

All samples were analyzed as continuous scans on a Perkin-Elmer LS-50B Luminescence Spectrometer. The resulting spectra are emission referenced with  $\Delta\lambda$  of 15 nm, scan speed of 750 nm/min, scanning range from 401 nm to 650 nm, and a 6.0 nm slit. Samples that contained dye concentrations exceeding the analysis limit of the fluorimeter were first analyzed as-is (Figure 7B). Following the initial analysis, the samples were diluted to a level that could be detected by the fluorimeter. For the samples in the summer 2013 trace, a 20% dilution (1 ml sample to 4 ml de-ionized water) was optimal for analysis. For the spring 2015 trace, a 33% dilution (3 ml sample to 6 ml de-ionized water) was optimal for analysis. The spectra produced were then normalized to 100% for comparison with the rest of the data.

All spectra were fitted using Fityk (version 0.9.8) curve fitting and data analysis program (Wojdyr, 2010). The spectra were fitted using Pearson Type VII functions. Peak fluorescence intensity values were converted to dye concentration in parts per billion (ppb) by creating a linear regression with the peak intensities of standards and their corresponding concentrations. The peak concentration for samples with quantifiable detections were plotted against time elapsed to construct breakthrough curves.

#### *July 2013 trace results*

Dye was detected at all monitoring sites downstream of Big Boiling Spring, and was not detected at either upstream monitoring sites or the control site (Figure 8). Peak concentrations and detection times for all monitoring sites are summarized in Table 2. One hundred twenty-eight grams of uranine dye was injected. Visually, uranine dye was strongly present at Big Boiling Spring and Anderson Spring (Figure 9). Sixteen grams of eosin dye was injected. Due to the small amount of dye, eosin was not visible at any monitoring site; however it was still detected at low levels at Big Boiling Spring.



Figure 8: Results of the summer 2013 dye trace test. Purple dots indicate locations of no dye detection. Green dots indicate spring and creek locations where uranine was detected. Arrows represent confirmations of groundwater flow between the injection point at Stagecoach Inn Cave Well and a spring.

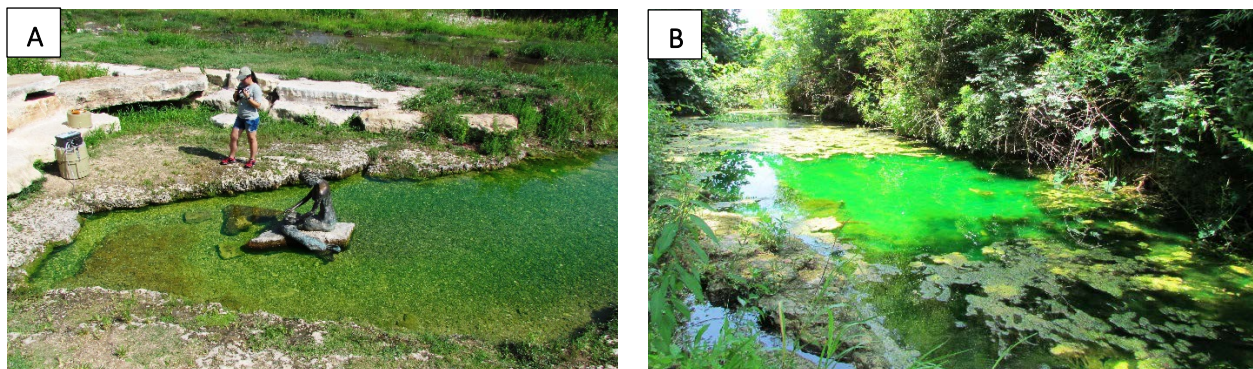


Figure 9: Big Boiling Spring (A) and Anderson Spring (B) both exhibited strong groundwater flow connection to Stagecoach Inn cave, as evidenced by visual detection of uranine at both sites.

Breakthrough curves for both uranine and eosin were plotted for samples collected using the ISCO auto-sampler at Big Boiling Spring (Figures 10 and 11). There are two major discharge points for Big Boiling Spring into the Big Boiling Spring pool; the ISCO auto-sampler sampled at the northern discharge point for the uranine trace and the southern discharge point for the eosin trace. The general shape of the breakthrough curves for uranine and eosin are similar, as are the peak detection times for both dyes (2.67 hours after injection of uranine, and 2.50 hours after injection of eosin). The amount of eosin injected was so small that the first portion of the breakthrough curve was not detected at quantifiable levels (that is, the dye was present at levels significantly above a blank, but was not quantifiable). However, a time of first detection for eosin may be estimated by extrapolating the breakthrough curve to its x-intercept. The extrapolated time of first detection for eosin is 2 hours after injection, which is comparable to the first detection time for uranine (1.83 hours). Groundwater velocities were estimated by dividing the distance between the injection site and Big Boiling spring pool (228 m) by the first and peak detection times for uranine and

eosin. The average groundwater velocity between the injection site and Big Boiling spring pool was determined to be 0.0284 m/s (1.526 mi/d). The first and peak detection times, and calculated groundwater velocities for the uranine and eosin traces are summarized in Table 3. The similarity of first arrival times, peak times, calculated groundwater velocities, and the overall shape of the breakthrough curves for uranine and eosin indicate similar flow paths from the injection site to the northern and southern discharge points in Big Boiling springs pool.

Table 2. Peak uranine concentrations and detection times for grab samples collected along Salado Creek on July 31, 2013. No dye detection at a given site is indicated by “ND” (“No detect”).

Site	Peak concentration (ppb)	Peak time (hh:ss)
Robertson Spring	Dry spring	--
Low water dam lake	ND	--
Main St. bridge	ND	--
Little Bubbly Spring	Dry spring	--
Side Spring	32.45*	12:31
Big Boiling Spring	137.45	10:40
Big Boiling confluence	20.82*	12:23
Big Boiling downstream	15.97*	12:26
Critchfield	2.20	10:37
Doc Benedict Spring	22.46	14:15
Doc Benedict fracture	22.16*	14:15
Anderson Spring	11.78*	14:02
USGS gage	10.08	16:33
North bank	30.26	14:03
Pace Park	12.81	18:36

*\* indicates peak concentrations that were also first detections.*

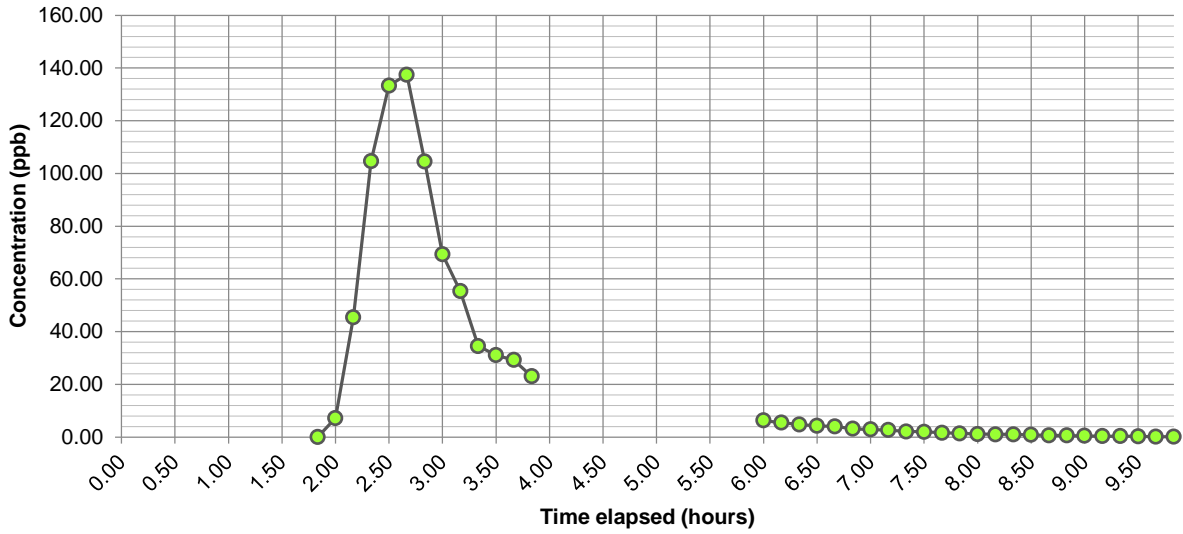


Figure 10. Breakthrough curve for uranine at Big Boiling Spring. Samples were collected with an auto-sampler at 10-minute intervals. First detection occurred at 1.83 hours after dye injection, and peak detection occurred at 2.67 hours (137.45 ppb). The data gap from hour 4 to 6 occurred while the auto-sampler was being re-set for the afternoon eosin trace.

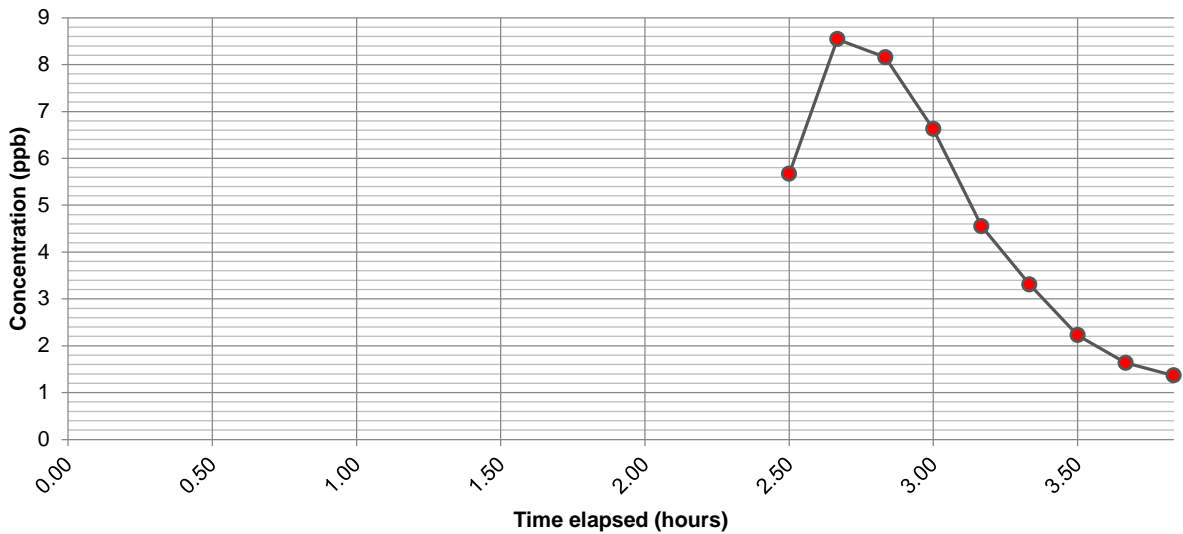


Figure 11. Breakthrough curve for eosin at Big Boiling Spring. Samples were collected with an auto-sampler at 10-minute intervals. First detection occurred at 2.50 hours after dye injection (5.67 ppb), and peak detection occurred at 2.67 hours (8.54 ppb).

Table 3. Groundwater velocity determined at Big Boiling Spring at first and peak detection times for both uranine and eosin traces. The injection point is 747 feet (228 meters) from Big Boiling Spring. The average groundwater velocity is 0.0284 m/s, or 1.526 mi/d. The first detection time for eosin was obtained by extrapolating the break-through curve to its x-intercept.

	URANINE			EOSIN		
	Time (h)	Velocity (m/s)	Velocity (mi/d)	Time (h)	Velocity (m/s)	Velocity (mi/d)
First detection	1.83	0.0346	1.858	2.0	0.0317	1.700
Peak detection	2.67	0.0237	1.273	2.67	0.0237	1.273

*April 2015 trace results*

Overall, the results of the second tracer test were very similar to those of the first test. Dye was detected at all monitoring sites downstream of Big Boiling Spring, and was not detected at any upstream monitoring sites (Figure 12). Peak concentrations and detection times for all monitoring sites are summarized in Table 4. Seventy-four grams of uranine dye was introduced to the Stagecoach Inn Cave Well. Visually, uranine dye was detected at Big Boiling, Side, Doc Benedict, and Anderson springs.



Figure 12: Results of the spring 2015 dye trace test. Purple dots indicate locations of no dye detection. Green dots indicate spring and creek locations where uranine was detected. Arrows represent confirmations of groundwater flow between the injection point at Stagecoach Inn Cave Well and a spring.

Groundwater velocities were estimated by dividing the distance between the injection site and each spring by the first and peak detection times for uranine. The average groundwater velocity between the injection site and Big Boiling spring was determined to be 0.0676 m/s. The average groundwater velocity from the injection site to Anderson Spring and Rock Spring were 0.0526 m/s and 0.0429 m/s respectively. The first and peak detection times, and calculated groundwater velocities for the traces are summarized in Table 5.

Table 4. Peak uranine concentrations and detection times for grab samples collected along Salado Creek on April 15, 2015. No dye detection at a given site is indicated by “ND” (“No detect”).

Site	Peak concentration (ppb)	Peak time (hh:ss)
Robertson Spring	ND	--
Low water dam lake	ND	--
Salado Creek (Main St. bridge to Side Spring)	ND	--
Little Bubbly Spring	Dry spring	--
Side Spring	>1000 intensity units <sup>†</sup>	9:46
Big Boiling Spring	>1000 intensity units <sup>†</sup>	10:00
Critchfield Spring	8.14*	15:40
Doc Benedict Spring	>1000 intensity units <sup>†</sup>	10:44
Anderson Spring	>1000 intensity units <sup>†</sup>	11:35
USGS gage	10.96*	14:53
Rock Spring (North bank)	>1000 intensity units <sup>†</sup>	11:30
Pace Park	16.54*	15:02

\* indicates peak concentrations that were also first detections.

<sup>†</sup> denotes a sample with dye concentration that exceeded the detection limit of the fluorimeter. These samples are being re-analyzed.

Table 5. Groundwater velocity determined at Big Boiling, Anderson, and Rock springs at first and peak detection times. The injection point is 747 feet (228 meters) from Big Boiling Spring, 1258 feet (384 meters) from Anderson Spring, and 869 feet (265 meters) from Rock Spring.

	Big Boiling			Anderson			Rock		
	Time (h)	Velocity (m/s)	Velocity (mi/d)	Time (h)	Velocity (m/s)	Velocity (mi/d)	Time (h)	Velocity (m/s)	Velocity (mi/d)
First detection	0.75	0.0844	4.53	1.58	0.0675	3.62	1.25	0.0589	3.16
Peak detection	1.25	0.0507	2.72	2.83	0.0377	2.02	2.75	0.0268	1.44
Avg. velocity	--	0.0676	3.63	--	0.0526	2.82	--	0.0429	2.30

#### Discussion

Results of the dye tracer tests at Salado Springs confirmed a previous tracer test (Mahler et al, 1998) and the potential that anecdotal stories might be true regarding flow paths between the Stagecoach Inn Cave Well and Big Boiling Spring. The dye tracer tests showed that groundwater flows freely between the injection point in the Stagecoach Inn Cave Well and the major springs along Salado Creek in the downtown area, demonstrating excellent communication between groundwater in all the flowing springs in the study area. The tracer tests revealed a spring system where the series of major springs in the downtown Salado area (with the exception of Robertson Spring) were interconnected to each other under low flow conditions experienced on July 31, 2013, as well as higher flow conditions like those on April 18, 2015.

The first tracer test was conducted under low-flow conditions when Little Bubbly Spring showed no visible flow, Robertson spring had only standing water and Critchfield Spring had only standing water. Side spring was barely flowing but was thought to possibly be connected to those two spring flows. The presence of dye detected in the seep indicates this is probably the case. It was unclear if the dye detected at the north bank of Salado Creek was the result of groundwater discharge at this location or if dye had been transported by surface flow in the creek from Big Boiling Spring discharge.

The second dye tracer test was conducted under higher flow conditions than the first test and in a different season (spring compared to summer). The results were similar and confirming in that all the same spring outlets received dye as they did in the previous test. The results indicate the connectivity among the springs and fracture system is present under both high and low flow conditions. However, as one might expect, the first detection and peak detection times were less for the second test under the higher flow conditions.

Flow was hypothesized to be toward Salado Creek with a downstream component and this appears correct as no dye was detected in the three upstream sites but was detected in all the downstream sites on both tracer tests. The dye reached Big Boiling Spring first and the amount was greater than at other sites except for Anderson Spring. Anderson Spring had a very strong showing of dye that appeared to be related to its strong discharge flow rate. Dye reached Anderson Spring later than Big Boiling Spring presumably because of a greater distance from the injection point. Results of the tracer tests suggest that on this localized scale of several hundred meters, even under low-flow conditions such as those during the summer 2013 tracer test, the springs are interconnected hydrogeologically and act as one system interacting with Salado Creek.

## Water Chemistry

### Cross sections

Seasonally, Salado Creek has been profiled at three cross sections near Big Boiling Spring. Cross sectional profiling helps to monitor physical and chemical conditions, as well as comparison with previously-collected data (water depth, temperature, and specific conductance) at Salado Creek. Flow measurements were also taken. Water samples were collected periodically to monitor natural radon levels in the area.

The three cross-sections were located in Salado Creek (Figure 13): within the spring flow of Big Boiling Spring (cross section one), in Salado Creek upstream of the confluence of Big Boiling Spring (cross section two), and in Salado Creek downstream of the confluence of Big Boiling Spring (cross section three).

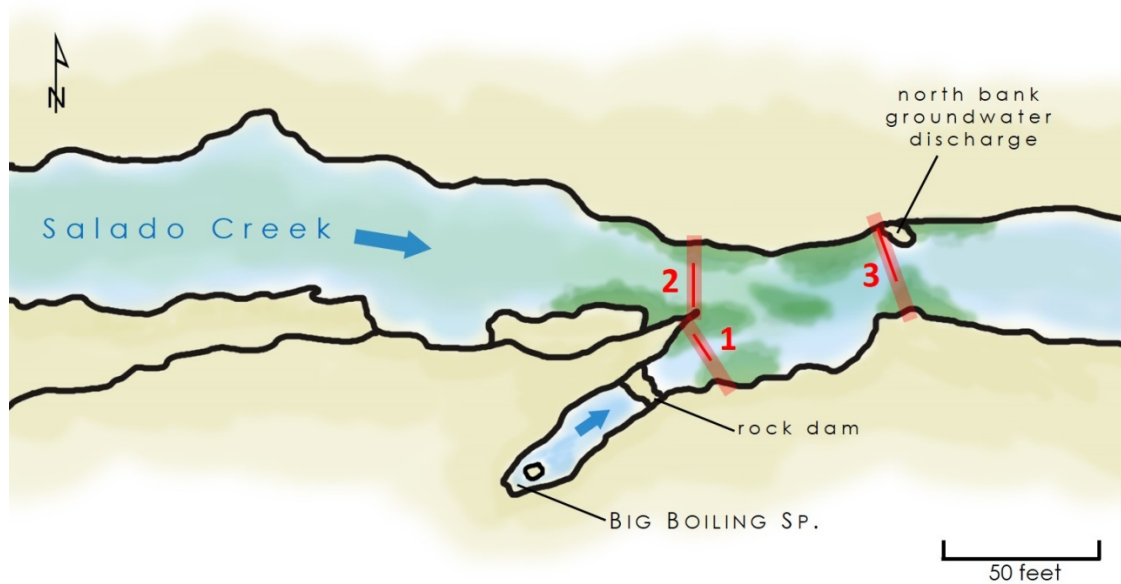


Figure 13. Diagram of Salado Creek showing key features. Cross-section locations are indicated by the red lines and labelled 1, 2, and 3.

### *Methods*

All three cross-sections were taken perpendicular to flow direction (Figure 13). The measured parameters included: depth in feet (ft.), temperature in degrees Celsius ( $^{\circ}\text{C}$ ), specific conductance in micro-Siemens ( $\mu\text{S}/\text{cm}$ ), and flow in feet per second (fps). Measurements were made across the creek using stadia rod or reel tape laid across the channel width. Depth was measured using a metal yard stick. Temperature and specific conductance were measured using a Solinst TLC meter (Solinst Model 107 TLC Meter; Solinst Canada Ltd., Georgetown, Ontario). Flow was measured using a Global Water flow meter (Global Water Instrumentation, College Station, Texas) or SonTek Flowtracker (SonTek, San Diego, California), and the discharge for each cross section was determined using the following equations:

$$Q = \sum q_x \quad (1.1)$$

where

$$q_x = \frac{(v_x d_x w_x)}{2} \quad (1.2)$$

where  $Q$  is the total discharge for a given cross section and is equal to the sum of each of the partial discharges ( $q_x$ ) in cubic feet per second (cfs),  $v_x$  is the measured flow velocity in feet per second (fps) at interval  $x$ ,  $d_x$  is the measured depth in feet, and  $w_x$  is the width of interval  $x$  in feet (equations modified from Michaud, 1991).

The specific conductance measurements were made in the natural water environment without the use of a stilling well or container, and without filtering the water. The water was very clear (spring flow and base flow conditions) but was flowing briskly except near the stream banks.

### *Results*

Cross-section one is characterized by unusual consistency in temperature and specific conductance (Figure 14 and 15). Steady depth and temperature values are understandable for a spring flow discharge channel and the landscaped, un-shaded nature of the Big Boiling Spring pool. The slight changes in specific conductance may be the result of variability in flow velocities that could affect the reading. Similar specific conductance values suggest a single source of water; in this setting it is groundwater discharging from Big Boiling Spring. Furthermore, specific conductance values are similar to those measured at the Stagecoach Inn Cave, located to the south and up-gradient with regard to groundwater flow. The similar specific conductance values suggest that Big Boiling Spring and the Stagecoach Inn Cave are part of the same groundwater system.

Cross-section two is located in the natural channel of Salado Creek. The cross-section is consistently shallow, with warm water that is characterized by lower specific conductance than cross-section one. Temperature and specific conductance values were again fairly consistent across the section. The variation in temperature and specific conductance near the north bank (feet 18-23) are the result of very shallow, muddy conditions. Higher temperature and lower specific conductance values than those measured at cross-section 1 suggest that flow in Salado Creek upstream of Big Boiling Spring is dominated by streamflow rather than direct groundwater. Although flow in Salado Creek during these observations was dominated by baseflow from groundwater, a low-water dam immediately upstream is partly responsible for increased temperatures and lower specific conductance.

Cross-section three is located in the natural channel of Salado Creek, downstream of the confluence with Big Boiling Spring. Temperature and specific conductance values at this location show more variability than cross-sections one or two. This is to be expected since cross-section three is below the confluence of the spring and stream flow. Temperature and specific conductance at this location are intermediate values of those measured at cross-sections one and two (Figures 14 and 15), suggesting a mixing of stream water (represented by cross-section two) and groundwater discharging from Big Boiling Spring on the south side of the channel (represented by cross-section one). Temperature and specific conductance values, beginning at about 20 ft. of cross-section three, are similar to measurements from Big Boiling Spring. The temperature rises and specific conductance decreases from the south to the north in the middle section as more surface water influences the total water flow. A probable groundwater discharge on the north side of the channel at the end of cross-section three is likely responsible for the change in temperature and specific conductance. Similar temperature and specific conductance values also suggest a groundwater connection between the two discharge points (that is, Big Boiling Spring and the north bank discharge point). Such a connection has been confirmed through dye tracing.

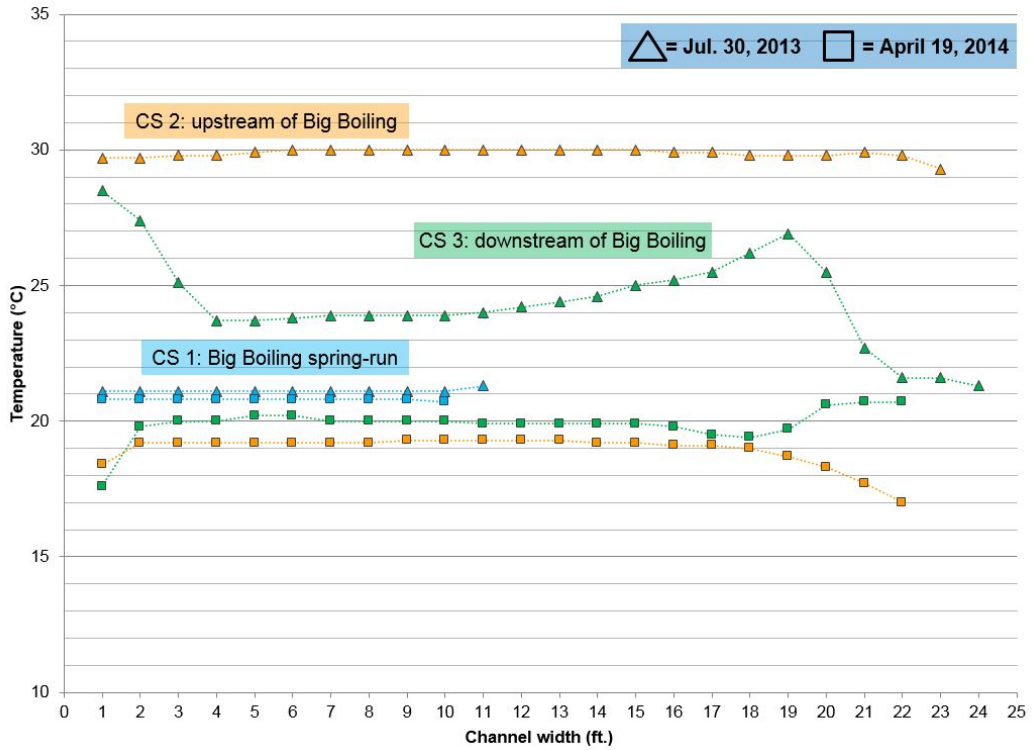


Figure 14: Temperature data for cross sections 1-3 at two time periods.

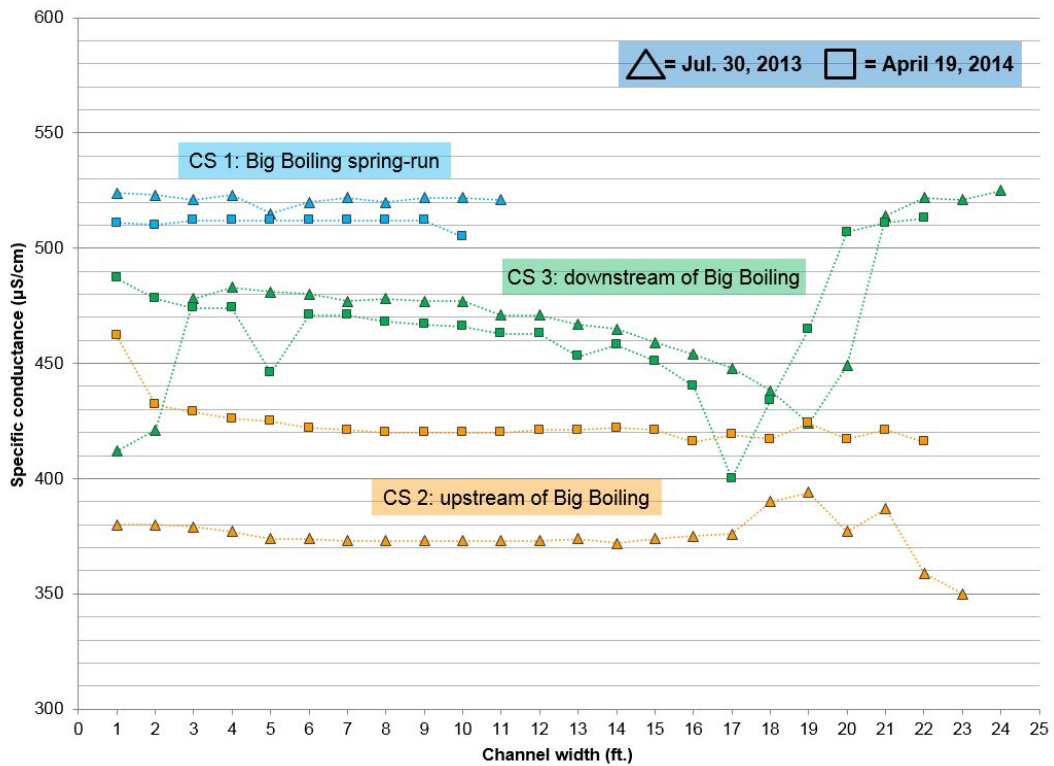


Figure 15: Specific conductance data for cross sections 1-3 at two time periods.

### Summary

Cross-sections one and two are characterized by consistent values in the three measured characteristics: depth, temperature, and specific conductance. Low temperatures and high specific conductance values confirm groundwater-dominated flow in cross-section one, while high temperatures and low specific conductance values in cross-section two indicate stream-dominated flow. Cross-section three showed the most variability in the three measured characteristics and, furthermore, the values range between those of cross-sections one and two. Values at cross-section three suggest a mixing of groundwater and stream water, with groundwater input from Big Boiling Spring in the south and a probable groundwater discharge point in the north bank of Salado Creek.

### Natural radon

Radon-222 is part of the decay chain of uranium-238 (due to the alpha-decay of radium-236), and has a relatively short half-life of 3.8 days. Radon is found naturally in trace amounts in the local soil and bedrock (Michel, 1987). It is assumed that there is no source material in the atmosphere and so the concentration of radon in rain is zero. As rain infiltrates the aquifer and interacts with source material (rocks and soils), the concentration of radon should increase until equilibrium is reached (Hoehn et al., 1992). As groundwater is discharged into a surface water body, the concentration of radon will decrease through decay and diffusion into the atmosphere (Figure 16), and is expedited through any aeration due to mixing and turbulence (Stellato et al., 2012; Neupane et al., 2014). Because of the short half-life of Rn-222, it has been useful for applications such as apparent age estimation of groundwater, infiltration rates, groundwater discharge location and magnitude, fracture aperture estimation, and contamination studies (Ellins et al., 1990; Lee and Hollyday, 1991). Radon was applied in the Salado Springs complex to identify locations and comparative magnitude of groundwater discharge. Radon is naturally-occurring and employs a minimally-invasive sampling method, which is especially attractive in a critical habitat setting such as Salado Springs.

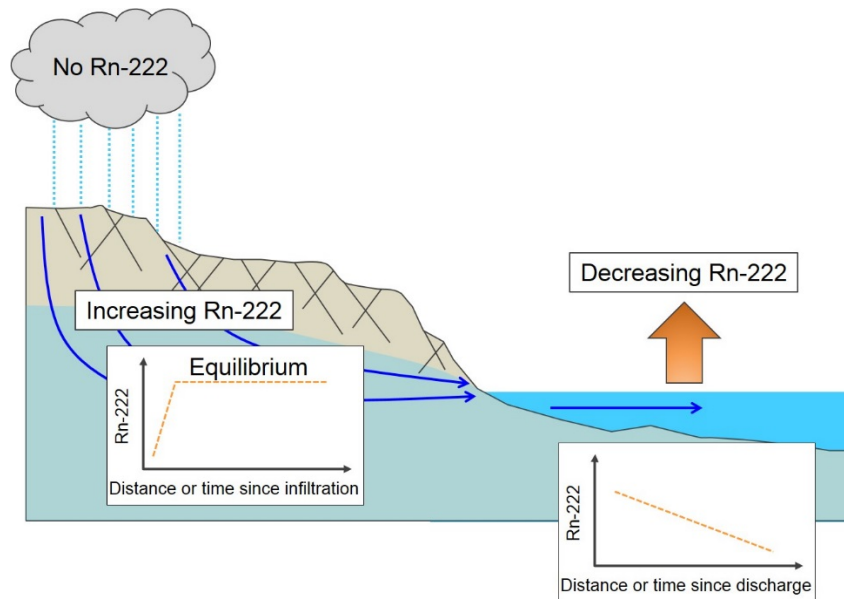


Figure 16: Conceptual model for radon-222 in a shallow groundwater system.

### Methodology

Water samples analyzed for Rn-222 were collected using air-dried 250 ml glass bottles with septum caps. Each bottle was triple-rinsed with sample water before sample collection. Where possible, samples were collected by completely immersing the bottles in the stream or spring discharge and, after the bottle had filled completely, capped underwater to avoid aerial exposure. Samples were collected with no headspace. For stream samples, water

was collected from the thalweg of the channel. Spring samples were collected as close to the point of discharge as possible. After collection, water samples were placed in a cooler for insulation from temperature fluctuations and protection during transport.

All the named springs in the Salado Springs complex were sampled to characterize the radon concentration of groundwater and monitor for seasonal change. Water was also collected at Main Street Bridge to characterize the radon concentration of surface water entering the Salado Springs system at downtown Salado. The complex was sampled in its entirety over three- to four-day campaigns during March 2014, May 2015, July 2015, and September 2015. On June 7, 2014, the main trunk of Salado Creek was sampled from its headwaters near Florence to the confluence with the Lampasas River to characterize radon concentration in the creek and identify points of groundwater addition.

Water samples were analyzed within 24 hours of collection to minimize loss of Rn-222 through radioactive decay. The activity of dissolved Rn-222 in each sample was measured using a RAD7 unit equipped with a RAD H<sub>2</sub>O radon-in-water accessory (DURRIDGE Company, Inc., Billerica, Massachusetts). The RAD7 is an electronic radon detector that quantifies radon activity through alpha spectrometry. Air is recirculated through the water sample and RAD7 unit in a continuous closed loop to extract dissolved radon gas. As Rn-222 nuclei decay, characteristic alpha energies emitted by radon daughters, specifically <sup>218</sup>Po (6.00 MeV) and <sup>214</sup>Po (7.69 MeV), are detected by a solid-state, ion-implanted, Planar, Silicon alpha detector as electrical signals which are then quantified and converted to digital form for output (DURRIDGE Company Inc., 2014a; 2014b). RAD7 results were corrected to account for radon activity decline due to radioactive decay from the time of sampling to analysis. The decay correction factor (DCF) was determined for each sample using the following equation:

$$DCF = e^{(T/132.4)}$$

where T is the decay time in hours, and 132.4 is the mean life of a Rn-222 atom in hours, calculated by dividing the product of 3.825 days (the half-life of Rn-222) and 24 hours per day by the natural logarithm of 2 (DURRIDGE Company Inc. 2014b).

Between every sample, the RAD7 was purged for a minimum of 15 minutes to flush the instrument of residual radon and lower the internal relative humidity to 6% or less. Also, a blank was measured between every sample to keep track of background radon levels.

### *Results*

Radon-222 concentrations observed at downtown Salado are summarized for the March 2014 sampling campaign in Figure 17. Average radon-222 concentrations for groundwater and surface water are summarized in Table 6 for all sampling campaigns. Radon-222 concentrations in groundwater samples were consistently greater than those of surface water, about two times greater. Radon-222 concentrations just above and below the low water dam shows the effect of aeration to expedite diffusion of radon into the atmosphere, resulting in a lower concentration immediately below the low water dam. Low radon-222 content at the Main Street Bridge is indicative of surface water which has had opportunity to de-gas its radon-222, while water sampled from a spring orifice would not have had time for gas exchange with the atmosphere (Cook et al. 2003). The radon-222 concentration for Salado Creek just downstream from the Big Boiling spring confluence is an intermediate value between Main Street Bridge and Big Boiling spring, suggesting a mixing of surface and groundwater at that location. Variations in groundwater radon-222 concentrations likely reflect differences in flow path through the aquifer and degree of water-rock interaction.

The radon-222 concentrations along Salado Creek are summarized in Figure 18. The lower basin exemplifies the radon-222 conceptual model; surface water samples had radon-222 concentrations less than 10 pCi/L, and increases where there is groundwater contribution. In the upper basin, there were less data collected and the pattern is not as clear. Looking at the data longitudinally, however, reveals a rise-and-fall pattern in radon-222 concentrations along Salado Creek, where high values correspond to proximity to a groundwater source and lower values further away from a source. From radon-222 data, there are three reaches of Salado Creek that can be distinguished by points of groundwater contribution (Figure 18).

*Discussion*

Analysis of radon in the waters of Salado Creek and the Salado Spring complex was found to be feasible and appropriate for the study area. The short half-life of radon-222 is suited to a karst setting which can have very quick flow paths. Relatively short times required for analysis allow for repeated sampling and monitoring of spring conditions. The short half-life of radon-222 does limit the number of samples that can be collected and analyzed before concentrations decay and render samples unusable; this limitation was addressed by focused sampling over a few days (under the same hydrologic conditions). Lastly, radon-222 has a couple of additional advantages in this study area. It is a naturally-occurring tracer and does not require adding chemicals to the spring system. Also, sampling methods were minimally-to-non-invasive, which is an important consideration in a critical habitat setting.

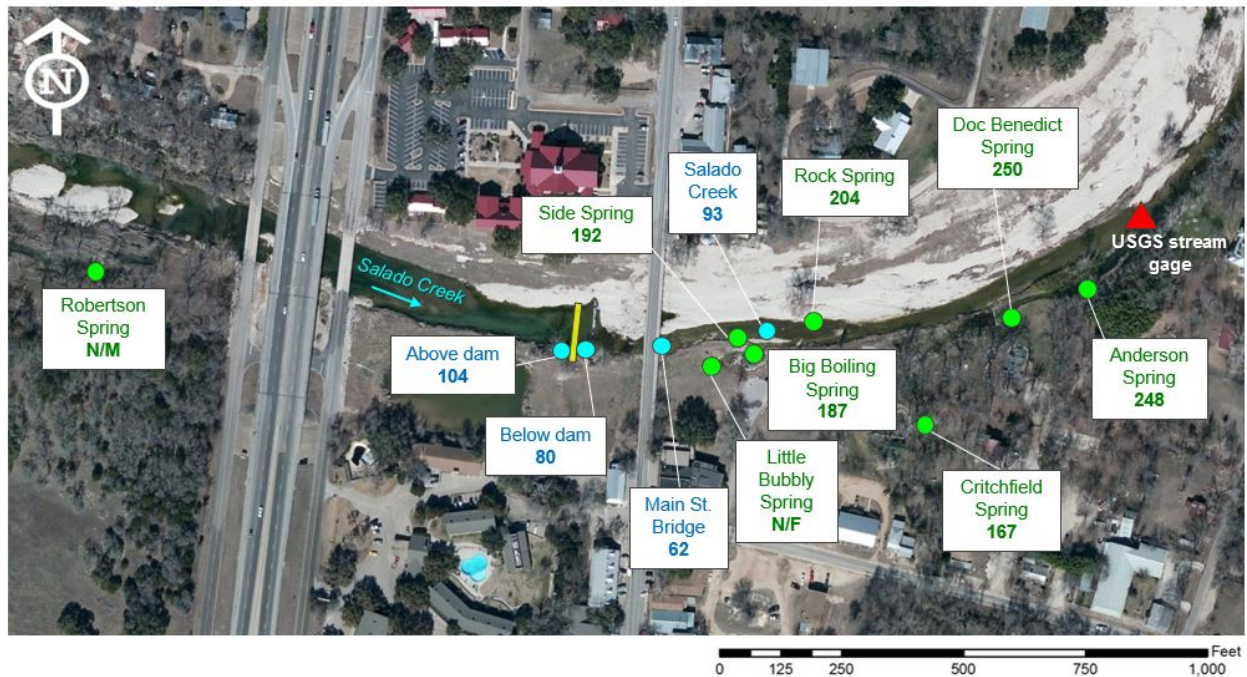


Figure 17: Synoptic radon-222 concentration in groundwater and surface water at Salado Springs. Radon-222 concentrations are given in pCi/L. The abbreviations “N/M” and “N/F” mean “not measured” and “no flow” respectively.

Table 6. Average radon-222 concentrations in pCi/L for groundwater and surface water in the Salado Springs complex for sampling campaigns in 2014 and 2015.

	March 2014	May 2015	July 2015	September 2015
Groundwater	200.16	257.25	244.56	262.10
Surface water	84.75	n/m*	124.87	167.60

\*n/m = not measured

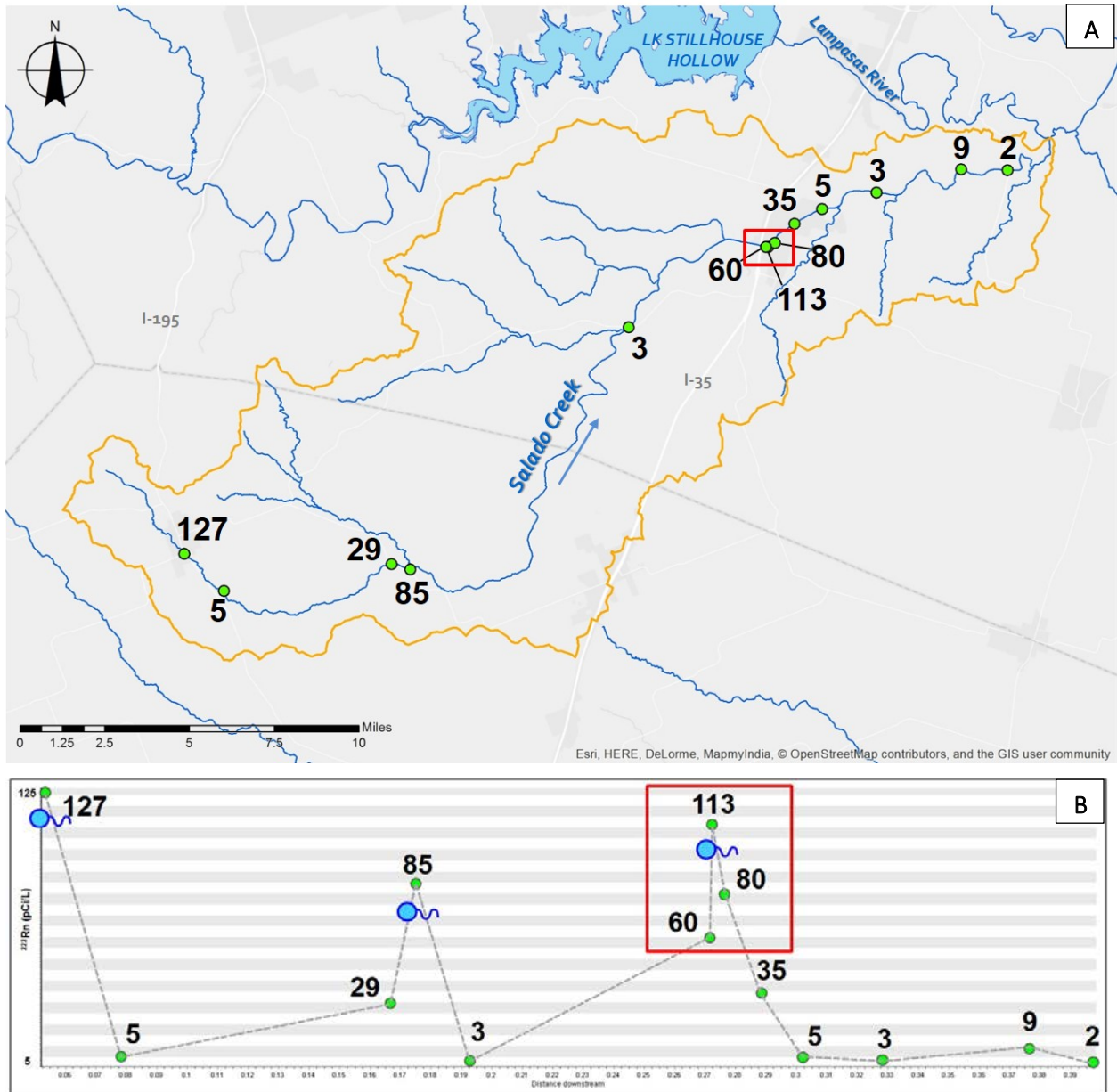


Figure 18: A) Map of the Salado Creek watershed, showing locations sampled for radon concentrations in June, 2014; B) A longitudinal plot of the same data, with radon concentrations on the Y-axis and distance down the channel on the X-axis, allowing spikes in radon concentration to be more easily seen.

Radon-222 concentrations in groundwater samples were consistently greater than those of surface water, which agrees with published research. Generally, a 2-4 times difference in surface and groundwater radon-222 concentrations have been reported (Burnett et al., 2010). The dichotomy of groundwater and surface water radon concentrations at Salado Springs can serve as end-members for groundwater and surface water in the study area. Radon concentration can complement other field measurements to identify, confirm, and monitor groundwater discharge sites. Radon concentrations also support the site of the USGS stream flow gauge (gauge #08104300) for tracking total spring complex discharge. As Figure 18 indicates, there are no major groundwater contributions to

Salado Creek downstream of the downtown springs. Additionally, tracer test data indicate that all the springs in the downtown section of the Salado Springs complex are connected. Radon and tracer test data indicate that the current site for the stream gauge is appropriate for monitoring Salado Springs.

### North bank groundwater discharge: Rock Spring

Through conducting stream profiles at Salado Creek, the water chemistry at the north end cross-section 3 was observed to closely mirror that of water discharging from Big Boiling Spring. A brief investigation was undertaken to confirm groundwater discharge from underneath a boulder on the north bank of Salado Creek, referred to in this project as “Rock Spring”.

After a rain event on September 21, 2013, a plume of clear water was seen to be discharging into Salado Creek, which was highly turbid due to fine sediment being suspended during and after the rain event (Figure 19A). From this event, we observed that water was being discharged from underneath the north bank boulder, and that it was clearly different from water in the creek. Repeated temperature, specific conductance, and radon-222 readings were taken at this site (Table 7). The mean temperature at Rock Spring for all sampling events is 20.64°C, the mean specific conductance is 531  $\mu\text{S}/\text{cm}$ , and the mean radon-222 concentration is 262.73 pCi/L. All these values fall into the range for what has been measured at the named springs in the complex, and confirm that the water being discharged from Rock Spring is groundwater.

Table 7. Water chemistry at Rock Spring confirming presence of groundwater.

Date	Temperature (°C)	Specific conductance ( $\mu\text{S}/\text{cm}$ )	Radon-222 (pCi/L)
April 19, 2014	20.7	513	236.98
November 6, 2014	20.9	513	239.21
January 15, 2015	16.2	525	286.95
July 29, 2015	22.7	505	252.24
September 18, 2015	22.7	601	298.28
<i>Averages</i>	<i>20.64</i>	<i>531</i>	<i>262.73</i>

After heavy rains and flooding in the spring of 2015, the Rock Spring site was unfortunately buried by gravels (Figure 19B). However, we were able to excavate some of the gravel to access the groundwater discharge point (Figure 19C). After allowing the disturbed sediment time to settle, water was sampled. The radon concentration was 252.24 pCi/L, indicating that groundwater was still discharging from this location.

The radon concentration, together with temperature and specific conductance data that mirror those of groundwater; strongly support the probability of a groundwater discharge point on the north bank of Salado Creek across from Big Boiling Spring. Previously, points of significant groundwater discharge into Salado Creek were identified on the south bank only. Positive dye detections at Rock Spring through the course of two tracer tests suggest connection with the groundwater flow system on the south side of Salado Creek. Additionally, augering on the north bank point bar caused turbidity in the water discharging from Rock Spring, suggesting groundwater contribution from the north side of Salado Creek (Figure 19D). Field observations, tests, and water analysis indicate that the water discharging from Rock Spring is groundwater, and that it is sourced from both the groundwater flow system from the south of Salado Creek as well as the north.

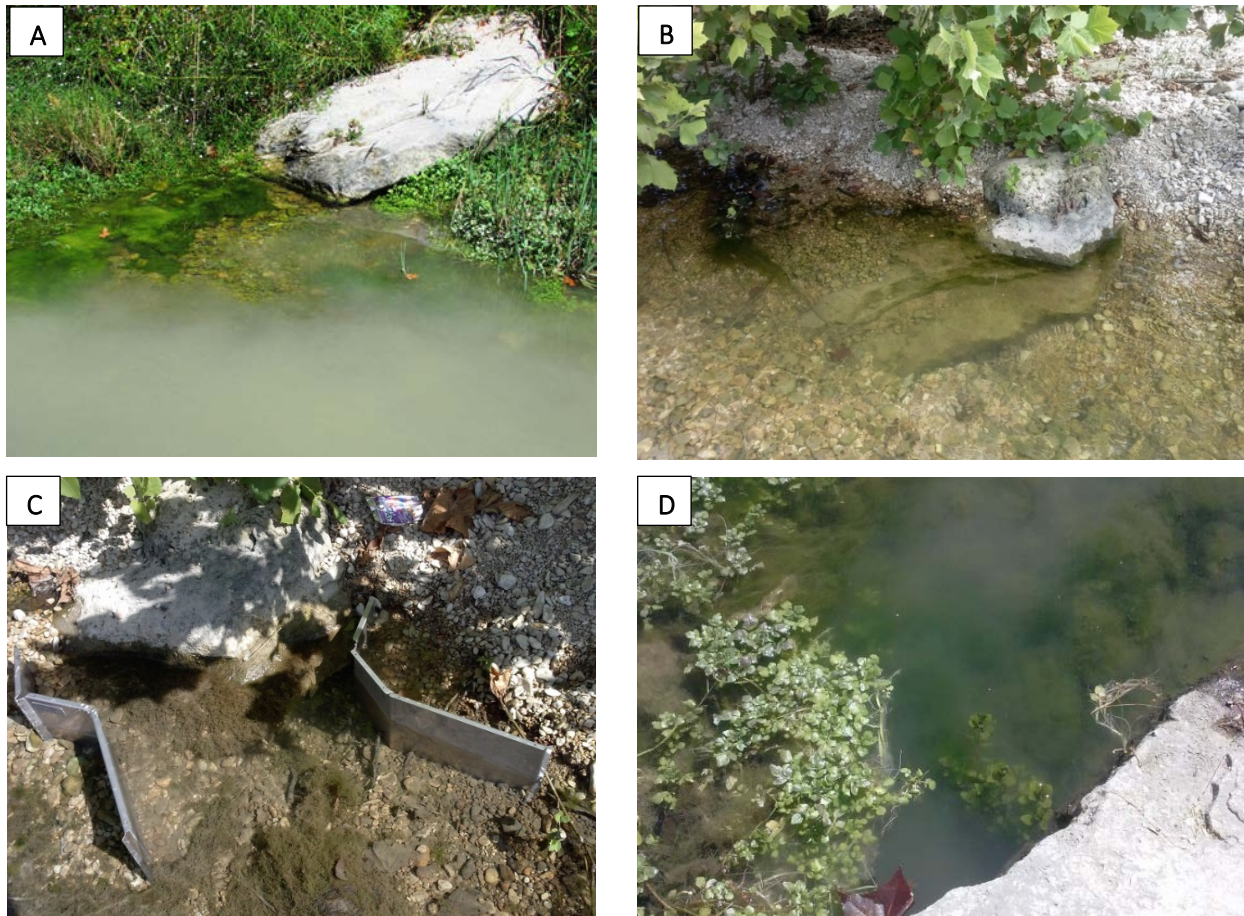


Figure 19: Groundwater discharge point from the north bank of Salado Creek. A) After a rain event, clear groundwater was observed to be discharging into Salado Creek which was cloudy due to suspended sediments (September 21, 2013); B) Rock Spring was buried by the gravel load carried by Salado Creek during spring flooding events (July 2, 2015); C) gravel around Rock Spring was excavated to sample the groundwater discharge point, and flume walls were used to prevent cave-in (July 29, 2015); D) augering on the north bank point bar caused sediment to be discharged from Rock Spring (March 28, 2015) .

### Aquifer water chemistry

In summer 2014, a sampling campaign of wells in the Northern Segment was undertaken to determine baseline water chemistry. Baylor and CUWCD collaborated to visit about 30 non-permitted domestic wells. Twenty wells out of the thirty were sampled; sampling was limited to those wells that had a point of access between the wellhead and storage tank. Tested parameters included: temperature ( $^{\circ}\text{C}$ ), specific conductance ( $\mu\text{S}/\text{cm}$ ), pH, radon-222 ( $\text{pCi}/\text{L}$ ), and field nitrate ( $\text{mg}/\text{L}$ ). Filtered samples were also collected and analyzed for dissolved nitrate and phosphate, and dissolved organic carbon at the Baylor Center for Reservoir and Aquatic Systems Research lab. Additionally, filtered samples were collected and sent to the USGS for nitrogen isotope analysis. Distribution of radon-222 and field nitrate in Northern Segment wells are mapped in Figures 20 and 21.

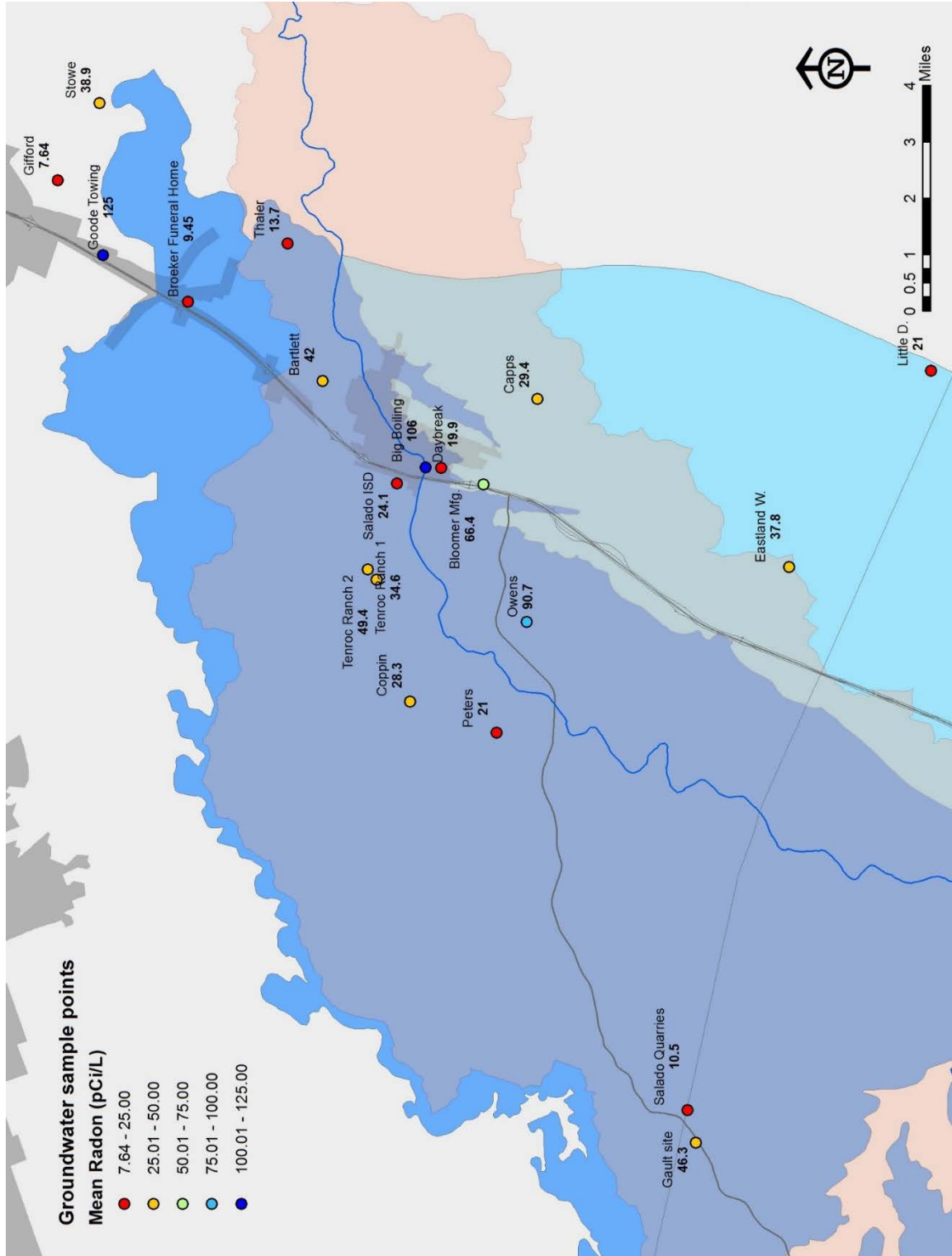


Figure 20: Concentration of radon-222 in water supply wells in the Northern Segment.

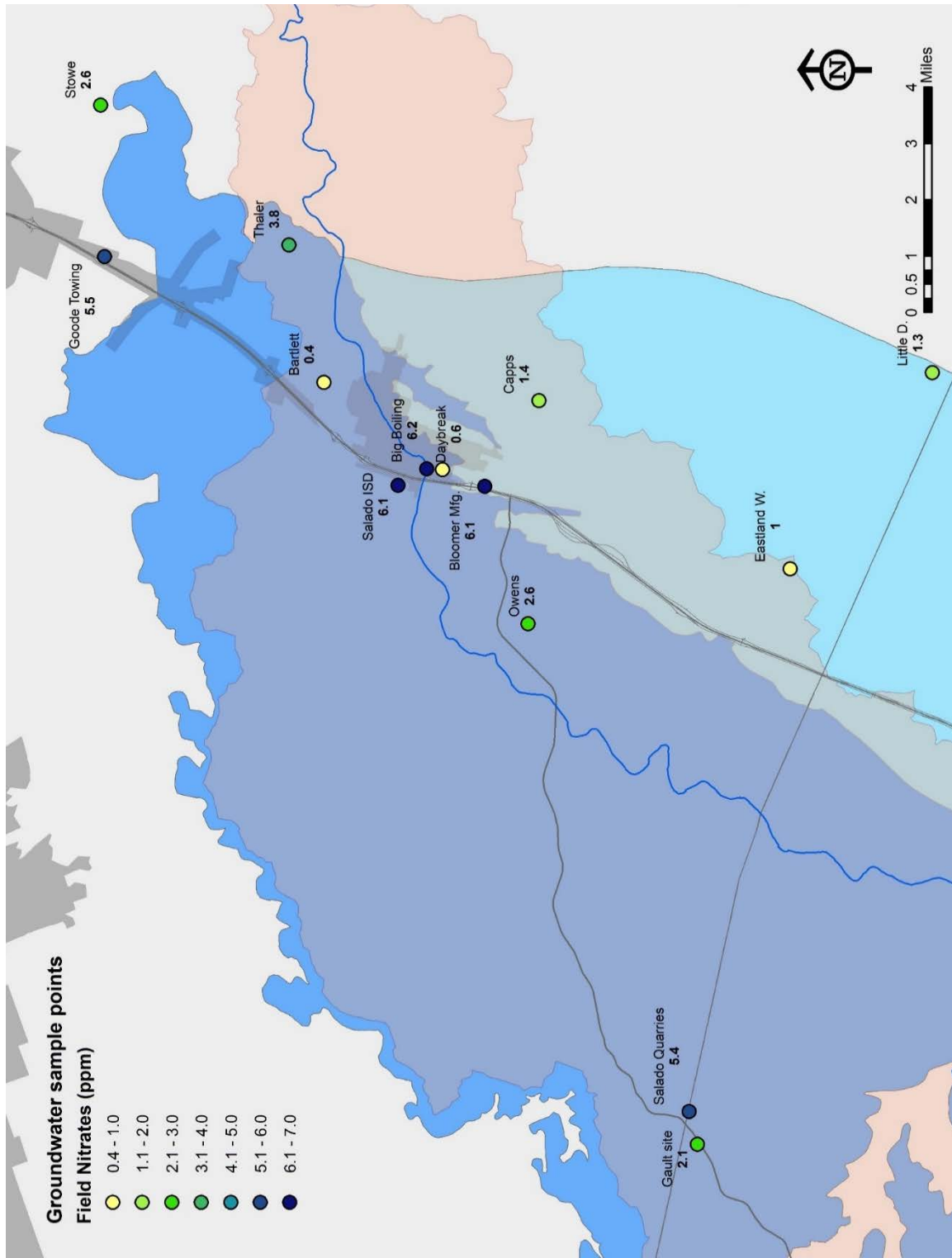


Figure 21: Concentration of nitrates in water supply wells, analyzed in the field.

## Aquifer Response to Recharge

### Weather stations and rain gauges

The distribution of rainfall over a given area can vary both spatially and temporally. Therefore, use of a single rain gauge and/or an average rainfall amount for an event may not be representative of reality. Accurately monitoring rainfall is relevant for flood prediction and hydrologic modelling (Arnaud et al., 2002; Singh, 1997). Since rainfall is the predominant form of recharge for the Northern Segment, it is important to monitor rainfall over the outcrop portion of the aquifer.

To begin capturing spatial and temporal rainfall variability over the Northern Segment, three Davis ISS (Integrated Sensor Suite) Vantage Pro2 weather stations (Davis Instruments, Hayward, California) were deployed to monitor precipitation. The positions of the three weather stations are shown in Figure 22. Precipitation amount is measured using a tipping bucket rain gauge that takes measurements in 0.01 inches. Other parameters monitored include temperature, wind speed, and barometric pressure. Weather conditions are logged once every 30 minutes. Weather station 1 was deployed at the Gault School of Archaeological Research near the county boundary between Bell and Williamson Counties on April 10, 2014. Weather station 2 was deployed on a private property in Salado on November 3, 2014; and the last weather station was deployed on a private property in the Hidden Springs housing development along FM 2843 on November 25, 2014. All weather stations have been in operation and collecting data for about a year, and are visited seasonally to download data and perform any necessary maintenance.

An advantage of the weather stations is their potential to ground-truth radar rainfall estimations, a product of the Next Generation Weather Radar (NEXRAD) program which utilizes Weather Surveillance Radar-1988 data and Precipitation Processing System (PPS) algorithms to estimate rainfall in a 4 km grid.

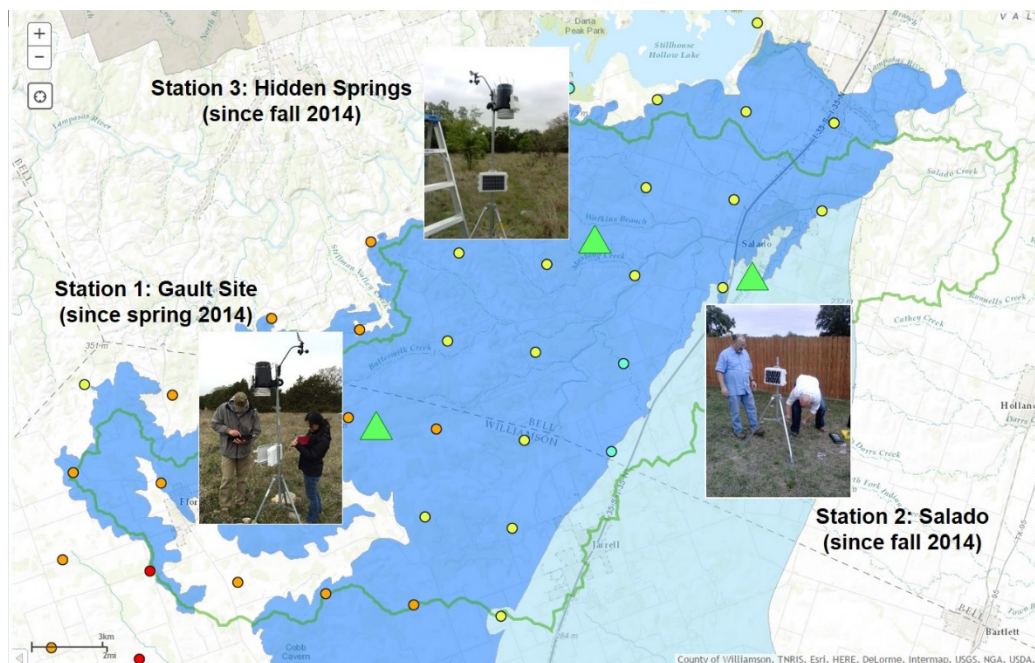
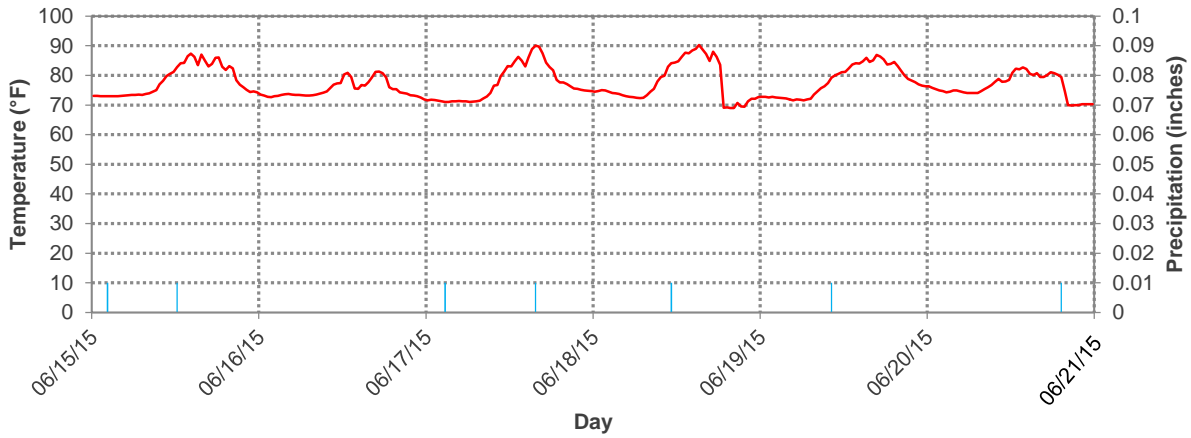


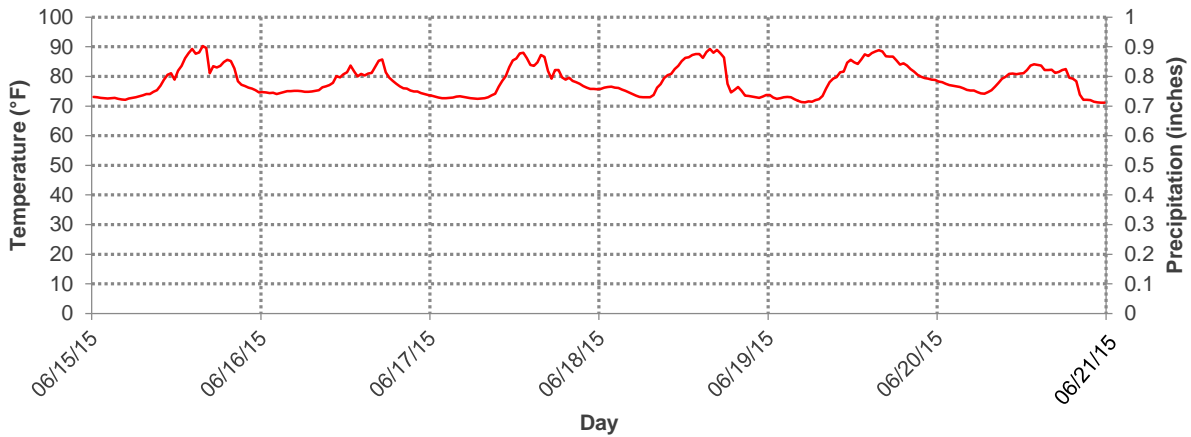
Figure 22: Location of where CUWCD weather stations are currently deployed. Locations were chosen to maximize coverage over the Northern Segment, particularly on the outcrop.

Temperature and precipitation data from June 15-20, 2015 are plotted in Figure 23 to illustrate the temporal, spatial, and intensity variability in rainfall over the Northern Segment; and highlight the importance of having more than one monitoring for these data. While temperature over the Northern Segment seems to by-and-large be

(A) Gault Site station



(B) Salado station



(C) Hidden Springs station

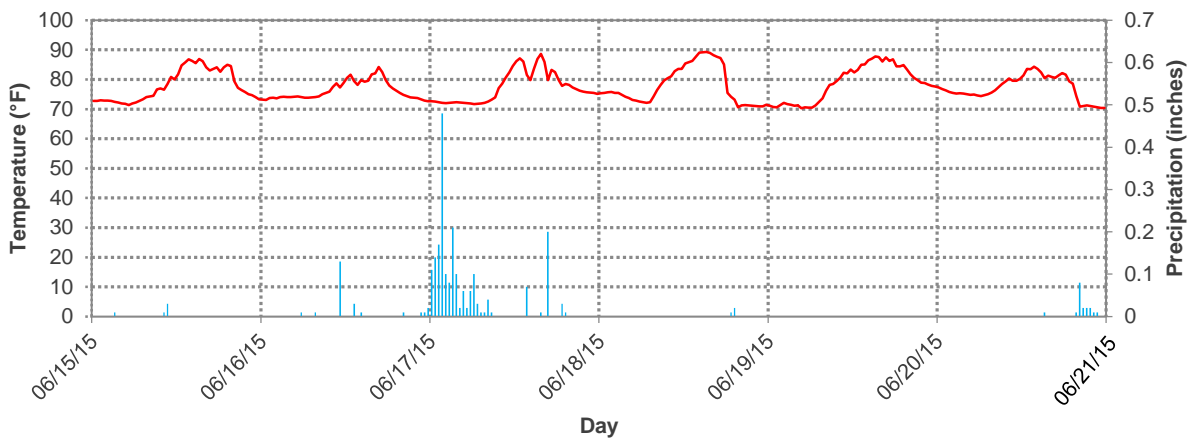


Figure 23: Example of data from CUWCD weather stations, June 15-20, 2015.

consistent in terms of amplitude (maximum and minimum temperatures ranging between 70-90°F) and pattern of daily fluctuation, rainfall over the Northern Segment is markedly different both in terms of amount and timing. For the rainfall that occurred over the period of June 15-20, the Gault Site weather station experienced small rains that were evenly spaced through time. Meanwhile, the Hidden Springs weather station experienced varying amounts of rain that peaked at 0.5 inches during the morning hours of June 17. No rainfall data is shown at the Salado weather station, but this is likely due to a faulty rain gauge. This rain gauge was replaced in fall 2015.

In addition to the weather stations, twelve 4-inch diameter rain gauges were obtained to gain additional ground-measurements of rainfall over the Northern Segment. Potential areas to deploy the rain gauges in the Northern Segment have been identified (Figure 24); Baylor will collaborate with CUWCD in spring and summer 2016 to finalize appropriate sites and set up the rain gauges. The rain gauges are standard CoCoRaHS (Community Collaborative Rain, Hail & Snow Network) gauges so that rainfall data can be uploaded to the National Weather Service CoCoRaHS national database.

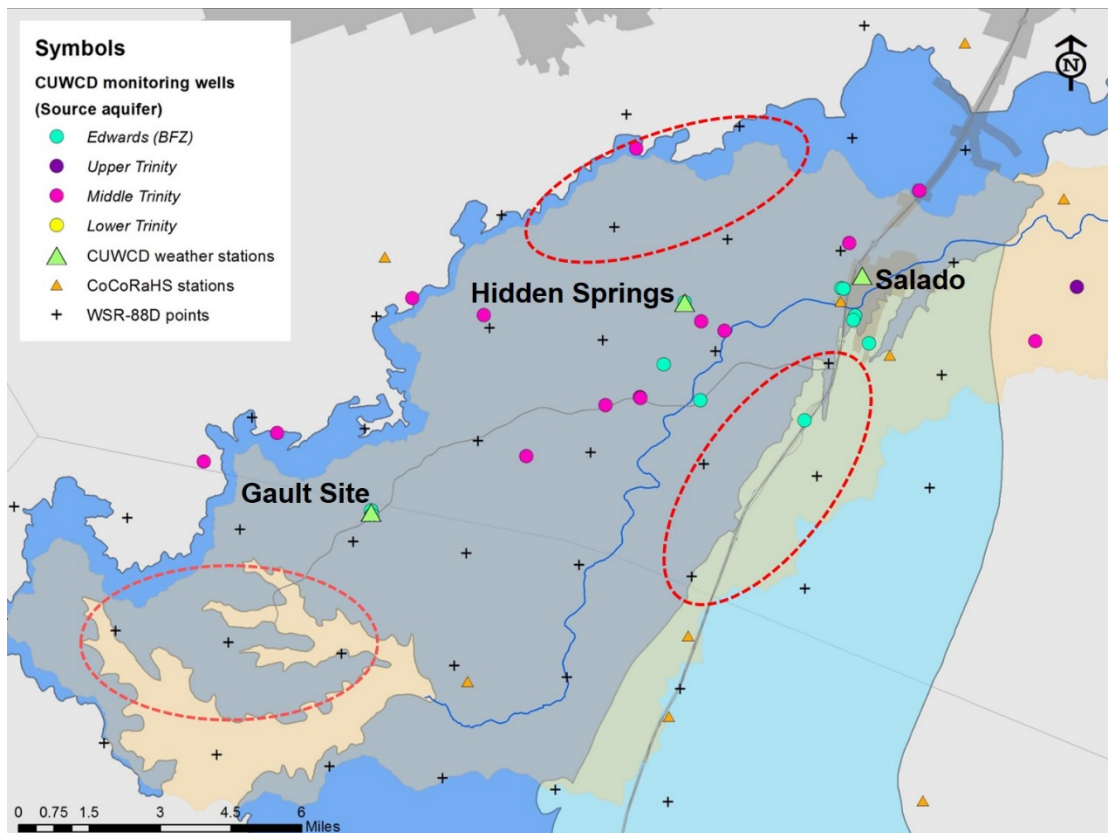


Figure 24: Map showing desirable areas to deploy twelve CoCoRaHS-standard rain gauges, indicated by red ovals. Baylor will work with CUWCD to choose the best sites.

### Multi-parameter monitoring

A data logger in a Northern Segment cave is being used to establish baseline levels of water level, temperature, and specific conductance; as well as to monitor response to precipitation events at this location in the Northern Segment. An OTT CTD data logger (OTT Hydromet, Loveland, Colorado) was installed in the cave well underneath the Stagecoach Inn in Salado Texas on May 23, 2013 (Figure 25A). Measurements of water level (feet above the sensor), temperature (°C), and specific conductance (μS) were taken at an interval of logging a reading every 5 minutes initially. Due to a connection problem, the data logger was removed on May 28<sup>th</sup>. It was re-installed on June

1, 2013. The recording interval is the same (one reading every 5 minutes). After a year of collecting data, we found the amount of data logged at 5-minute intervals to be unnecessarily large especially during periods of no rain. The logging interval was therefore adjusted to once every 10 minutes to conserve battery power and datalogger memory in May of 2014. A large recharge event on May 26, 2015 dislodged the datalogger (Figure 25B). It was therefore removed from the cave for the summer. A datalogger was re-deployed on October 6, 2015 to continue monitoring; an identical OTT CTD datalogger with a longer vented cord was used.

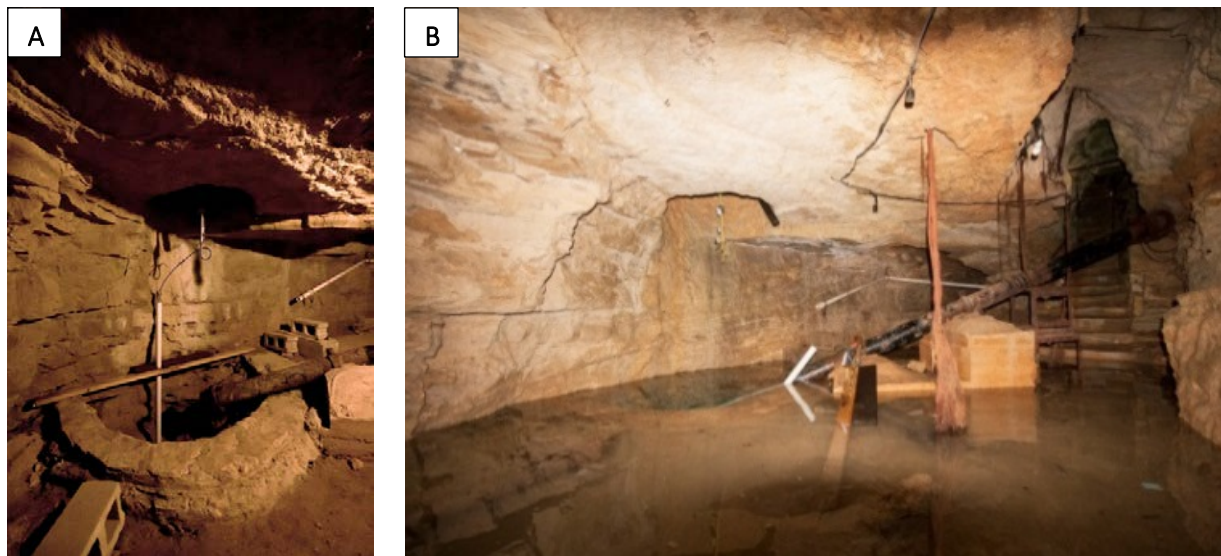


Figure 25: A multi-parameter datalogger has been deployed in the Stagecoach Inn cave well since May 2013 to collect data on water level, temperature, and specific conductance. (A) Setting of the datalogger in the cave well. The sensor is set inside a 2-inch PVC that is attached to a wooden board for stability, and the datalogger and connection port is suspended above the well to prevent submersion in a recharge event. (B) A large recharge event in May 2015 caused water level in the cave well to rise above the sides of the well and destabilized the datalogger, PVC, and wooden board.

Figure 26 shows water level, temperature, and specific conductance data respectively from May 1<sup>st</sup> until the 26<sup>th</sup> (2015), when the Stagecoach Inn Cave was flooded and destabilized the datalogger. Water level ranged from 3 ft. to 9.1 ft. above the sensor. Temperature values ranged between 69.40°F and 69.67°F with sharp, temporary drops in temperature that coincide with recharge events and the introduction of colder rain water to the aquifer. Specific conductance values ranged between 578  $\mu\text{S}/\text{cm}$  and 595  $\mu\text{S}/\text{cm}$  over the recording period. Following each rain, water level stabilized at a higher level, compared to water level at the beginning of May. Specific conductance seemed to peak with each rain event, and then stabilize at a lower level; this likely reflects the influence of more lower-specific conductance water producing a dilution effect. Although all the changes were slight in magnitude, they were the response one would expect from aquifer recharge in this season.

These data support several ideas about the Northern Segment at the Stagecoach Inn. A rise in water level before changes in chemistry indicate more remote recharge that changed head in the aquifer and “pushed old water out”. The small change in temperature and specific conductance indicate that the amount of recharge was small. Relatively rapid responses in temperature and specific conductance (i.e., less than four hours) indicate that groundwater velocities are fairly high, or that recharge is fairly close, or both.

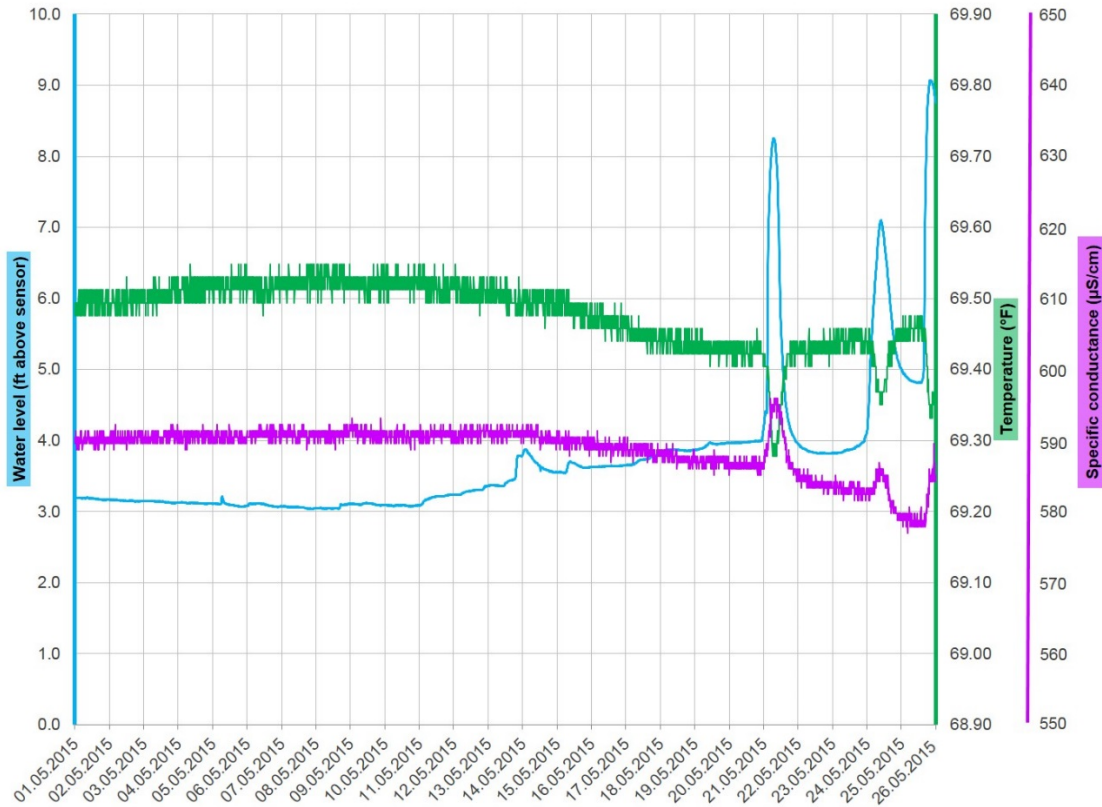


Figure 26: Hydrologic conditions at the Stagecoach Inn cave well in May 2015.

Four Solinst Levelloggers (Solinst Canada Ltd., Georgetown, Ontario) were also obtained through this contract. These dataloggers are able to monitor water level change, temperature, specific conductance. They are smaller, uncabled dataloggers that allow them to be easily hidden in spring openings and piezometers, which make them ideal for event-based deployments to monitor conditions at multiple springs over the course of a recharge event. Since they monitor the same parameters as the OTT CTD datalogger in the Stagecoach Inn Cave, the data can be correlated to gain further insight of aquifer response to recharge and spring connectivity.

An example of data collected using the Solinst Levelloggers is shown in Figure 27. By placing the Solinst Levelloggers in several spring outlets we were able to observe responses to recharge events with respect to specific conductance and temperature for multiple springs during the same event. The responses in Doc Benedict and Anderson springs shown in Figure 27 are similar but exhibit slight differences. The response patterns of decreased specific conductance as a result of the recharge event are similar in magnitude for both springs but the timing is distinctly different. Doc Benedict Spring appears to experience the decrease in SC slightly delayed after Anderson spring experiences this change. This is a little surprising because Doc Benedict Spring is closer to the cave well where connectivity was determined with the dye tracer test. The similarity of the responses again confirms the connectivity but the timing indicates Anderson Spring may be connected more directly with a separate fracture that is wider or straighter or perhaps Doc Benedict spring is connected with a fracture that branches off the main fracture going from the Stagecoach Inn Cave Well to Anderson Spring.

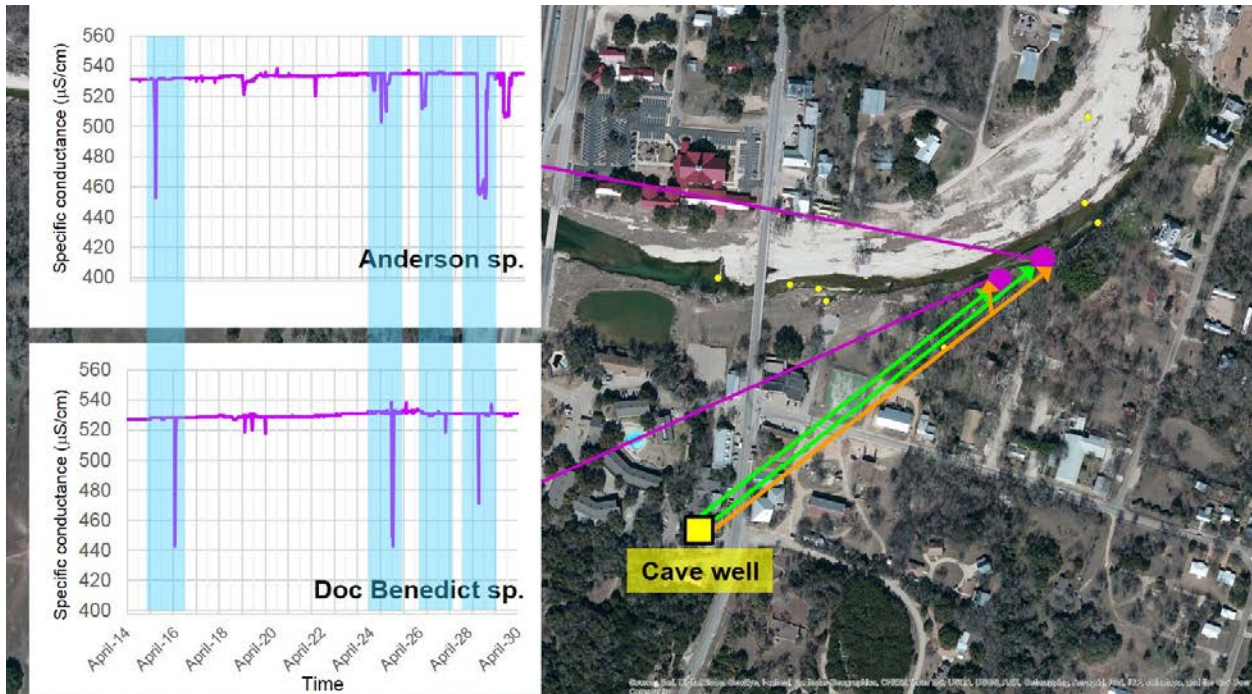


Figure 27: An example of specific conductance data from Anderson and Doc Benedict springs, collected using Solinst Levelloggers. The sampling frequency of the Levelloggers allows further interpretations to be made regarding spring connectivity and response to recharge.

### Flumes and weirs

Flumes and weirs are two devices that can be used with pressure transducer data loggers to record flow and evaluate response to recharge. We have constructed several weirs and purchased two flumes. We have tested the flumes and weirs on Side Spring and Little Bubbly (Figures 28 and 29). Recent flow increases indicate redesigning some of the weirs is necessary. The flumes work fine but need protection and maintenance. Negotiations and planning for long-term monitoring at two locations (Critchfield and Robertson) are progressing and placement for all the flumes and weirs is anticipated in Spring 2016. Two other locations have been proposed and several other locations are needed.



Figure 28: Cutthroat flume at Side Spring, Salado, Texas, September 3, 2015. Volumetric discharge was calculated at 240 gallons per minute but the conditions did not meet the criteria for acceptable accuracy.



Figure 29: Cutthroat flume at Little Bubbly Spring, Salado, Texas, September 3, 2015. Volumetric discharge was 13 gallons per minute with an estimated 5% leakage.

## Recharge Features Characterization

### LiDAR

LiDAR, which stands for light detection and ranging, is an active remote sensing technology that utilizes pulsed lasers to measure various properties of targets of interest. LiDAR technology measures the relative distance between the scanning laser (air- or ground-based) and a target, and generates a point cloud representing the target surface (Figure 30-1). Each point has an associated x, y, and z coordinate. Surfaces can be generated from the point cloud using interpolation methods, which can then be analyzed for lineaments.

For this project, the original objectives were to: identify lineations and depressions using LiDAR data, differentiate between geologic and anthropogenic lineations and depressions, and identify geologic lineations that are potential recharge features by combining LiDAR output with rain data. LiDAR data that was commissioned by Bell County was obtained from the Central Texas Council of Governments in fall 2013. A proof-of-concept exercise to manipulate the LiDAR data and see if karst features could be detected was completed in summer 2015 (Figure xx). The workflow for identifying karst features involves generating digital elevation models and shaded surfaces from the LiDAR point cloud (Figure 30-2), then isolating and extracting those pixels that may indicate karst features. In our proof-of-concept exercise, those pixels were those that represented the lowest points of elevation (Figure 30-3). At this point in time, pixel extraction is through manual selection, which is slow due to the density of data generated by LiDAR – only very small areas can be dealt with at a time. Moving forward, the goal is to: 1) Expand the workflow to other areas of interest, and 2) Attempt to automate the selection process for lineations and depressions.

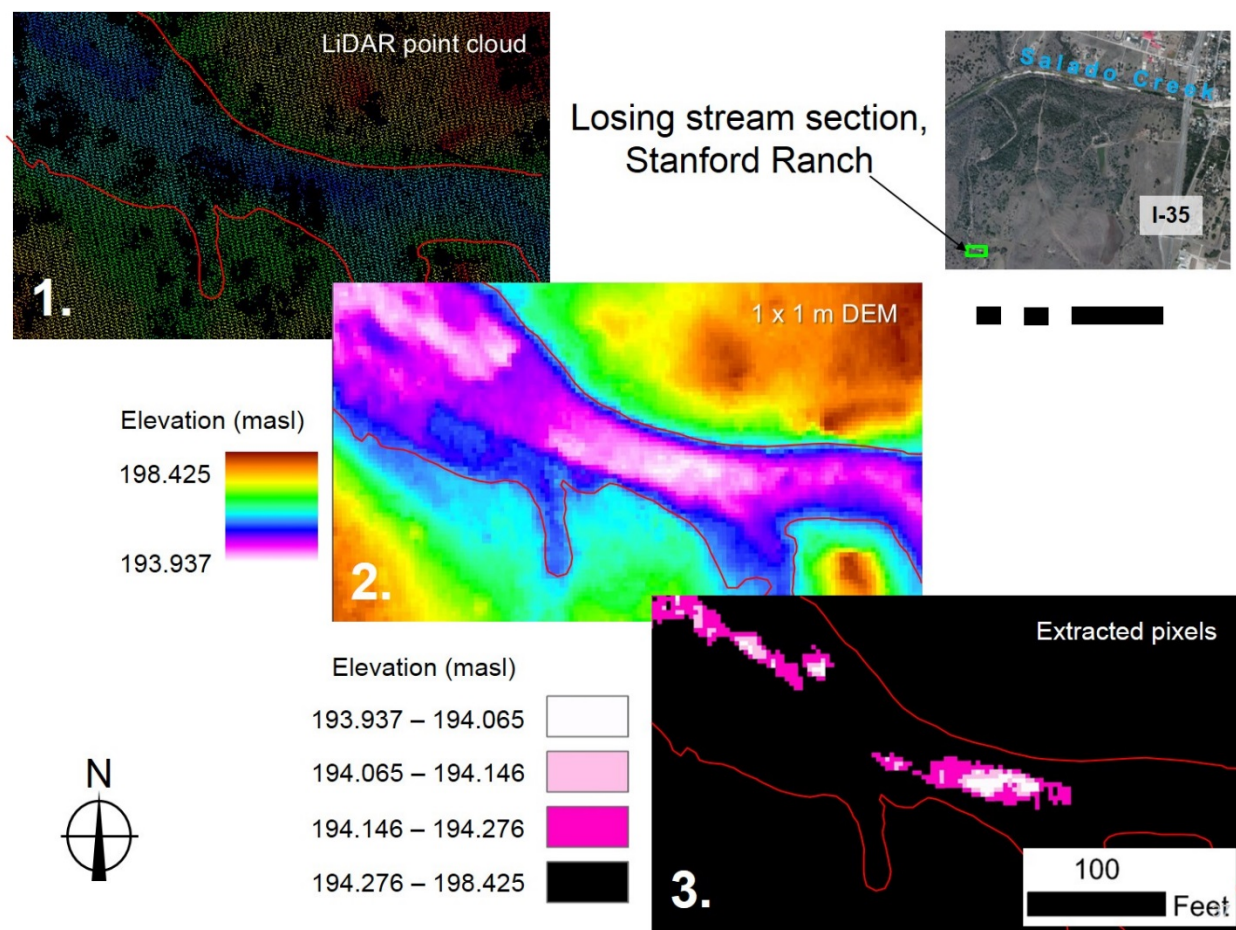


Figure 30: Overview of workflow for identifying karst features using LiDAR data.

## Summary and Project Conclusions

This project has produced new data and new insights into the groundwater flow systems of the Northern Segment of the Edwards Balcones Fault Zone aquifer in the Salado Springs area. The findings are summarized below.

A clear difference between spring water (groundwater) and stream water (Salado Creek) has been documented for Specific Conductance and natural Radon concentrations. The spring water definitely possesses a higher specific conductance than the stream water. The higher specific conductance in the spring water compared to the surface water indicates higher dissolved solids values from longer residence times within the aquifer which resulted from more dissolution of the aquifer material. The turbulence of the stream and biota of the stream water allows for ionic components to be removed through bio-geochemical processes thereby decreasing the total dissolved solids and the specific conductance. The spring water also has higher radon concentrations interpreted as equilibrium conditions between the water and the aquifer material compared to water in the stream which has been able to de-gas more rapidly.

The connectivity for the known spring discharge points in the downtown area of Salado, Texas, east of Interstate Highway 35 has been documented under two different flow conditions. Two dye tracer tests were conducted that showed dye from the Stagecoach Inn Cave Well flowed to all the springs even though the flow rates varied. The connectivity implies that mobile aquatic organisms, such as the Salado Salamander, may be able to move throughout the spring system and that the entire group of springs could be considered as one overall spring system.

Recharge responses to the aquifer as represented by changes in water level, specific conductance and temperature in the Stagecoach Inn Cave Well are rapid. Water levels responded within an hour for the large rainfall event May 24<sup>th</sup> and the water quality represented by specific conductance and temperature responded within a few hours. The rapid response is indicative of direct recharge paths and local recharge components.

Synoptic water level measurements indicated little change occurred between pre-drought and post-drought measurements in the Edwards aquifer even though the stream and spring flow had decreased. These data would indicate the aquifer was managed well and that current usage patterns appear sustainable under the current management.

New discharge points in the downtown area spring complex were documented during this study. A new discharge point named Rock Spring was documented on the North bank of Salado Creek in the downtown area across from Big Boiling Spring and the dye tracer tests indicated it was connected to the springs on the South side of the creek. A spring discharging from the south side of the creek through the alluvium just upstream from Big Boiling Spring discharge was also documented by dye as connected to the Stagecoach Inn Cave Well. This spring was named Side Spring and occurs near Little Bubbly Spring.

## Project Experience / Concluding Thoughts

The results of this research contributed to the USFWS listing the Salado Salamander as threatened rather than endangered. The results also indicate the water quantity in the Northern Segment of the Edwards Balcones Fault Zone aquifer is being managed in a sustainable way in Bell County.

The results of the dye studies showing connectivity among the springs in the downtown Salado area indicate the USGS gage that is placed downstream of the springs can be used appropriately to monitor the water quantity in the spring system.

The application of data loggers to monitor water levels and water quality indicators appears feasible. A monitoring system using multi-parameter data loggers and periodic water sampling should be considered as development in the area continues. It is important to establish baseline parameters that can be used to assess changes that may occur over time.

## References

- Arnaud, P., C. Bouvier, L. Cisneros, and R. Dominguez, 2002. Influence of rainfall spatial variability of flood prediction. *Journal of Hydrology*, 260(1-4): 216-230.
- Burnett, W.C., R.N. Peterson, I.R. Santos, and R.W. Hicks, 2010. Use of automated radon measurements for rapid assessment of groundwater flow into Florida streams. *Journal of Hydrology*, 380(2010): 298-304.
- Cook, P.G., G. Favreau, J.C. Dighton, and S. Tickrell, 2003. Determining natural groundwater influx to a tropical river using radon, chlorofluorocarbons and ionic environmental tracers. *Journal of hydrology*, 277(1-2): 74-88.
- Department of the Interior, Fish and Wildlife Service, 2014, Endangered and Threatened Wildlife and Plants; Determination of Threatened Species Status for the Georgetown Salamander and Salado Salamander Throughout Their Ranges; Final Rule. *Federal Register*, 79(36): 59 pp.
- Durrige Company, Inc. 2014a. RAD7 Radon Detector User Manual. Durrige Company, Inc., Billerica, MA. 79 pp.
- Durrige Company, Inc. 2014b. RAD H<sub>2</sub>O User Manual. Durrige Company, Inc., Billerica, MA. 31 pp.
- Ellins, K.K., A. Roman-Mas, and R. Lee, 1990, Using <sup>222</sup>Rn to examine groundwater/surface discharge interaction in the Rio Grande de Manati, Puerto Rico. *Journal of Hydrology*, 114(1-4):319-341.
- Hoehn E., H.R. Von Gunten, F. Stauffer, T. Dracos, 1992, Radon-222 as a groundwater tracer: a laboratory study. *Environment Science and Technology*, 26:734-738.
- Lee, R.W. and E.F. Hollyday, 1991, Use of radon measurements in Carters Creek, Maury County, Tennessee, to determine location and magnitude of groundwater seepage. *In* *Field Studies of Radon in Rocks, Soils, and Water*. L.C.S. Gundersen and R.B. Wanty (eds.), pp.237-242. C.K. Smoley, Boca Raton, Florida.
- Mahler, B.J., P.C. Bennet, M. Zimmerman, 1998, Lanthanide-labeled clay: a new method for tracing sediment transport in karst. *Ground Water*, 36(5): 835-843.
- Michaud, J.P., 1991. *A Citizens' Guide to Understanding and Monitoring Lakes and Streams*. Washington State Department of Ecology, Olympia, WA.
- Michel, J., 1987, Sources *In* *Environmental Radon*, C.R. Cothorn and J.E. Smith, Jr. (Eds.). Plenum Press, New York, 363 pp.
- Neupane, R.P., J.D. White, P.M. Allen, and S.I. Dworkin, 2014, A snapshot comparison of environmental tracers for estimating groundwater contribution to recession flow in a mountain stream. *Hydrological Processes*, *in press*.
- Singh, V.P., 1997, Effect of spatial and temporal variability in rainfall and watershed characteristics on stream flow hydrograph. *Hydrological Processes*, 11: 1679-1669.
- Stellato, L., F. Terrasi, F. Marzaioli, M. Belli, U. Sansone, and F. Celico, 2013, Is <sup>222</sup>Rn a suitable tracer of stream-groundwater interactions? A case study in central Italy. *Applied Geochemistry*, 32: 108-117.
- Wojdyr, M. 2010. Fityk: a general-purpose peak fitting program. *Journal of Applied Crystallography*, 2010 (43): 1126-1128.

Appendix  
Radon-222 concentrations for Salado Springs

Table A1. Radon-222 content in groundwater and surface water at Salado Springs.

Site	March 2014	May 2015	July 2015	September 2015
Stagecoach Inn Cave Well	160.17	212.15	230.67	218.62
Robertson Spring	N/M	408.90	303.59	363.13
Main Street Bridge	61.52	N/M	124.87	167.60
Side Spring	192.12	185.08	222.42	236.88
Little Bubbly Spring	N/F	252.42	238.63	N/F
Big Boiling Spring	178.35	252.62	217.39	235.88
Critchfield Spring	167.44	310.64	238.27	244.69
Doc Benedict Spring	249.87	306.26	262.14	276.71
Anderson Spring	248.89	253.28	235.65	222.59
Rock Spring (North bank)	204.28	133.67	252.24	298.28

**Phase II**

# A Follow-up Investigation into the Recharge Pathways and Mechanisms in the Northern Segment of the Edwards Aquifer, Bell County, Texas



*A research report submitted to the Clearwater Underground Water Conservation District, Bell County, Texas*

Final Report, December 2016

Submitted By:

Stephanie S. Wong, graduate student

Dr. Joe C. Yelderman Jr., Ph.D., P.G.

Baylor University, Department of Geosciences



## Executive Summary

Efforts to learn more about the hydrologic processes in the Northern Segment of the Edwards Balcones Fault Zone aquifer, specifically in the Salado Springs complex, revealed several important discoveries that will aid water management and direct future research needs. These discoveries are listed below with interpretations regarding their potential significance.

1. Progress using LiDAR data to detect recharge features has been difficult and time consuming but is progressing slowly. A work-flow for identifying potential karst features using a mixture of manual and semi-automatic processes has been developed for the study area. The LiDAR data still look promising for determining areas of important recharge potential. Some potential fractures have been identified for further analysis.
2. Data collected with a multi-parameter datalogger in the Stagecoach Inn Cave well indicated rapid groundwater responses to large rainfall events. The data also show slight water quality changes. The responses to recharge captured by the datalogger provide important timing information to aid in the development of future monitoring strategies.
  - a. Nitrogen data from field and laboratory analysis showed values that are interpreted to be slightly above expected background levels but no nitrate values were observed to be over the drinking water limit.
  - b. The nitrogen data warrant further investigation and monitoring.
3. Data collected with a Solinst hand-held meter along cross-sections of Salado Creek and adjacent springs show patterns helpful in understanding groundwater/surface-water interactions and potential areas of salamander habitat.
  - a. Specific conductance (SC) and temperature (T) measurements in cross sections of Big Boiling Spring as well as upstream and downstream of the confluence between Big Boiling Spring discharge and Salado Creek confirm the mixing patterns of groundwater and surface water from Big Boiling Spring.
  - b. The cross section data are important to quantify groundwater/surface water mixing, aid in habitat assessments, and aid in water sample location selection.
4. Thermography using a handheld FLIR camera has helped delineate potential salamander habitat in the springs and spring runs at several springs. The thermography also has better delineated the exact areas of groundwater interaction with surface water and confirmed previous cross section studies.
5. Spring Inventory protocol (SIP) and Spring Ecosystem Assessment Protocol (SEAP) were used to categorize the springs in the downtown area with internationally published protocols for comparisons of baseline and possibly future management conditions.

# Contents

Executive Summary .....	i
Contents .....	ii
List of Figures .....	iii
Project Overview .....	1
- Project area	
Recharge features characterization.....	3
Groundwater monitoring.....	7
- Multi-parameter monitoring	
- Multi-parameter monitoring data	
- Nitrate monitoring	
Groundwater – surface water interaction.....	15
- Stream profiling	
- Thermography (FLIR)	
Springs assessment.....	25
- SIP and SEAP	
Summary & Project Conclusions .....	30
Recommendations .....	31
References .....	32
Appendices .....	33
- Appendix A: Dissolved nitrate /nitrite concentrations for Salado Springs	
- Appendix B: Springs Assessment: SIP and SEAP datasheets	
- Appendix C: Sunpath diagrams for Salado Springs	

## List of Figures

Figure 1. This study was conducted in Northern Segment of the Edwards Balcones Fault Zone aquifer in Bell County (modified from Jones, 2003).....	2
Figure 2. Location of springs in the Salado Springs complex.....	2
Figure 3. Overview of LiDAR data collection to produce elevation surfaces which can then be used for analysis.....	3
Figure 4. Overview of workflow for identifying karst features using LiDAR data.....	4
Figure 5. Map of depressions at Robertson Ranch.....	5
Figure 6. Aspect map of Robertson Ranch, with manually-determined lineations.....	5
Figure 7. Rose diagram plotted using GeoRose 0.5.1.....	6
Figure 8. A major lineation extrapolated from Robertson Ranch matches the field-determined orientation of a lineation observed at Big Boiling springs.....	6
Figure 9. A multi-parameter datalogger has been deployed in the Stagecoach Inn cave well since May 2013 to collect data on water level, temperature, and specific conductance.....	7
Figure 10. Hydrologic conditions at the Stagecoach Inn cave well from June 2013 to September 2016.....	9
Figure 11. Hydrologic conditions at the Stagecoach Inn cave well in May 2015.....	10
Figure 12. Nitrate trend data collected by the Troll 9500 sonde from October 7 to November 30, 2015 at the Stagecoach Inn Cave well.....	11
Figure 13. Map of nitrate sampling locations around downtown Salado.....	12
Figure 14. Nitrate concentrations at Salado Springs over the Labor Day long weekend.....	13
Figure 15. Nitrate trend data collected by the Troll 9500 sonde and grab samples from September 1-21, 2016 at the Stagecoach Inn Cave well.....	14
Figure 16. Diagram of downtown Salado Creek showing key features.....	15
Figure 17. Discharge, specific conductance and temperature measurements at cross-section 1, located in the spring flow of Big Boiling Spring.....	16
Figure 18. Discharge, specific conductance and temperature measurements at cross-section 2, located in the natural channel of Salado Creek.....	17
Figure 19. Discharge, specific conductance and temperature measurements at cross-section 3, located in the natural channel of Salado Creek, downstream of the confluence with Big Boiling Spring.....	18
Figure 20. Abrupt contrast between clear groundwater flowing from Big Boiling Springs and sediment-laden surface water in Salado Creek after a small rainfall and during low spring flow conditions.....	20
Figure 21. No contrast between clear groundwater flowing from Big Boiling Springs into clear baseflow in Salado Creek.....	20
Figure 22. FLIR E63900 handheld infrared camera.....	23
Figure 23. Side Spring looking northward from the south bank of Salado Creek in downtown Salado, Texas.....	23
Figure 24. Temperature profiles in Salado creek and Big Boiling Spring, April 6, 2016.....	22
Figure 25. Specific conductance profile at section 3 April 6, 2016.....	22
Figure 26. FLIR infrared image of profile Section 3 downstream from Big Boiling Spring showing the warmer temperatures associated with the groundwater discharge of Big Boiling Spring along the REW edge of the creek.....	23

Figure 27. <i>Ludwigia</i> growing near the REW bank of Salado Creek downstream from the spring discharge of Big Boiling Spring, April 6, 2016.....	23
Figure 28. Rheocrene spring (Springer and Stevens, 2009).....	26
Figure 29. Limnocrene spring (Springer and Stevens, 2009).....	26
Figure 30. The Solar Pathfinder™ .....	27
Figure 31. Robertson Spring has characteristics of both a rheocrene spring as well as a limnocrene spring.....	27
Figure 32. Big Boiling Spring has characteristics of a rheocrene spring and a limnocrene spring.....	28
Figure 33. Little Bubbly Spring is best classified as a rheocrene spring.....	28
Figure 34. Side Spring is best classified as a rheocrene spring.....	28
Figure 35. Critchfield Spring has characteristics of both a limnocrene spring as well as a rheocrene spring.....	29
Figure 36. Doc Benedict Spring is best classified as a limnocrene spring.....	29
Figure 37. Anderson Spring is best classified as a limnocrene spring.....	29

## Project Overview

A body of research was undertaken by Baylor University (“Baylor”), in collaboration with the Clearwater Underground Water Conservation District (CUWCD), to gain a deeper understanding of the Northern Segment of the Edwards Balcones Fault Zone (BFZ) Aquifer (the Northern Segment) for the purposes of providing insight for groundwater resource management and supporting collaboration between the district and community stakeholders. Phase 1 of this research began in 2013 and focused on instrumentation, field tests, and feasibility studies to help build knowledge of how much recharge occurs and the pathways that recharge takes to the aquifer. Over the course of phase 1 research, Baylor and CUWCD realized that further efforts were necessary to continue data collection and interpretation. Phase 2 research, which spanned spring and summer 2016, focused on continuing monitoring activities while adding new monitoring parameters, refining field tests and samples, as well as analysis and interpretation of data gathered during phase 1 research. After a brief description of the study area, this report is divided into sections regarding recharge features characterization, groundwater monitoring, groundwater-surface water interaction, and springs assessment. Each section describes the rationale for a given work, methods and instrumentation employed, and results.

Although this report serves as a final summary of the research efforts completed under the 2016 contract between Baylor and CUWCD, there is still much to learn about the Northern Segment system. Collaborative efforts, monitoring, and data gathering are on-going.

### Project area

This body of research was conducted in the outcrop portion of the Northern Segment in Bell County (Figure 1). Focus was placed on the Salado Springs complex in downtown Salado due to their importance as critical habitat for the Salado salamander, their use as a measure of the CUWCD’s DFC, and ease of access (Figure 2).

There are three formations that comprise the Northern Segment of the Edwards Balcones Fault Zone aquifer. They are in ascending order: the Comanche Peak Formation, the Edwards Formation and the Georgetown Formation. All of these units are sedimentary rocks, Cretaceous in age, and comprised mainly of carbonate (limestones). The Edwards and Comanche Peak formations are part of the Fredricksburg Group and the Georgetown is part of the Washita Group. They are fairly well connected hydraulically and considered as one hydrostratigraphic unit referred to as the Edwards aquifer; specifically the Northern Segment of the Edwards Balcones Fault Zone aquifer. The underlying confining unit is the uppermost member of the Walnut formation, the Keys Valley Marl, which is a carbonaceous clay. The overlying confining unit is the Del Rio Formation, a carbonaceous clay-rich unit that is often referred to as the Del Rio Clay (sometimes referred to as the Grayson Formation). Upper Cretaceous units overlying the Del Rio Formation and cropping out in the Salado Creek basin include the Buda Formation, Eagle Ford Group and the Austin Chalk. None of these are considered aquifers in this area. (Jones, 2003)

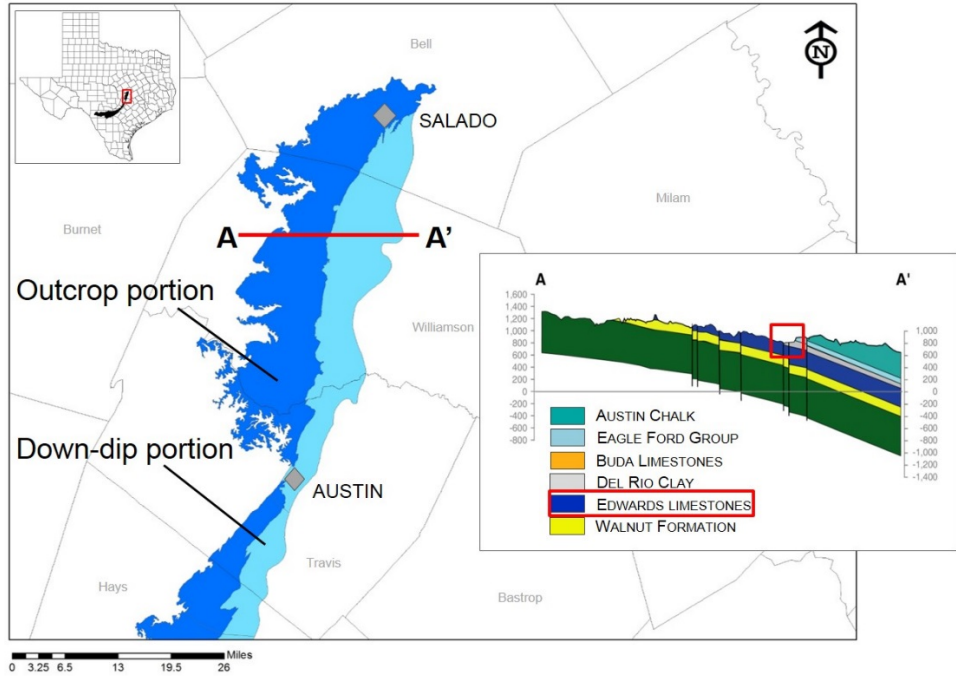


Figure 1. This study was conducted in Northern Segment of the Edwards Balcones Fault Zone aquifer in Bell County (modified from Jones, 2003).

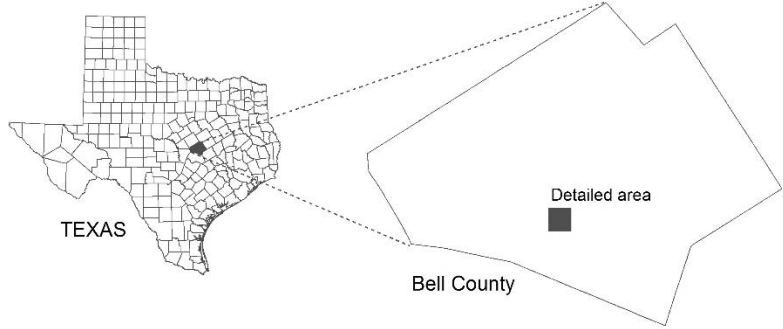


Figure 2. Location of springs in the Salado Springs complex, which was a focus area for this body of research due to ease of access and the springs' importance as a management parameter for CUWCD.

## Recharge Features Characterization

### Lidar

Lidar, which stands for *light detection and ranging*, is an active remote sensing technology that utilizes pulsed lasers to measure various properties of targets of interest. Lidar technology measures the relative distance between the scanning laser (air- or ground-based) and a target, and generates a point cloud representing the target surface (Figure 3-1; 3-2). Each point has an associated x, y, and z coordinate. Surfaces can be generated from the point cloud using interpolation methods, which can then be analyzed for karst features (Figure 3-3).

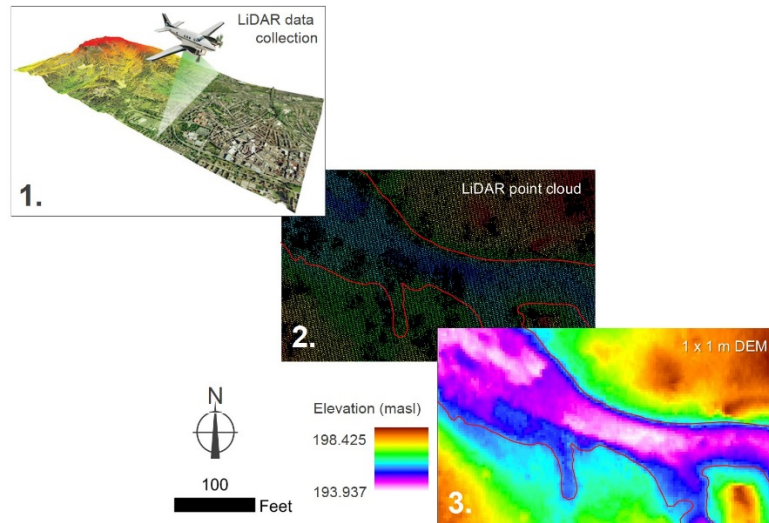


Figure 3. Overview of Lidar data collection to produce elevation surfaces which can then be used for analysis.

### *Approach*

For this project, the original objectives were to: identify lineations and depressions using Lidar data, differentiate between geologic and anthropogenic lineations and depressions, and identify geologic lineations that are potential recharge features. Lidar data and 1 x 1 m DEMs were obtained from the Central Texas Council of Governments (CTCOG) in fall 2013. Bell County Lidar data were acquired through a partnership between CTCOG and TNRIS during spring of 2011. A Leica ALS50 phase II+ and a Leica ALS60 Lidar sensor (Gonzales Block) were used to collect multiple return data in the x, y, and z, dimensions; as well as intensity data (TNRIS, 2017). In our proof-of-concept exercise (phase 1), the workflow for identifying karst features involved manually isolating and extracting pixels that may indicate karst features, which were represented by pixels of lowest elevation. This process was slow due to the density of data generated by LiDAR, and only very small areas could be dealt with at a time.

Through consultation with colleagues and published literature, separate workflows were developed to identify depressions and lineations that allowed dealing with more LiDAR data at once (Figure 4). Both the depressions workflow and lineations workflow utilize ArcGIS capabilities and tools. To identify depressions, the 1 x 1 m DEM was first filled using the Fill tool. DEM datasets normally contain sinks which arise due to data resolution errors or rounding elevations to the nearest integer value (ESRI, 2017a). However in glacial or karst areas, data sinks may represent actual depressions in the landscape. Processing the DEM using the Fill tool created a continuous surface with no sinks. The original DEM and the filled DEM were subtracted from each other using the Raster Calculator, creating a difference surface. Pixels that were less than 1 m (3.28 ft) difference were filtered out since the spatial resolution of the Lidar DEM is 1 m. The surface after filtering represents depressions identified through this semi-

automatic workflow. A similar workflow was described by Gritzner (2006) to identify wetland depressions in Devils Lake Basin, North Dakota.

To identify lineations, a map of aspect was created from the original 1 x 1 m DEM. Aspect is the slope direction. The value of every cell in an aspect map is the maximum rate of change (or slope) for that cell relative to its neighbors, range from 0-360° as in a full circle (where 0° and 360° equal due north, 90° equals due east, 180° equals due south, and 270° equals due west), and indicates the compass direction that the surface faces at that location (ESRI, 2017b). Since most lineations in the area of interest are associated with the Balcones Fault Zone which runs NE-SW, developing an aspect map helped highlight lineations that were present. Additionally, aspect helped to differentiate geologic lineations which would mostly also be oriented NE-SW from anthropogenic lineations such as fence lines, unpaved paths, and roads. Lineations were identified and digitized manually. Comparison with aerial imagery aided in differentiating anthropogenic versus geologic lineations. Both depression and lineation workflows were applied to the Robertson Plantation property.

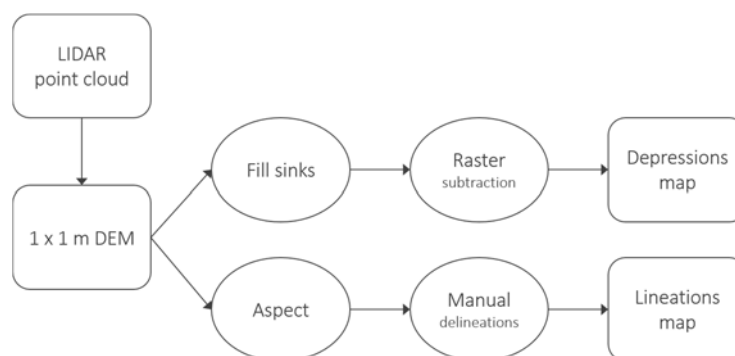


Figure 4. Overview of workflow for identifying karst features using LiDAR data. After a feasibility test in phase 1 research, separate workflows were developed to identify lineations and depressions.

#### *Results and Discussion*

The final depressions map is presented in Figure 5. Two main depression features are immediately apparent: the constructed pond towards the middle of the Robertson property, ranging from about 3 to 12 ft depth; and another depression near the eastern property line, ranging from about 3 to 9 ft depth. The spring run for Robertson Springs also shows up as a depression in the northeastern corner of the property.

The final lineations map is presented in Figure 6. Measured lineation orientation ranged from 4 – 359°, with an average orientation of 77°. When the orientations are summarized using a rose diagram (Figure 7), most lineations are oriented southwest-northeast, which agrees with the trend of the Balcones Fault Zone. The measured orientations also correlated with field observations. A lineation extending past the eastern property line was extrapolated to downtown Salado. By combining Lidar and aerial imagery, the Robertson lineation appeared to line up with a lineation making up the north edge of the Big Boiling Spring run (Figure 8). The Robertson lineation, measured using ArcGIS, is 236°. The lineation measured in the field at Big Boiling Spring is 220°. The length of apparent lineations on the Robertson property ranged from 69 – 2203 ft, with an average length of 353 ft.

Blackwell and Wells (1999) noted that resampling 1x1 m, bare-earth Lidar data to 5x5 m and 10x10 m cells allowed Lidar data to be more easily-processed. Resampling was not done on Bell County Lidar data because the karst features of interest would have been lost in a coarser-resolution dataset. The limitation of not resampling was that the volume of data was large, limiting the amount of data that could be processed at any given time and resulting in a smaller study area. While the 1x1 m resolution data confirmed the presence of the largest depressions and lineations on the Robertson property, the ability to identify smaller features, which may be important from a recharge perspective, is still limited.

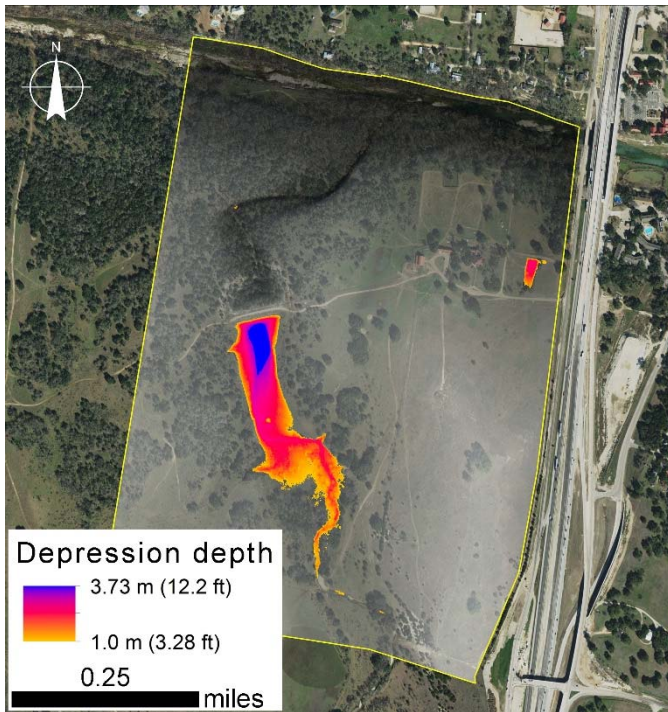


Figure 5. Map of depressions at Robertson Ranch, produced using semi-automatic sink determination.

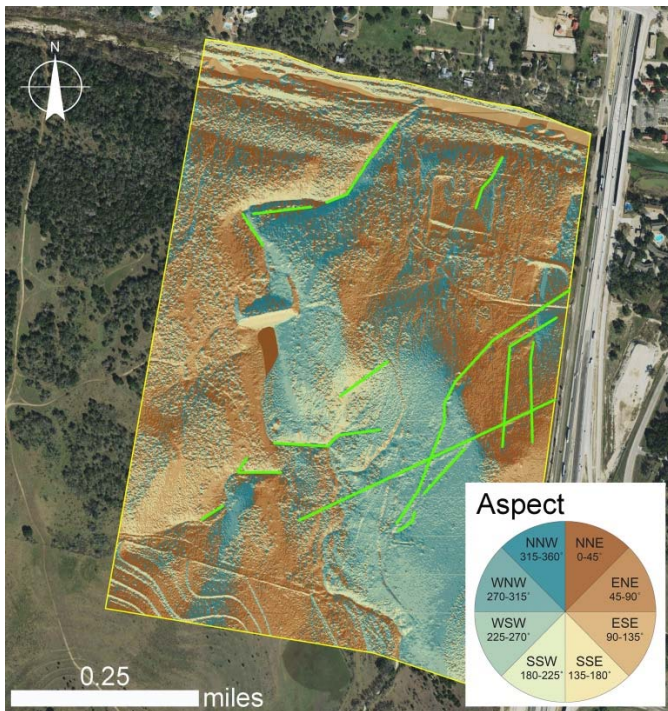


Figure 6. Aspect map of Robertson Ranch, with manually-determined lineations shown in green.

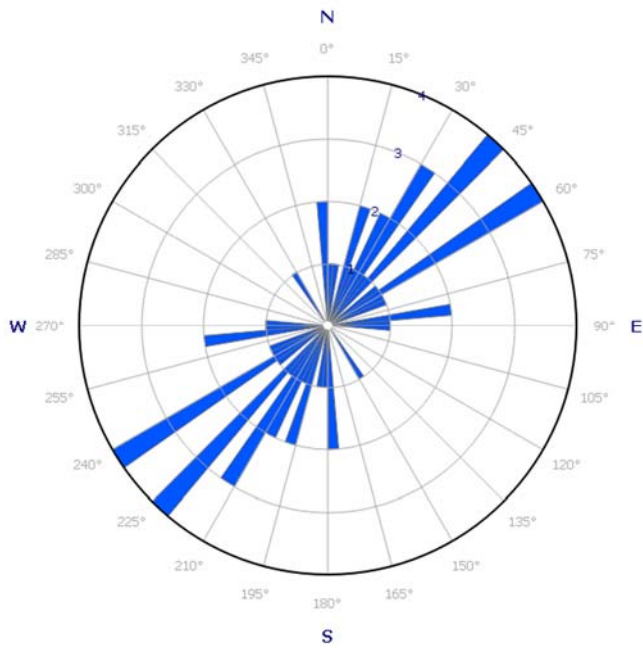


Figure 7. Rose diagram plotted using GeoRose 0.5.1 (Yong Technology Inc., 2015).

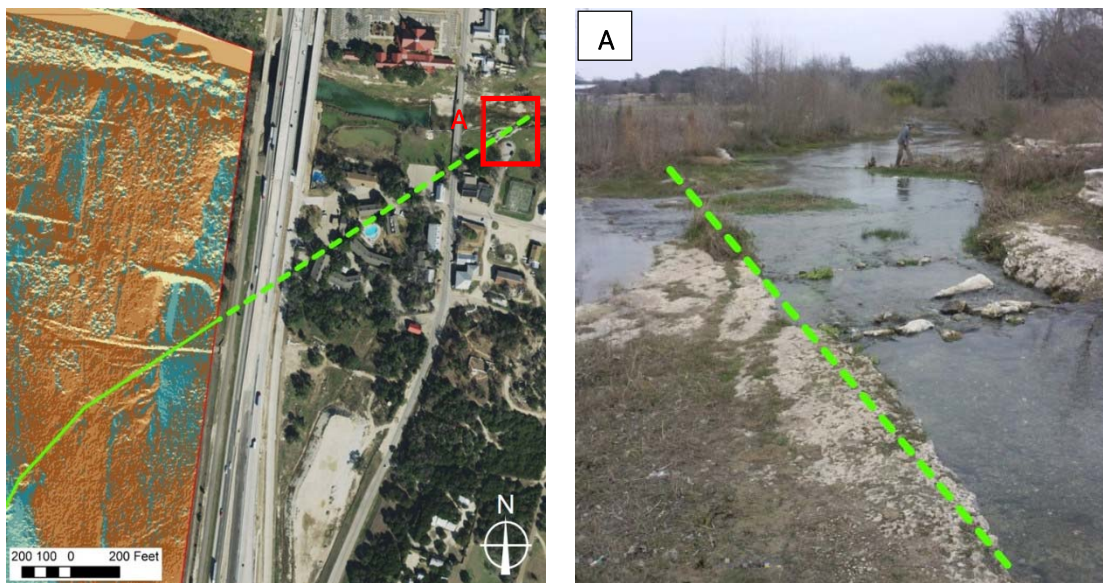


Figure 8. A major lineation extrapolated from Robertson Ranch, *left*, matches the field-determined orientation of a lineation observed at Big Boiling springs (A), *right*. Although the images were taken from different angles, the lineation from Robertson Ranch measured from ArcGIS is 236 degrees and the fracture lineation at Big Boiling Springs measured in the field with a Brunton Compass was 220 degrees. These orientations are closely aligned and fall in the range of the strongest trends on the Rose diagram.

## Groundwater Monitoring

### Multi-parameter monitoring

A data logger in a Northern Segment cave is being used to establish baseline levels of water level, temperature, and specific conductance; as well as to monitor response to precipitation events at this location in the Northern Segment. An OTT CTD datalogger (OTT Hydromet, Loveland, Colorado) was installed in the cave well underneath the Stagecoach Inn in Salado Texas on May 23, 2013. Measurements of water level (feet above the sensor), temperature ( $^{\circ}\text{C}$ ), and specific conductance ( $\mu\text{S}/\text{cm}$ ) were taken at an initial interval of logging a reading every 5 minutes, then adjusted to once every 10 minutes to conserve battery power and datalogger memory in May 2014. The datalogger was replaced with an identical OTT CTD datalogger with a longer vented cord on October 6, 2015.

A second multi-parameter sonde was installed on October 6, 2015 as a test for monitoring additional chemical parameters (Figure 9). An In-Situ Troll 9500 sonde and datalogger (In-Situ, Fort Collins, Colorado) was installed alongside the OTT CTD datalogger that has the ability to monitor pH, specific conductance ( $\mu\text{S}/\text{cm}$ ), dissolved oxygen ( $\text{mg}/\text{L}$  or % saturation), and dissolved nitrate ( $\text{ppm}$ ). Of particular interest is the change in groundwater nitrate over time. During a routine battery replacement on February 11, 2016, water seeped into the datalogger casing, causing the Troll 9500 to cease functioning. The entire unit was rebuilt and recalibrated over the following months, and re-deployed on September 1, 2016.

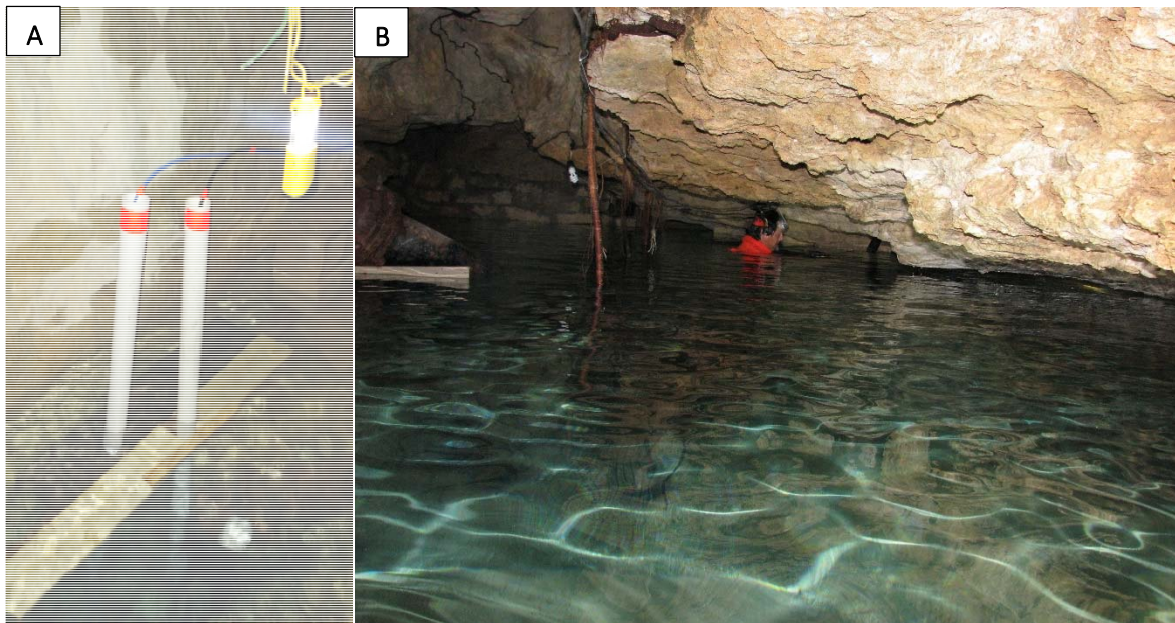


Figure 9. A multi-parameter datalogger has been deployed in the Stagecoach Inn cave well since May 2013 to collect data on water level, temperature, and specific conductance. (A) Setting of the OTT CTD (right side, black cord) and In-Situ Troll 9500 (left side, blue cord) sondes in the cave well. The sensors are set inside 2-inch PVC slotted near the bottom and attached to a wooden board for stability, with cinder blocks on top of the board to prevent movement during high water levels. The sondes are located in the lower portion of the PVC pipe which is screened. The dataloggers and connection ports are run along the cave wall to the foot of the stairs for easier access. (B) A large recharge event in May 2016 caused flooding in the cave; photo is of FWS biologist Pete Diaz retrieving a water sampler from the bottom of the cave well during high water levels.

## Multi-parameter monitoring data

### *Long-term trends*

Figure 10 shows daily water level, specific conductance, and temperature data from June 1<sup>st</sup> 2013 until September 21<sup>st</sup> 2016, giving an overview of hydrologic conditions in the Northern Segment at SCI cave over the past three years. Two notable gaps exist in the monitoring data collected by the OTT CTD datalogger. The first data gap occurs in May 2014 and was due to a loss of battery power. The datalogger was decommissioned on May 21<sup>st</sup>, brought back to Baylor University for routine maintenance and battery replacement, and re-deployed on June 1, 2014. The second data gap occurred in May 2015, when a large recharge event on May 26, 2015 dislodged the datalogger. It was therefore removed from the cave for the summer. An identical datalogger with a longer vented cable was re-deployed on October 6, 2015 to continue monitoring. Data collection has been consistent since then.

Water level ranged from 570.40 ft to 580.68 ft elevation, with an average of 573.81 ft elevation, or 19.44 ft below ground surface. Water levels increased after rains in late 2013 but returned to previous levels by late 2014. Since that time, rainfall and subsequent recharge have had a cumulative effect and the aquifer level has increased after rainfall events; following each rain, water level “stabilized” at a higher level compared to the previous water level. Over the recording period, overall water level increased; the first water elevation reading on June 2<sup>nd</sup>, 2013 was 571.64 ft and the last reading on September 21<sup>st</sup>, 2016 was 576.72 ft. Addition of water to the aquifer through recharge events are evident in peak responses in the hydrograph. The magnitude of response to recharge events appear to be greater in 2015-2016 than previously in the recording period, evident by sharper peaks in the hydrograph. Temperature values over the recording period remained fairly constant, ranging between 68.90°F and 69.93°F. The average temperature was 69.56°F. Sharp, temporary changes in temperature coincided with recharge events and the introduction of rain water that reflect the ambient surface air temperature (that is, colder rain water during winter months and warmer rain water during summer months). Specific conductance values, which are related to the concentration of ions dissolved in water, ranged between 544  $\mu\text{S}/\text{cm}$  and 606  $\mu\text{S}/\text{cm}$  over the recording period, with an average value of 580  $\mu\text{S}/\text{cm}$ . Sharp drops in specific conductance were observed shortly after each rain event, and then increased as water levels receded. The drops may reflect introduction of lower-specific conductance rainwater, producing a dilution effect. Inversely, as water level declines over a dry season, specific conductance increases.

### *High-resolution data*

Examining high-resolution monitoring data collected at 15-minute intervals allows a closer look at recharge response of the Northern Segment at SCI cave. An example of such data is provided for May 2015 (Figure 11). Aquifer response to recharge appears to be a function of both the amount of rainfall, antecedent moisture and possibly the location within the basin. By coupling data logged in the SCI cave well with precipitation data, smaller rains were observed to have little or no effect on temperature and specific conductance (Figure 11; contrast locations *A* and *B* with location *C*), while all rainfall caused change in water level to some degree. Antecedent moisture refers to the relative wetness of the unsaturated zone preceding a rain event. If a given rainfall is preceded by a long dry period, the antecedent moisture of the unsaturated zone will be low and any rainfall will fill pores in the zone instead of infiltrating by gravity to the water table. However, if the time is short between rain events, antecedent moisture will be high (that is, the zone will be near saturation). More rain will infiltrate to the water table, and an increase in aquifer level will be observed. The impact of antecedent moisture conditions on groundwater recharge has been documented in other studies such as those of Zhang and Schilling (2006), and Sorman and Abulrazzak (1993); it was also observed at SCI cave. The effect of antecedent moisture on groundwater level may be observed by contrasting a 0.3” rain event on May 12<sup>th</sup> (Figure 11; location *A*) and 0.17” rain event on May 14<sup>th</sup> (Figure 11; location *B*). Water level rose less than two inches at SCI cave after the May 12<sup>th</sup> rainfall; meanwhile, despite less recorded rainfall on May 14<sup>th</sup>, water level rose about four inches. A slight lag time between change in water level preceding any change in temperature or specific conductance (Figure 11; location *C*) suggests that recharge entered the aquifer at some point away from the SCI cave, changing head in the aquifer and displacing

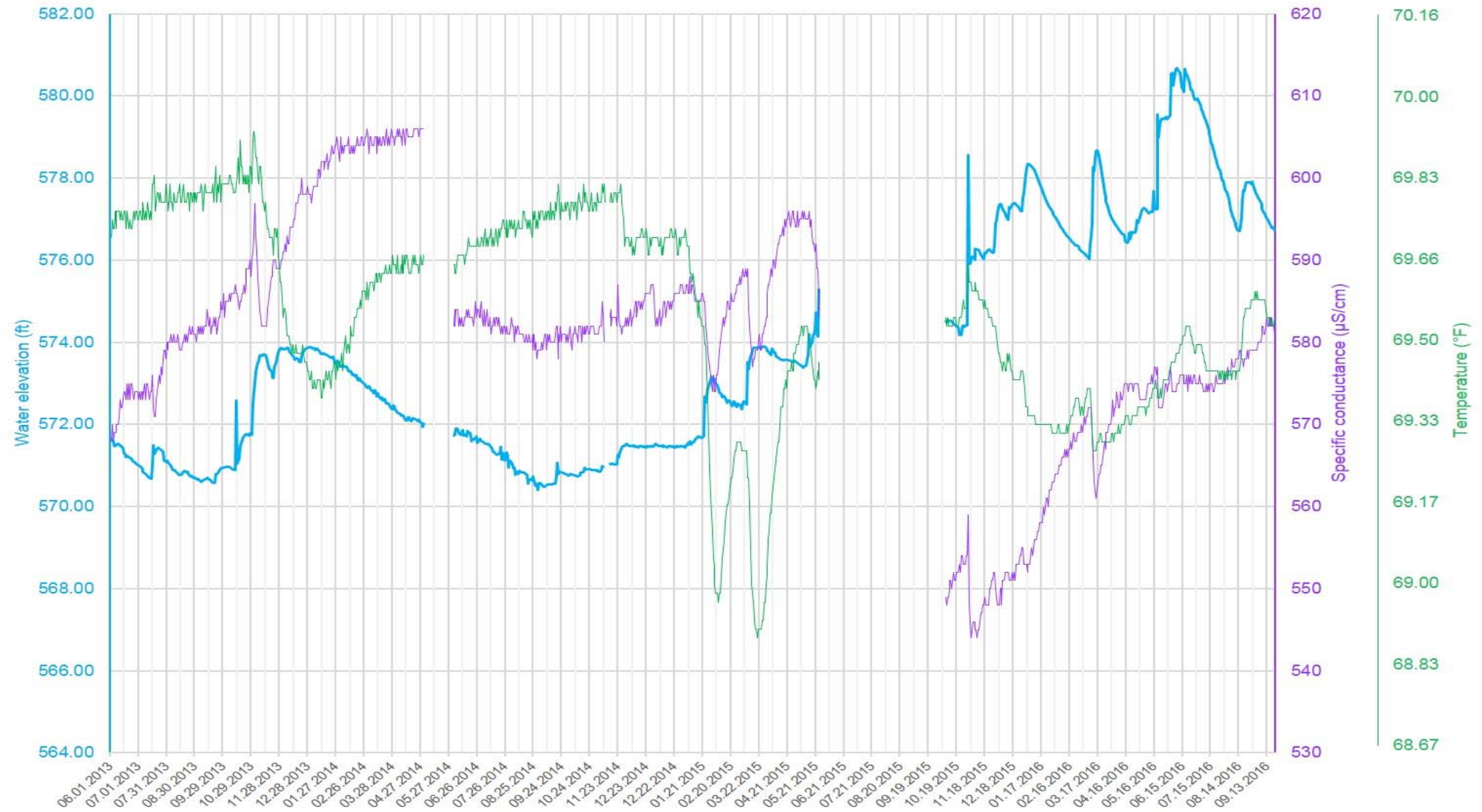


Figure 10. Hydrologic conditions at the Stagecoach Inn cave well from June 2013 to September 2016. Daily values are plotted.

antecedent water. Water level at SCI cave responds to the addition of water, while temperature and specific conductance remain unchanged until new water flows through the cave.

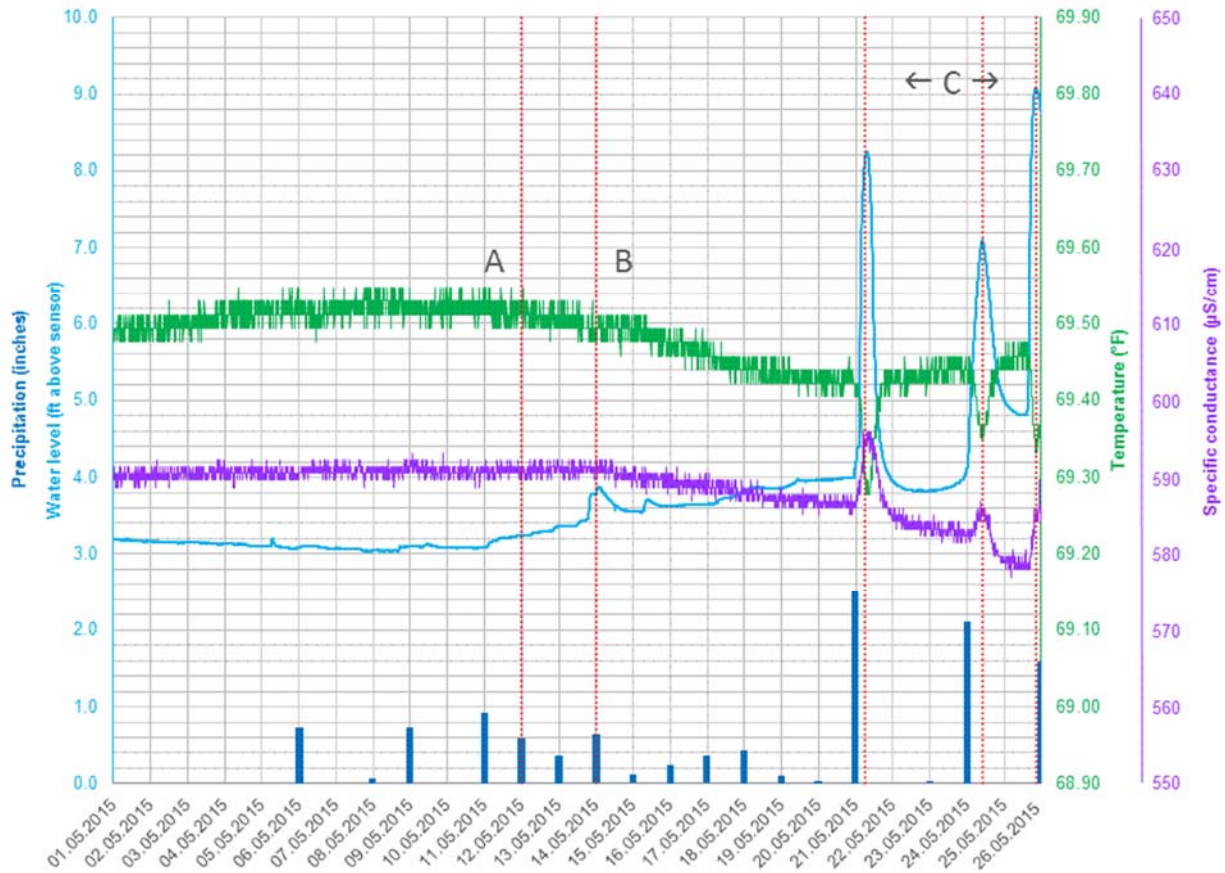


Figure 11. Hydrologic conditions at the Stagecoach Inn cave well in May 2015. Water level, temperature, and specific conductance measurements were logged every 15 minutes. Rainfall data from the nearest NOAA WSR-88D station (Geo ID #609938) are plotted as bars.

### Nitrate monitoring

Monitoring data (Figures 12) show that nitrate levels in the aquifer appear to respond to episodic loading or recharge events, and return to pre-episode levels within a few days. From the monitoring conducted in this study, nitrate levels do not appear to exhibit an increasing trend through time; however, the monitoring period was short (a few months), and a longer monitoring period may provide a better perspective.

Initial monitoring data collected from October to November of 2015 (Figure 12) prompted additional grab sampling before, during, and after high-traffic weekends (ie, holiday or Salado event weekends). Conceptually, nitrate concentrations in groundwater should be low before a high-traffic weekend, highest during the weekend, and returning to a low level after the weekend; this was observed in the initial data (Figure 12; see locations A, B, and C). The objective of grab sampling was: 1) to obtain more accurate nitrate concentrations, as the Troll 9500 functions better as a trending instrument; and 2) to see if nitrate concentrations would correlate with the increase and decrease of nitrate as recorded by the Troll 9500.

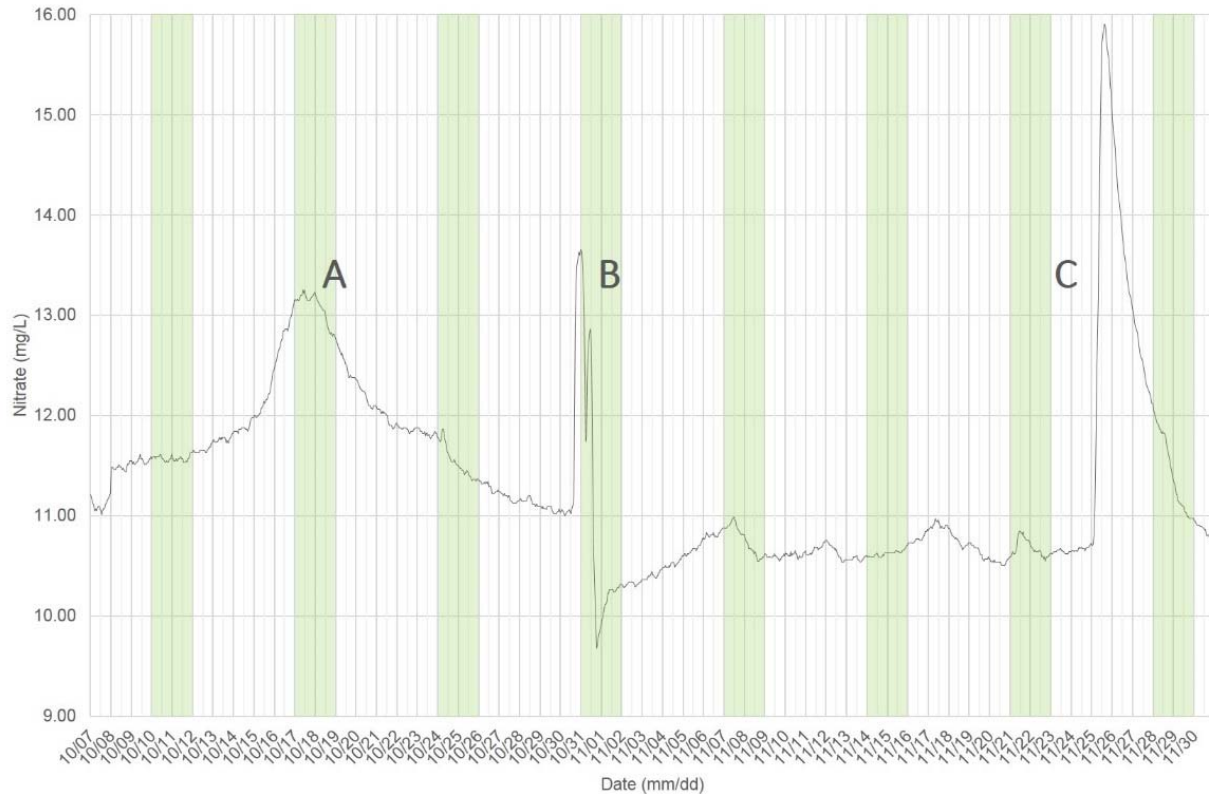


Figure 12. Nitrate trend data collected by the Troll 9500 sonde from October 7 to November 30, 2015 at the Stagecoach Inn Cave well. Green-shaded days indicate weekends (Saturday-Sunday). The spikes at A, B, and C correlate with high-traffic weekends in Salado; A correlates with the Halloween Fright Trail, B correlates with Halloween, and C correlates with Thanksgiving.

### Methods

Grab-sampling was conducted over the following weekends: Easter (March 23-30), Labor Day (September 1-8) and the Salado Chocolate and Wine Weekend (September 14-21). Grab-sampling was also conducted over a low-traffic weekend on February 11-16 (ie, not a holiday or Salado event weekend) as a control. Samples were collected before the weekend on either Wednesday or Thursday, during the weekend on Saturday, and after the weekend on Wednesday or Thursday. During each sampling event, water was collected from each downtown spring outlet (Big Boiling, Little Bubbly, Side, Critchfield, Doc Benedict, and Anderson Springs), Salado Creek upstream of the spring complex at Main Street Bridge and downstream of the complex at Inn on the Creek, and Stagecoach Inn Cave. Forty milliliters of water were filtered through a 0.45  $\mu\text{m}$  syringe filter, and collected in triple-rinsed 50 ml PPE centrifuge tubes. As quality controls, a trip blank and field blank were collected on each sample day, and one site was randomly selected to collect a duplicate sample. Samples were stored in ice and transported back to the Baylor CRASR (Center for Reservoir and Aquatic Systems Research) lab for analysis.

### Results and Discussion

Results from all sampling events are tabulated in Appendix A. A summary of sampling locations and mean nitrate concentrations are provided in Figure 13. Surface water just upstream from the downtown springs has an average nitrate concentration of 1.93 mg/L. The springs are a source of nitrate input to Salado Creek; all sampled springs had average nitrate concentrations between 3.10-3.50 mg/L. Surface water downstream of the springs contains an average 2.28 mg/L nitrate, reflecting the addition of nitrate from groundwater.

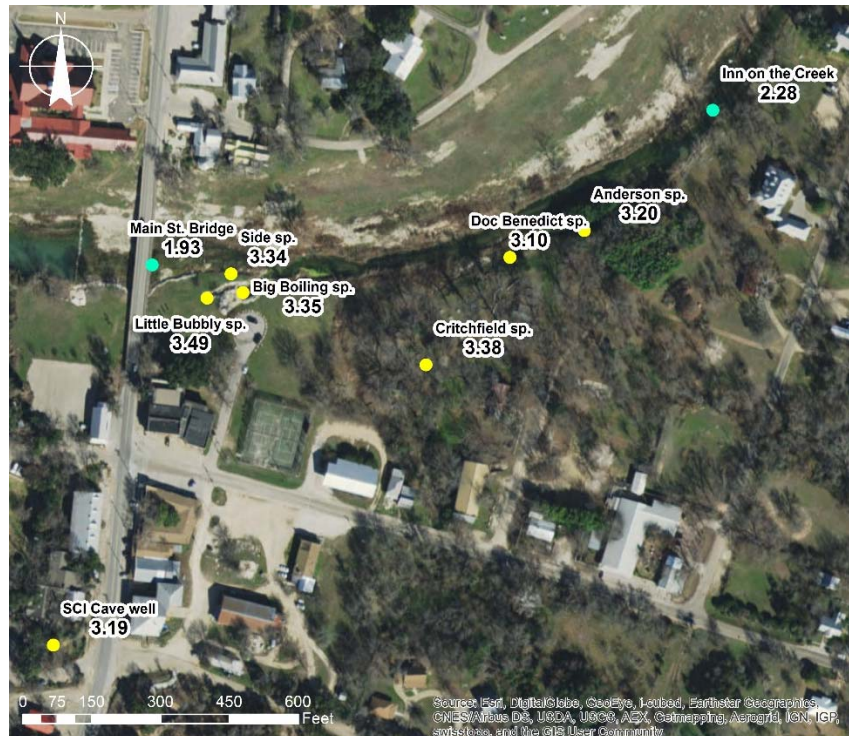


Figure 13. Map of nitrate sampling locations around downtown Salado showing average nitrate concentrations from all sampling events in mg/L. Specific nitrate concentrations for each event can be found in Appendix A.

Nitrate concentrations from the Labor Day long weekend sampling are shown in Figure 14. It is evident that quite a few of the sampling locations exhibit the low-high-low pattern, again supporting the observation that nitrate content in the Salado Springs complex be influenced by high-use, episodic loading. Measured nitrate concentrations for all surface water and groundwater sample locations ranged from 1.19 mg/L to 3.84 mg/L, with a mean concentration of 2.71 mg/L. At groundwater sampling locations (ie, the springs and the Cave well), nitrate concentrations ranged from 1.88 mg/L to 3.84 mg/L, with a mean concentration of 2.99 mg/L.

Critchfield spring is notably different from other springs, exhibiting a high-low-high pattern. We know from eye-witness accounts (Tim Brown, personal communication) that Critchfield Spring developed as a result of excavation in the area for Mr. Critchfield’s fish pond as opposed to natural exposure. As a result, Critchfield Spring, while being hydrologically connected to other springs in the downtown Salado Complex (established through dye tracing), is slightly different in geomorphologic setting and chemistry. Taking Critchfield Spring out of the statistical analysis for nitrate concentration does not change the range observed in groundwater sampling points; however, the mean concentration is 2.97 mg/L which is slightly lower.

Measured nitrate concentrations in the Salado Springs complex is within the range of nitrate measured in the unconfined portions in the San Antonio and Barton Spring segments of the Edwards BFZ aquifer. Krietler and Browning (1983) measured groundwater nitrate concentration as well as nitrogen isotopes in both the unconfined and confined portions of the San Antonio Segment. Nitrate concentration in unconfined groundwater ranged from 1.8-190 mg/L, but only two samples had concentrations greater than 15 mg/L (190 mg/L in a Bexar County well, and 29.0 mg/L in a Medina County well). Without these two high values, groundwater in the unconfined portion of the San Antonio Segment ranged from 1.8-14.9 mg/L, with a mean concentration of 7.06 mg/L and a median concentration of 6.1 mg/L. Slade and others (1986) assessed the hydrology and water quality of the Edwards Aquifer at Barton Springs. They reported a nitrate concentration of 1.0 mg/L for three samples collected between 1941 and 1955. Samples collected for the 1986 assessment contained a mean nitrate concentration of 1.5 mg/L. Slade and

others suggested that the increase in nitrate could be due to cattle and septic tanks, sanitary sewer systems in residential developments, or privately-owned sewage-treatment plants. Slade and others also observed highest nitrate levels in shallower wells, or wells located in the recharge area of the aquifer.

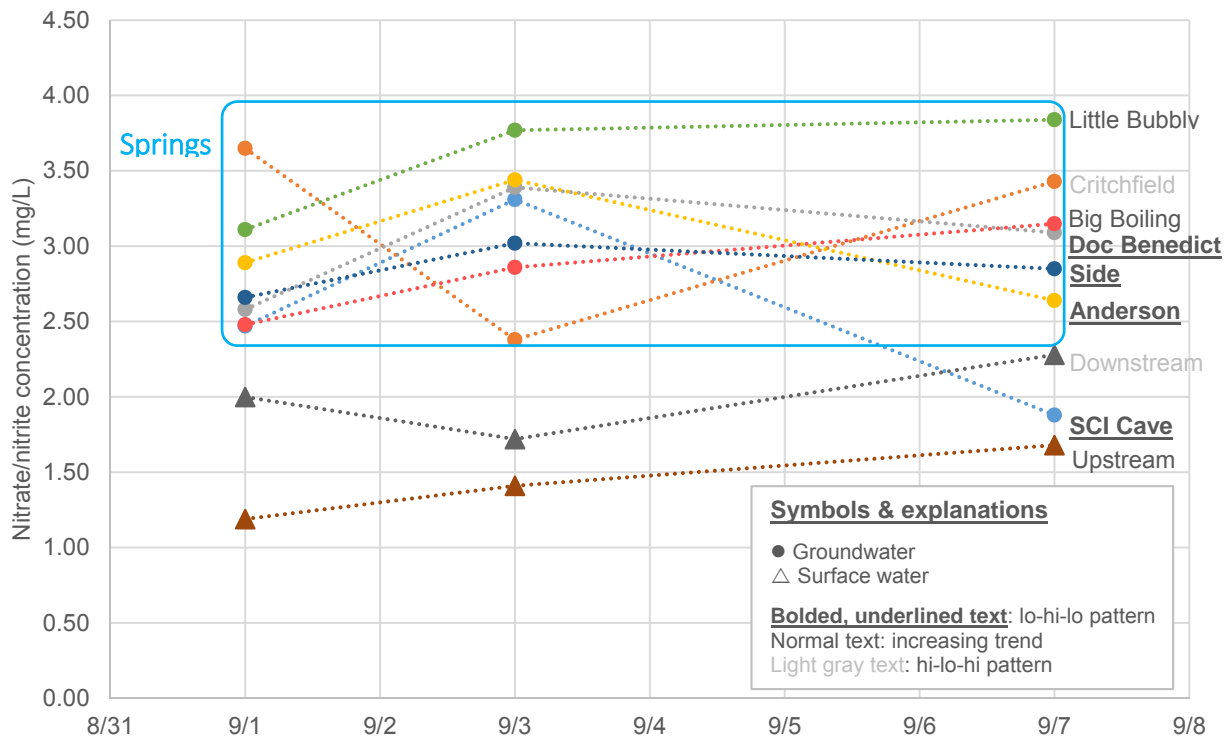


Figure 14. Nitrate concentrations at Salado Springs over the Labor Day long weekend (September 1<sup>st</sup>, 3<sup>rd</sup>, and 8<sup>th</sup>). Each spring outlet was sampled, as well as points upstream and downstream of the downtown spring complex.

Surface water appears to have a lower concentration of nitrate than groundwater. Because Salado Creek is a baseflow, perennial stream that is fed primarily from springs and seeps sourced from the Edwards aquifer, the lower concentration may be the result of plants taking nitrogen out of solution as a grown nutrient. Much of the nitrogen may return to the water when the plants senesce in the winter.

Grab-sample concentrations were compared to the Troll 9500 monitoring data, and did not seem to correlate well in the amount of nitrate detected nor in temporal trend. While nitrate concentrations do appear to increase during weekend events, they do not appear to correlate to the timing of nitrate peaks recorded by the Troll 9500 (Figure 15). It was not expected for the magnitude of nitrate to be comparable; nitrate sensors in general have difficulty remaining calibrated. However, the hope was that the nitrate sensor could provide trend data and indicate times to collect grab-samples, which could then be analyzed using lab techniques to obtain accurate nitrate concentrations.

The nitrate sensor on the Troll 9500 did not give accurate or dependable trend results.

- a. The sensor measured concentrations larger than the chemical analysis of the same water
- b. Grab sampling during sensor peaks was not consistent and did not show the same trends as the Troll 9500.

The nitrate sensor is difficult to calibrate and maintain. Therefore, it is probably more effective to collect periodic water samples to be analyzed in a lab and monitor for temporal changes.

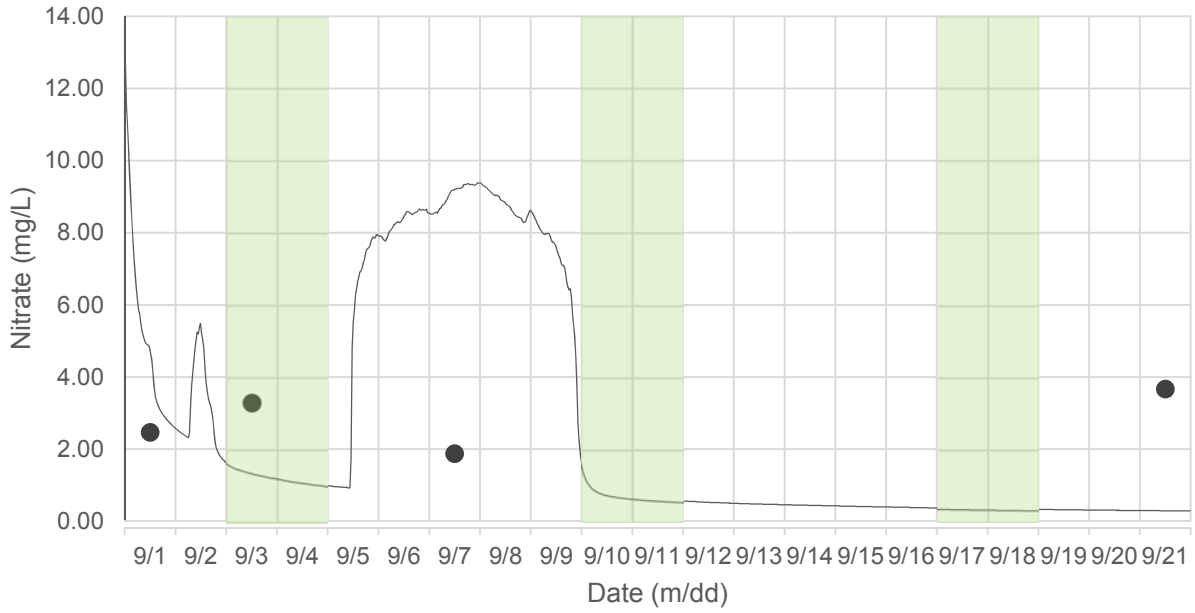


Figure 15. Nitrate trend data collected by the Troll 9500 sonde and grab samples from September 1-21, 2016 at the Stagecoach Inn Cave well. Points represent nitrate concentrations for grab samples collected from Stagecoach Inn Cave over the labor day long weekend and after the Salado Chocolate and Wine Weekend event. Green-shaded days indicate weekends (Saturday-Sunday).

## Groundwater-surface water interaction

### Stream Profiling

Profiling Salado Creek at three cross-sections near Big Boiling Spring has continued. Cross-sectional profiling helps to monitor physical and chemical conditions, as well as comparison with previously-collected data (water depth, temperature, and specific conductance) at Salado Creek. Flow measurements were also taken.

The three cross-sections were located in Salado Creek (Figure 16): within the spring flow of Big Boiling Spring (cross-section one), in Salado Creek upstream of the confluence of Big Boiling Spring (cross-section two), and in Salado Creek downstream of the confluence of Big Boiling Spring (cross-section three).

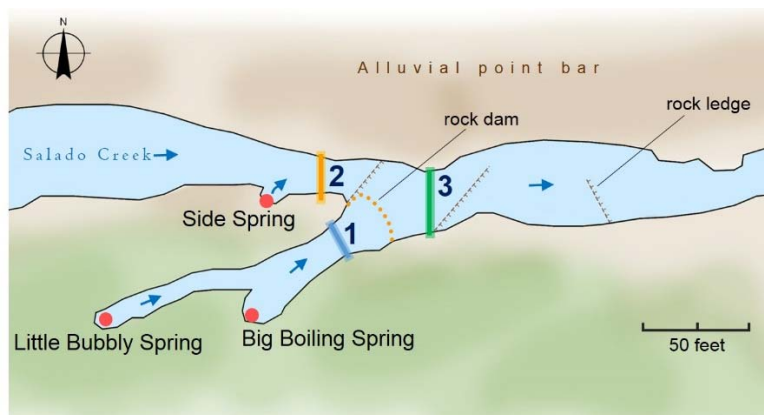


Figure 16. Diagram of downtown Salado Creek showing key features. The area around Big Boiling Spring, Little Bubbly Spring, Side Spring, and the adjacent section of Salado Creek was the focus of the study. Cross-section locations used for stream profiling are indicated by the colored lines and labelled 1, 2, and 3.

### *Methods*

All three cross-sections were taken perpendicular to flow direction. The measured parameters included: depth in feet (ft.), temperature in degrees Celsius (°C), specific conductance in micro-Siemens ( $\mu\text{S}/\text{cm}$ ), and flow in feet per second (fps). Measurements were made across the creek using stadia rod or reel tape laid across the channel width. Depth was measured using a metal yard stick. Temperature and specific conductance were measured using a Solinst TLC meter (Solinst Model 107 TLC Meter; Solinst Canada Ltd., Georgetown, Ontario). Flow was measured using a SonTek Flowtracker (SonTek, San Diego, California). The discharge at each profile was calculated using the midsection method, a standard discharge calculation method utilized by SonTek/YSI Inc. and the U.S. Geological Survey (SonTek, 2007). The midsection method assumes that a measured velocity is representative of the mean velocity for a rectangular segment of a stream profile (Turnipseed and Sauer, 2010). The partial discharge at each rectangular segment is calculated using the following formula, then summed to determine the total discharge of the stream profile (Turnipseed and Sauer, 2010).

$$q_i = v_i \left[ \frac{b_{(i+1)} - b_{(i-1)}}{2} \right] d_i$$

where  $q_i$  is the partial discharge through section  $i$ ,  $v_i$  is the mean velocity at location  $i$ ,  $b_{(i+1)}$  is the distance from the starting point of the profile to the next location,  $b_{(i-1)}$  is the distance from the starting point to the preceding location, and  $d_i$  is the depth of water at location  $i$ .

The specific conductance measurements were made in the natural water environment without the use of a stilling well or container, and without filtering the water. The water was very clear (spring flow and base flow conditions) but was flowing briskly except near the stream banks.

*Results and Discussion*

Cross-section one is characterized by unusual spatial consistency in temperature and specific conductance (Figure 17). Flow velocity ranged from 0.0381 ft/s towards the left edge-of-water of the Big Boiling spring run, to 0.351 ft/s towards the center of the profile. The average velocity was 0.2343 ft/s, and total discharge at cross-section one was calculated to be 5.0 cfs. Specific conductance and temperature readings were consistent across the profile. Specific conductance measured 483  $\mu\text{S}/\text{cm}$  across the profile except from 3-6 ft where specific conductance was 482  $\mu\text{S}/\text{cm}$ , and temperature measured 20.9°C across the profile. Steady depth and temperature values are understandable for a spring flow discharge channel and the landscaped, un-shaded nature of the Big Boiling spring run. The slight changes in specific conductance may be the result of variability in flow velocities that could affect the reading. Similar specific conductance values suggest a single source of water; in this setting it is groundwater discharging from Big Boiling Spring. Furthermore, specific conductance values are similar to those measured at the Stagecoach Inn Cave, located to the south and up-gradient with regard to groundwater flow. The similar specific conductance values suggest that Big Boiling Spring and the Stagecoach Inn Cave are part of the same groundwater system.

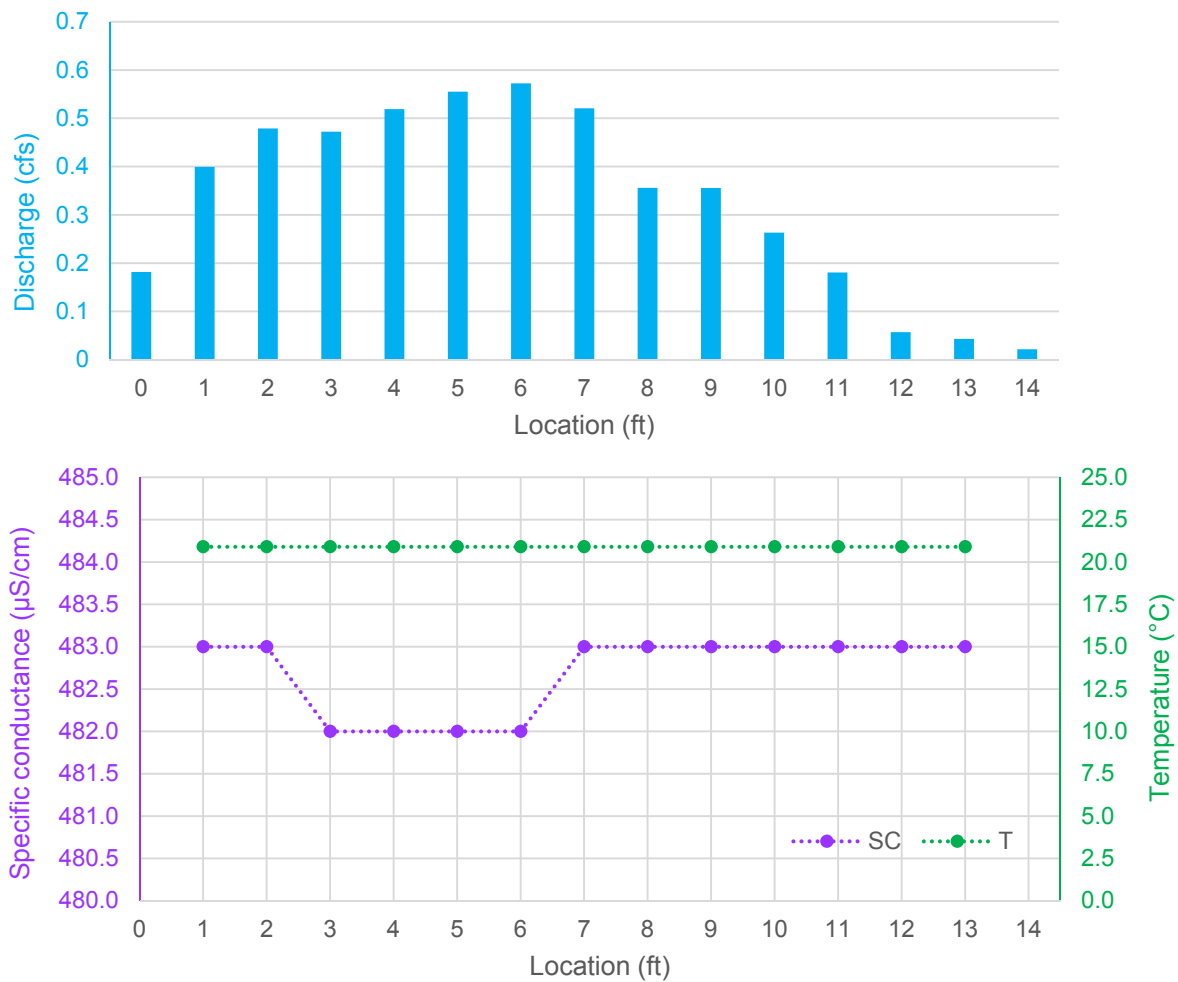


Figure 17. Discharge (*top*), specific conductance and temperature (*bottom*) measurements at cross-section 1, located in the spring flow of Big Boiling Spring. Measurements were taken on July 29, 2016.

Cross-section two is located in the natural channel of Salado Creek, upstream from Big Boiling Spring (Figure 18). Flow velocity ranged from 0 ft/s at the north bank of Salado Creek (left edge-of-water; 28 ft) which is a gently-sloping alluvial point bar, to 2.1962 ft/s near the south bank of Salado Creek (4 ft), where the thalweg is located. The average velocity was 1.1338 ft/s, and total discharge at cross-section two was calculated to be 28.7 cfs. Specific conductance ranged from 430 to 442  $\mu\text{S}/\text{cm}$ ; the average value was 433  $\mu\text{S}/\text{cm}$ . Temperature ranged from 23-24.7°C; the average value was 23.7°C. The cross-section is consistently shallow, with comparatively warm water and lower specific conductance relative to cross-section one. Temperature and specific conductance values were again fairly consistent across the section. Increased in temperature and decreased specific conductance near the north bank (feet 27-30) are the result of very shallow, muddy conditions. In contrast, decreased temperature and increased specific conductance near the south bank (feet 1-2) suggest groundwater influence, possibly through bank seepage. Overall, higher temperature and lower specific conductance values than those measured at cross-section 1 suggest that flow in Salado Creek upstream of Big Boiling Spring is dominated by streamflow rather than direct groundwater. Although flow in Salado Creek during these observations was dominated by baseflow from groundwater, a low-water dam immediately upstream is partly responsible for increased temperatures and lower specific conductance.

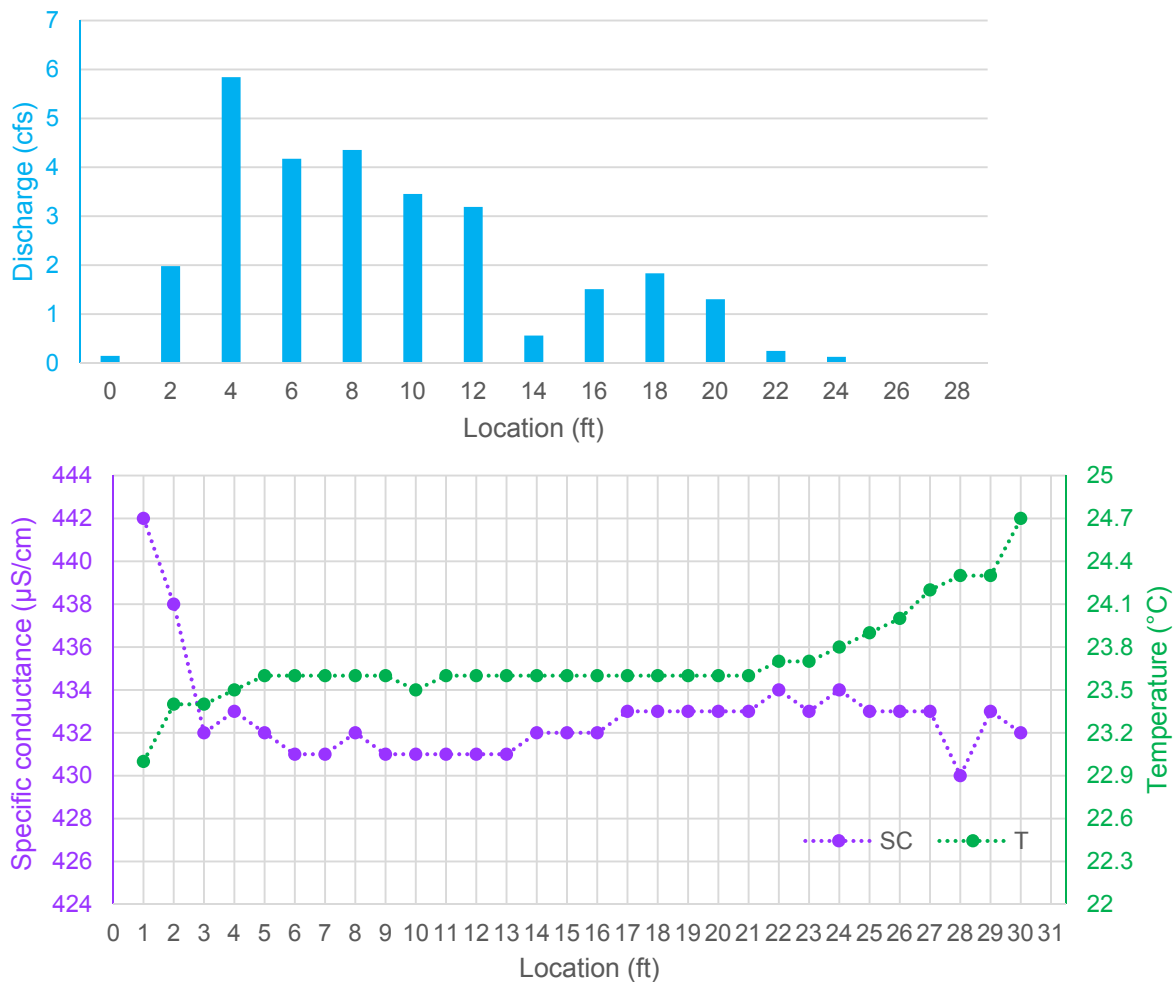


Figure 18. Discharge (*top*), specific conductance and temperature (*bottom*) measurements at cross-section 2, located in the natural channel of Salado Creek. Measurements were taken on July 29, 2016.

Cross-section three is located in the natural channel of Salado Creek, downstream of the confluence with Big Boiling Spring (Figure 19). Flow velocity ranged from 0 ft/s at the north bank of Salado Creek (left edge-of-water; 44 ft)

which is an alluvial point bar, to 2.6362 ft/s (26 ft). The average velocity was 1.5569 ft/s, and total discharge at cross-section two was calculated to be 34.0 cfs. The flow distribution at cross-section three is bimodal, reflecting the contribution of groundwater to Salado Creek at this location. The peak centered at 4 ft is primarily groundwater flow from Big Boiling Spring, while the peak centered around 28 ft is surface water from upstream. Specific conductance ranged from 420 to 483  $\mu\text{S}/\text{cm}$ ; the average value was 442  $\mu\text{S}/\text{cm}$ . Temperature ranged from 21.2-23.7°C; the average value was 23.0°C. Temperature and specific conductance values at this location exhibit a larger range than cross-sections one or two. This is to be expected since cross-section three is influenced by both spring and stream flow. Temperature and specific conductance at this location are intermediate values of those measured at cross-sections one and two, suggesting a mixing of stream water (represented by cross-section two) and groundwater discharging from Big Boiling Spring on the south side of the channel (represented by cross-section one). The width of groundwater influence is clearly evident in temperature and specific conductance values from 1 ft to about 8 ft of the cross-section, which are similar to measurements from Big Boiling Spring. The temperature rises and specific conductance decreases from the south to the north in the middle section as more surface water influences the total water flow. Since the burial of Rock Spring at north bank in the spring 2016, groundwater influence on temperature and specific conductance values is no longer evident.

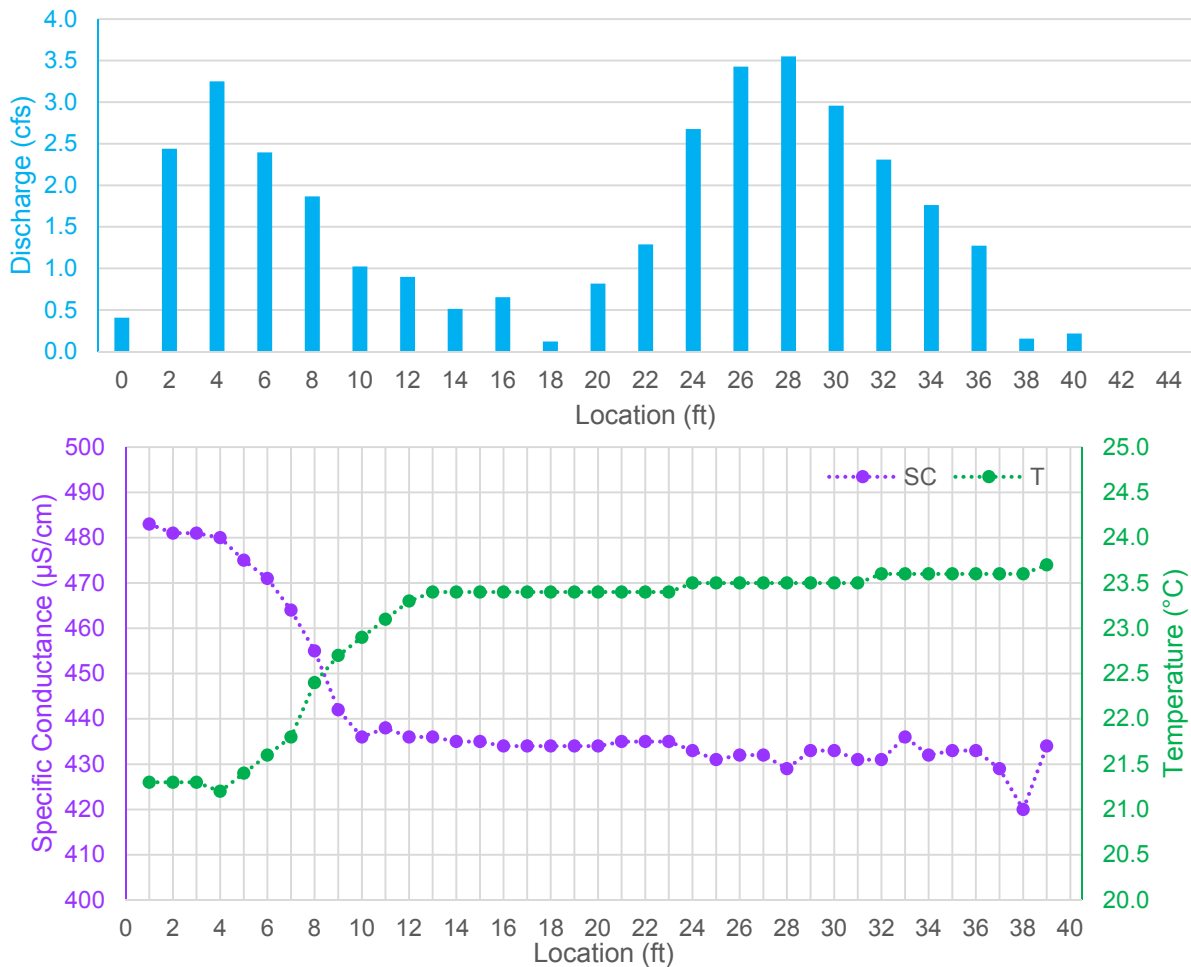


Figure 19. Discharge (*top*), specific conductance and temperature (*bottom*) measurements at cross-section 3, located in the natural channel of Salado Creek, downstream of the confluence with Big Boiling Spring. Measurements were taken on July 29, 2016.

## Thermography (FLIR)

Habitat for the Salado Salamander is associated with springs in the Northern Segment of the Balcones Fault Zone Edwards aquifer. However, questions remain as to how far back into the aquifer and how far beyond the spring orifices suitable habitat may occur. Temperature is quite consistent within the aquifer and has always been a critical habitat factor but determining the temperature consistency beyond the spring orifice can be difficult and time consuming. Differences between surface water and groundwater can be visible immediately after rains when sediment from runoff is suspended in the surface water but groundwater discharging from the springs remains clear (Figure 20). However, after the runoff event ends, the sediment settles out and the stream flow is supported primarily by baseflow which appears clear and is difficult to distinguish visually from the groundwater discharge (Figure 21). An infrared camera capable of measuring and displaying temperatures over an area was useful for providing insight into the extent of groundwater-dominated temperatures in spring runs, receiving streams, and the types of groundwater/surface-water interactions that may occur. Additionally, stream portions influenced by groundwater temperatures were observed to contain vegetation associated with springs and potential salamander habitat.

Because no published literature existed on the temperature distribution within this specific area of Salado Springs, the first efforts consisted of data gathered with a handheld FLIR-E63900 Infrared camera (Figure 22; FLIR® Systems, Inc.). The camera setting for emissivity did not change during the study but stayed as a constant setting of 0.95 which is thought to represent the emissivity of water. Distance settings were estimated for each image and ranged from 3-16 meters. When air temperatures were less than 40°F, the cold air absorbed some of the infrared energy over distances greater than about 10 meters and resulted in poor results. The spot check feature was used and the spot values compared closely with temperatures of the water measured with a probe. On January 22, 2016, the spot check on the FLIR was compared against temperatures measured using the Solinst TLC meter, which was also used for stream profiling. The temperature at the Big Boiling Spring orifice measured with the Solinst meter was 20.7°C while the FLIR spot check registered 20.9°C. Little Bubbly Spring measurements that day were 20.6°C at the orifice with the Solinst and 20.6°C with the FLIR. Because the water of greatest interest was groundwater discharging from a given spring, the spot check feature was used as both a hot spot and as a cool spot depending upon the type of temperature contrast between the groundwater from the springs and the surface water in the stream.

When the water is clear, temperature measurements and the FLIR camera can be used to determine the extent of groundwater/surface-water interactions. Essentially, in the summer when the air temperatures are high and the sun warms the surface water, groundwater is significantly cooler than the surface water; and in the winter when the air temperatures are cold and the surface water is also cold, then groundwater is relatively warmer. An example FLIR camera image compared to the visible light digital camera image can be seen in figure 23. In this figure, Side spring is discharging into Salado Creek when the groundwater from Side Spring is warm (68.5°F) and the surface water of Salado Creek is much cooler (47.2°F).

In addition to infrared imaging, profiles of temperature (T) and specific conductance (SC) along cross-sections in the Big Boiling spring run, and in Salado Creek upstream and downstream of the confluence of Big Boiling Spring were compared to the FLIR images to better understand temperature trends in relation to water flow and perhaps the chemistry as well. The study area focused on the area upstream and downstream of Big Boiling Spring although it included Side Spring and Little Bubbly Spring as well. Figure 16 shows the focus area. Temperature and specific conductance profiles were measured on April 6, 2016, in the area around Big Boiling Springs for direct comparison to FLIR images.



Figure 20. Abrupt contrast between clear groundwater flowing from Big Boiling Springs and sediment-laden surface water in Salado Creek after a small rainfall and during low spring flow conditions (October 7, 2013).



Figure 21. No contrast between clear groundwater flowing from Big Boiling Springs into clear baseflow in Salado Creek (July 31, 2013).



Figure 22. FLIR E63900 handheld infrared camera.

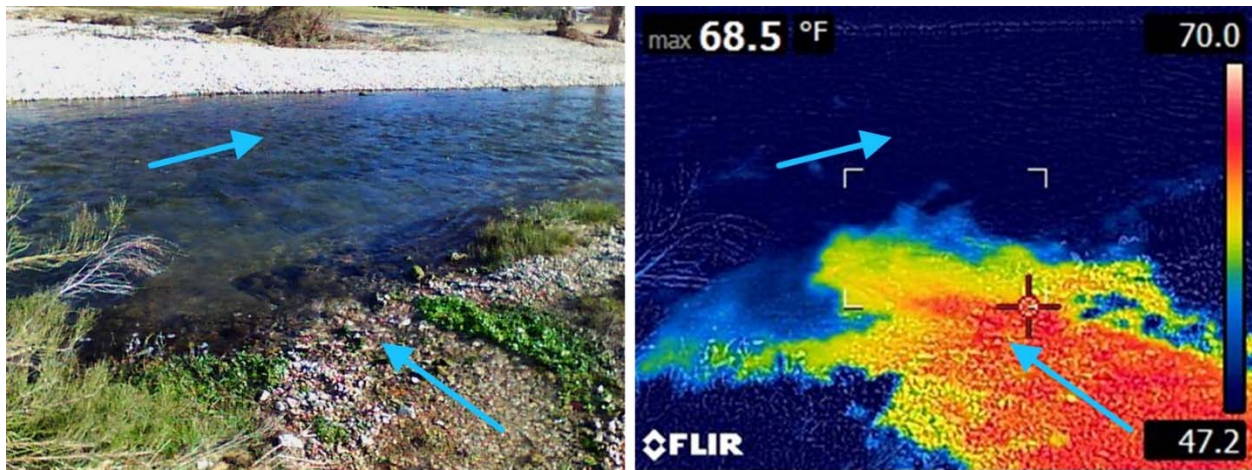


Figure 23. Side Spring looking northward from the south bank of Salado Creek in downtown Salado, Texas (January 27, 2016). The *left image* is a digital photograph and the *right image* is the infrared photograph showing temperature distribution. In the visible light image (*left*) it is impossible to see the boundaries and extent of the groundwater from Side Spring but these are readily observed in the infrared image below.

The temperature profile values showed remarkable consistency in Section 1 (Big Boiling Spring run). Section 2 which is upstream of Big Boiling Spring discharge also shows a consistent but cooler temperature profile than Section 1 with the exception of shallow water warming effects near the left edge-of-water (LEW), or north bank. Section 3 contains more overall variability than sections 1 and 2 but shows a shallow water warming trend on the LEW edge similar to Section 2. However, there is a warm water section about 4 feet wide along the right edge-of-water (REW) in Section 3 that did not appear on Section 2, and the magnitude of those temperatures match the temperatures for Big Boiling Spring discharge (Figure 24).

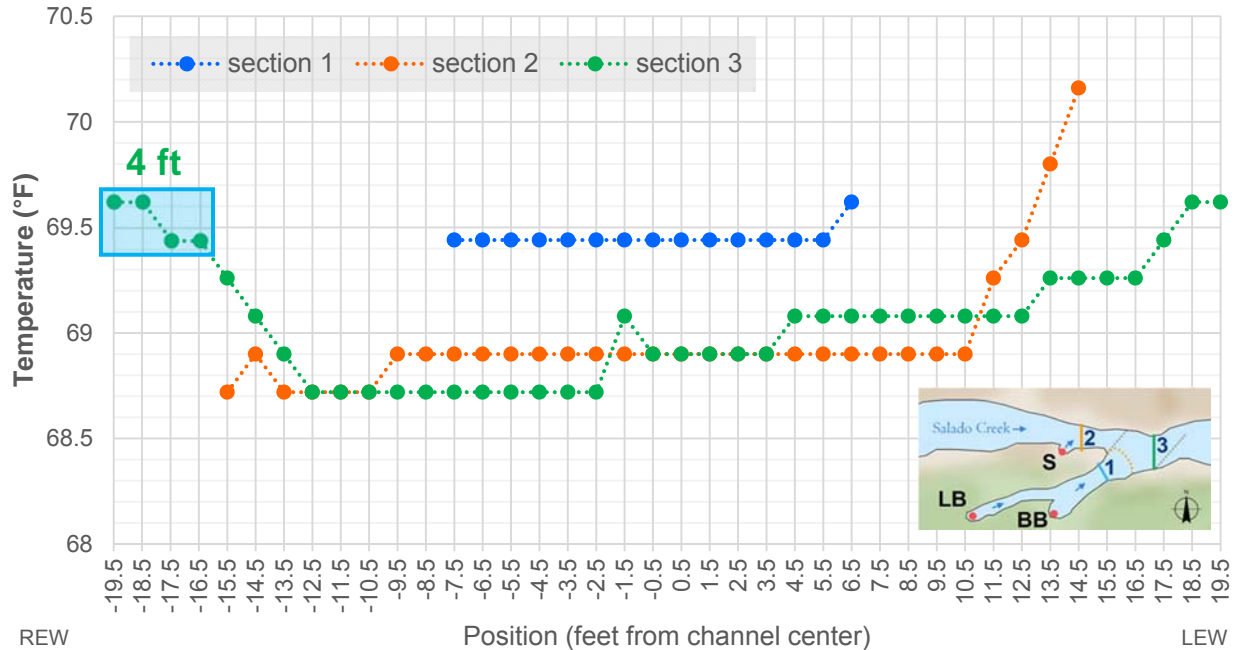


Figure 24. Temperature profiles in Salado creek and Big Boiling Spring, April 6, 2016.

The specific conductance profile measured on April 6, 2016 showed the same 4-foot wide area on the REW stream bank that the T profile showed, but in an even more dramatic fashion (Figure 25). The FLIR image also showed a 4-foot wide area of warmer temperatures on the REW side of the stream (Figure 26). The temperature values from the FLIR image are a few degrees lower than those recorded with the probe. The groundwater has not mixed with the surface water at this point downstream from the spring discharge. In addition, *Ludwigia*, a plant indicative of spring flow and known to provide habitat for salamanders, was found in this 4-foot section of the stream dominated by spring discharge (Figure 27).

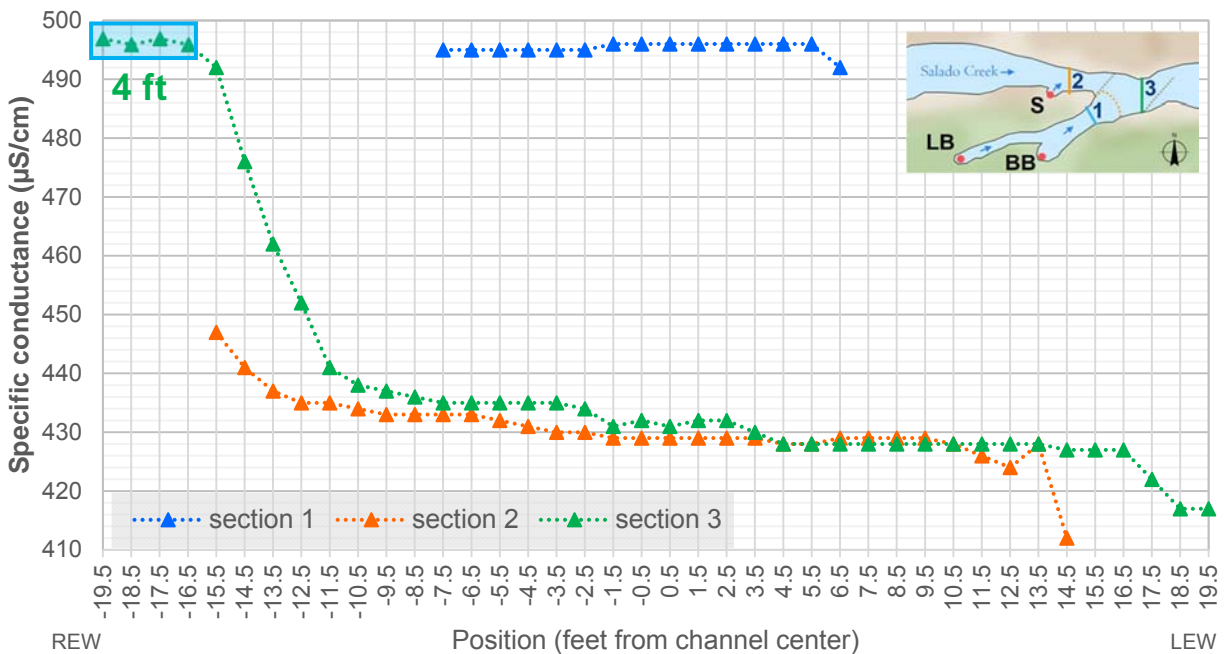


Figure 25. Specific conductance profile at section 3 April 6, 2016.

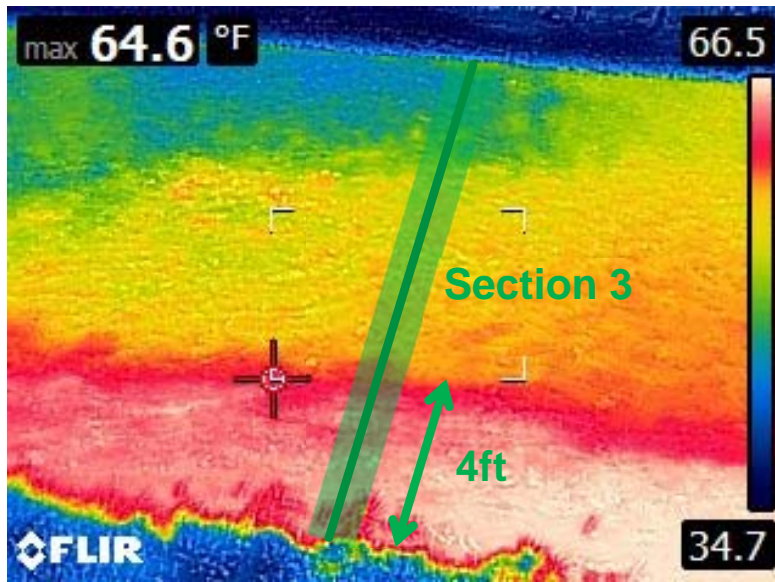


Figure 26. FLIR infrared image of profile Section 3 downstream from Big Boiling Spring showing the warmer temperatures associated with the groundwater discharge of Big Boiling Spring along the REW edge of the creek.



Figure 27. *Ludwigia* (submerged reddish plant) growing near the REW bank of Salado Creek downstream from the spring discharge of Big Boiling Spring, April 6, 2016.

*Discussions and conclusions regarding the FLIR camera*

The camera produces dramatic images that can be used to better understand interactions between groundwater and surface water. Although the spot check feature can produce similar temperatures to measurements from thermistors or thermometers, the FLIR readings represent surface temperatures and are most appropriate for shallow water where temperatures do not change drastically between the top and bottom of the water column. The infrared imagery is most efficient when there are drastic differences in temperatures between subjects of interest. When studying springs and interactions between groundwater and surface water in Central Texas, winter and summer are the preferred seasons compared to spring and fall. If the technology is used for locating groundwater

discharge during summer, it is best to do the field work in the morning and if working in the winter it is best to use the camera late in the day. Before dawn and after dusk are tempting application times, but the low lighting loses the ability to use visible light images for direct comparison.

The study showed variability in the stream areas impacted by groundwater discharge over time. The area affected by groundwater temperatures and chemistry (SC) was dependent upon the amount of spring discharge in relation to the amount of stream discharge. Big Boiling Spring has a larger impact area than Side Spring because its discharge is greater. Salado Creek is a fairly “flashy” stream, and during floods, the stream is the dominant flow contributor and groundwater does not impact a large area. However, groundwater levels rise quickly in conjunction with stream levels during floods and surface water does not appear to affect the T or SC of groundwater. The presence of *Ludwigia* and other vegetation indicative of spring flow and potential salamander habitat are dependent upon the length of time in which the area is consistently dominated by the groundwater flow. The floods appear to remove the spring-associated vegetation but regrowth occurs when baseflow conditions re-establish previous flow regimes.

## Springs Assessment

### SIP/SEAP

Salado Springs is recognized locally as an important natural resource, cultural landmark, and ecosystem that needs thoughtful and sustainable management. While springs are often considered as important and sensitive ecosystems, researchers recognize that a consistent language to describe and classify springs is lacking. Stevens and others (2011) propose a set of protocols for the holistic inventory and monitoring of springs. The objective of a consistent language and classification system for springs is to facilitate consistent guidelines for the conversation, management, restoration, and research of spring ecosystems. The classification system described by Stevens and others (2011) was applied to Salado Springs as a summation of the hydrogeological knowledge that has been collected at the springs through this body of research. Using terminology that is consistent with other spring researchers may allow researchers and managers of Salado Springs to better compare Salado Springs to other spring systems.

The classification process developed by Stevens and others aims to integrate pre-existing spring classification systems into a methodology that can be consistently applied to different spring ecosystems at differing levels of effort. The process involves two steps: The first step is an integrated *springs inventory protocol* (SIP) to quickly and reliably provide information on spring ecosystem components, processes, threats, and stewardship options (Stevens and others, 2011). Results from the SIP may be uploaded to an online database for comparison with other springs at the national and international levels. Furthermore, SIP results feed into a comprehensive secondary assessment, the *springs ecosystem assessment protocol* (SEAP). SEAP facilitates comparison of springs within a landscape, determination of stewardship priorities, monitoring, and measurement of the effectiveness of management actions (Stevens and others, 2011). Data sheets for both the SIP and SEAP are included in Appendix B for reference.

As part of the SIP and SEAP, springs of interest are classified into 12 spring types. Each spring type is described as a “sphere of discharge”, which is the idea that springs may be distinguished from each other by the environmental setting, or “sphere”, into which groundwater is discharged (Springer and others, 2008). The 12 spheres of discharge of springs originally described by Springer and others (2008) and further explained by Springer and Stevens (2009) are: Cave springs, exposure springs, fountain springs, geyser springs, gushet springs, hanging garden springs, helocrene springs, hillslope springs, hypocrene springs, limnocrene springs, mound-form springs, and rheocrene springs. In the Salado Springs complex, springs may be classified as rheocrene springs or limnocrene springs; characteristics of certain springs fit into and be classified as a combination of spring types.

A rheocrene spring (Figure 28) is defined as a flowing spring that emerges into one or more stream channels, or “spring runs”. The relatively uniform temperature and de-oxygenated groundwater in a spring run can create unique habitat conditions. Hydrogeochemical stability of a spring run is modified by groundwater interaction with surface water or runoff, disturbance frequency, and geomorphology (Springer and others, 2008); these factors influence the microhabitats that exist in a rheocrene spring setting, which in turn may support specialist aquatic species and evolutionary adaptation (in groundwater-dominated spring runs) or generalist, weedy species (surface water-dominated spring runs (Griffiths and others, 2008; McCabe, 1998). In Salado, parts of groundwater-dominated spring runs are habitat for the Salado salamander (*Eurycea chisolmensis*).

A limnocrene spring (Figure 29) is defined as a groundwater that is discharged from a confined or unconfined aquifer into one or more lentic, or still-water, pools. Limnocrene springs may be inhabited by pond and aquatic species, but their relatively uniform temperature and chemistry may support different species than those that are present in an adjacent surface water-dominated water body (Springer and Stevens, 2009).

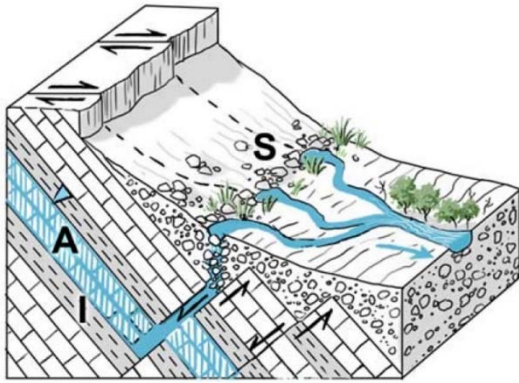


Figure 28. Rheocrene spring (Springer and Stevens, 2009). In the spring diagrams, A represents the aquifer, I is impermeable stratum, S is the spring source, and the inverted triangle represents the water table.

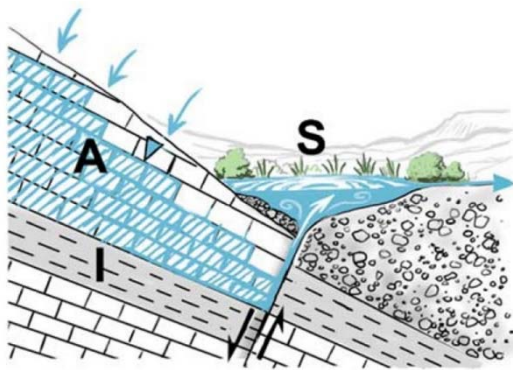


Figure 29. Limnocrene spring (Springer and Stevens, 2009). In the spring diagrams, A represents the aquifer, I is impermeable stratum, S is the spring source, and the inverted triangle represents the water table.

#### *Solar budget (Solar Pathfinder™)*

One aspect of the SIP assessment is performing a solar budget evaluation for each spring site. Knowing the amount of exposure a spring site has to the sun can be important for understanding the ecology of the spring, including temperature dynamics and what types of plants and animals can thrive. Using a Solar Pathfinder™ (SPF; The SolarPathfinder Company, Linden, Tennessee), the shading pattern across a given site is determined (Figure 30, left). A highly polished, transparent, convex dome gives a panoramic view of the entire site and shows tall plants or rock outcrops that can potentially shade a spring site. The edge of possible shade-structures are traced onto latitude-specific sunpath diagrams, specialized charts with rays that show solar time and arcs that show months of the year (Figure 30, right). By combining the tracing with the sunpath diagram, researchers can determine when a spring site will be shaded during the year. A SPF evaluation was performed for each spring in the Salado Springs complex on September 22, 2016 and the sunpath diagrams are documented in Appendix C. Results from SPF evaluations are entered into the “SPF” field of the SIP datasheet as part of the overall spring assessment.

#### *SIP Results and Recommendation*

In 2016, springs in the Salado Springs complex, Robertson Spring as well as all the major downtown springs, were categorized according to their spheres of discharge. Robertson Spring is comprised of multiple orifices, some which discharge into spring runs, and others that discharge from the floor of a stream or spring run; Robertson Spring is best described as both a rheocrene spring and a limnocrene spring (Figure 31). At Big Boiling Spring, groundwater discharges from one major ground-level orifice at the head of a large spring run and pool; because of these characteristics, Big Boiling Spring is best described as both a rheocrene spring and a limnocrene spring (Figure 32). Little Bubbly spring, which discharges into a spring run (61 ft) that flows into the pool of Big Boiling Spring, is best described as a rheocrene spring (Figure 33). Side Spring is also described as a rheocrene spring because groundwater discharges into a short spring run (11 ft) that flows into Salado Creek (Figure 34). Critchfield Spring discharges from a ground-level orifice that forms a groundwater pool. Water flows out of the northern end of the

pool to feed a spring run that flows parallel to Salado Creek for about 250 ft before flowing into the Doc Benedict Spring pool. Critchfield Spring is best described as both a limnocene spring and a rheocene spring (Figure 35), while Doc Benedict Spring is best described as a limnocene spring (Figure 36). Lastly, Anderson Spring, which also discharges from a ground-level orifice, is best described as a limnocene spring (Figure 37).

The SIP process was initiated in 2016. However, more time and study are necessary to develop a reasonably complete SIP document for each of the springs. It is recommended that the SIP process continue until the files are more complete and then the results presented in a separate report to the CUWCD board for approval.

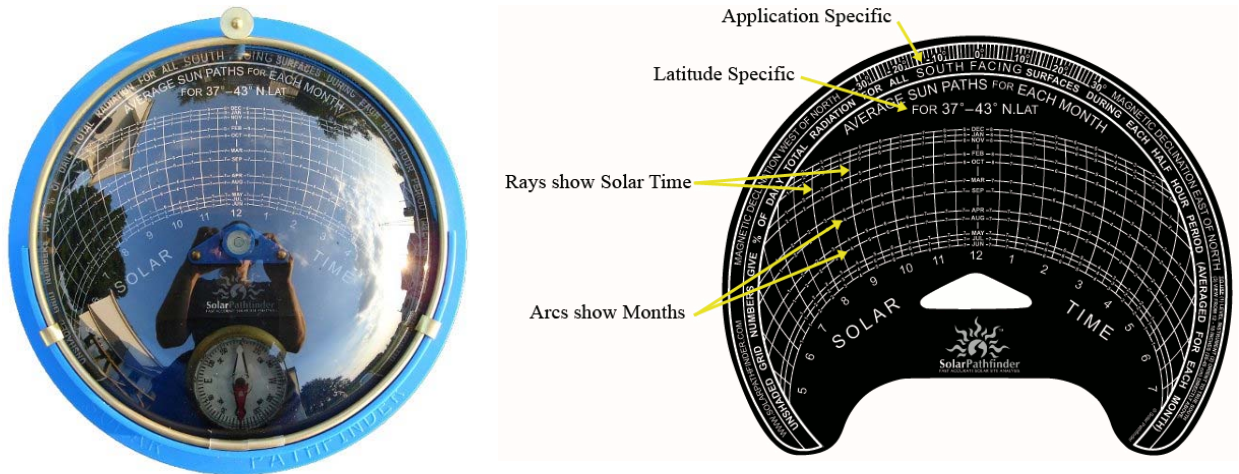


Figure 30. The Solar Pathfinder™. *Left*, a transparent dome gives a panoramic view around a site, showing surrounding shade structures. *Right*, an example sunpath diagram. (Images from Solar Pathfinder™, 2017).



Figure 31. Robertson Spring has characteristics of both a rheocene spring (*left*) as well as a limnocene spring (*right*). Location of the Solar Pathfinder™ is indicated by the crossed circle (⊕) in the *left* photo.



Figure 32. Big Boiling Spring has characteristics of a rheocrene spring and a limnocrene spring. Location of the Solar Pathfinder™ is indicated by the crossed circle (⊕).



Figure 33. Little Bubbly Spring is best classified as a rheocrene spring. Location of the Solar Pathfinder™ is indicated by the crossed circle (⊕).



Figure 34. Side Spring is best classified as a rheocrene spring. Location of the Solar Pathfinder™ is indicated by the crossed circle (⊕). The photo on the *right* shows Stephanie Wong working with the Solar Path Finder at Side Spring.



Figure 35. Critchfield Spring has characteristics of both a limnocrene spring as indicated by the pool on the *left*, as well as a rheocrene spring as indicated by the spring run on the *right*. Location of the Solar Pathfinder™ is indicated by the crossed circle (⊕) in the photo on the *left*.



Figure 36. Doc Benedict Spring is best classified as a limnocrene spring. Location of the Solar Pathfinder™ is indicated by the crossed circle (⊕).



Figure 37. Anderson Spring is best classified as a limnocrene spring. Location of the Solar Pathfinder™ is indicated by the crossed circle (⊕).

## Summary and Project Conclusions

The continuation of research on the Northern Segment has produced new data and new insights into the groundwater flow dynamics of the Northern Segment of the Edwards Balcones Fault Zone aquifer, particularly the downtown Salado Springs complex. Findings are summarized below.

1. Using LiDAR data to detect recharge features still looks promising for determining areas of important recharge potential. Several depressions in the Robertson ranch were detected and an aspect map identified lineations which parallel faults/fractures associated with the springs and warrant further analysis. However, the efforts to this point indicate an analysis of temporal and spatial rainfall patterns coupled with the Cave Well hydrographs may be more insightful in delineating important areas of recharge.
2. Data collected with a multi-parameter datalogger in the Stagecoach Inn Cave well indicated rapid groundwater responses to large rainfall events. The data also show slight water quality changes. The responses to recharge captured by the datalogger provides important timing information to aid in the development of future monitoring strategies.
  - a. Nitrogen data from field and laboratory analysis showed values that are interpreted to be slightly above expected background levels but no nitrate values were observed to be over the drinking water limit.
  - b. The nitrogen data warrant further investigation and monitoring.
3. Data collected with a Solinst hand-held meter along cross-sections of Salado Creek and adjacent springs show patterns helpful in understanding groundwater/surface-water interactions and potential areas of salamander habitat.
  - a. Specific conductance (SC) and temperature (T) measurements in cross sections of Big Boiling Spring as well as upstream and downstream of the confluence between Big Boiling Spring discharge and Salado Creek confirm the mixing patterns of groundwater and surface water from Big Boiling Spring.
  - b. The cross section data are important to quantify groundwater/surface water mixing, aid in habitat assessments, and aid in sample location selection.
  - c. The groundwater from Big Boiling Spring appears to mimic laminar flow and hug the south bank of Salado Creek for tens of yards before structural features in the stream enable mixing with the surface water of the creek. The groundwater influence is dependent upon the ratio of the flow between the creek and the spring.
4. Thermography using a handheld FLIR camera has helped delineate potential salamander habitat in the springs and spring runs at several springs. The thermography also has better delineated the exact areas of groundwater interaction with surface water and confirmed previous cross section studies.
5. Spring Inventory protocol (SIP) and Spring Ecosystem Assessment Protocol (SEAP) were used to categorize the springs in the downtown area with internationally published protocols for comparisons of baseline and possibly future management conditions.

## Recommendations

### Recharge feature characterization

While providing new insights on methods for characterizing the aquifer, the large data volume and time required to perform Lidar data analysis is not efficient for aquifer-wide analysis in general. A more efficient work-flow may be to examine spatial distribution of precipitation and pair these data with hydrograph analysis to determine important recharge areas, then perform a second-level examination of the area using Lidar data to identify recharge features.

### Groundwater monitoring

#### *Aquifer conditions*

The OTT CTD datalogger is a reliable instrument that provides consistent data and requires minimal maintenance; recommended that CUWCD continue monitoring at the SCI Cave well with this instrument. There is a need to determine a fixed benchmark in the cave to tie all water level measurements to through time. Maintenance once every 4-6 months is recommended, including replacement of desiccant tablets and recalibration of specific conductance sensor. Visits to the site are recommended once every month. This is necessary to download data, check battery power, and observe site conditions.

#### *Nitrate*

Calibration and maintenance of the In-Situ Troll 9500 instrument has been an involved process. Magnitude of nitrate concentrations from the In-Situ Troll 9500 do not compare well with results from lab analysis. Therefore, we recommend monitoring the long-term nitrate trend through periodic (annual or semi-annual) grab samples at key springs and monitoring wells.

### Groundwater – surface water interaction

The FLIR infrared camera and profiling of spring discharge using temperature, specific conductance, and flow produced some useful insights into groundwater and surface water interactions. This technique may be useful at other spring locations within the Salado Creek Basin.

### Springs assessment

While the spring assessment process has been started, more time and study are necessary to develop a reasonably complete SIP document for each of the springs. It is recommended that the SIP process continue until the files are more complete and then the results presented in a separate report to the CUWCD board for approval.

## References

- Blackwell, P.R., and G. Wells, 1999, DEM resolution and improved surface representation. *In* ESRI Users Conference, Proceedings, June 1999.
- ESRI, 2017a, Hydrology toolset concepts: How Fill works *in* Tool Reference. <<http://pro.arcgis.com/en/pro-app/tool-reference/spatial-analyst/how-fill-works.htm>> *Last accessed 12 April 2017.*
- ESRI, 2017b, Surface toolset concepts: How Aspect works *in* Tool Reference. <<http://desktop.arcgis.com/en/arcmap/10.3/tools/spatial-analyst-toolbox/how-aspect-works.htm>> *Last accessed 13 April 2017.*
- Griffiths, R.E., A.E. Springer, and D.E. Anderson, 2008, The morphology and hydrology of small spring-dominated channels. *Geomorphology*, 102(3-4): 511-521.
- Gritzner, J.H., 2006, Identifying wetland depressions in bare-ground LIDAR for hydrologic modeling. *In* Proceedings of the twenty-sixth annual ESRI user conference, July 2006. 13 pp.
- Jones, I.C., 2003, Groundwater Availability Modeling: Northern Segment of the Edwards Aquifer. Texas Water Development Board Report 358, Austin, Texas, 75 pp.
- Kreitler, C.W., and L.A. Browning, 1983, Nitrogen-isotope analysis of groundwater nitrate in carbonate aquifer: Natural sources versus human pollution. *Journal of Hydrology*, 61:285-301.
- McCabe, D.J., 1998, Biological communities in springbrooks. *In* Studies in Crenobiology: The biology of springs and springbrooks, Botosaneanu, L. (Ed.). Backhuys, Leiden, The Netherlands.
- Slade Jr., R.M., M.E. Dorsey, and S.L. Stewart, 1986, Hydrology and water quality of the Edwards Aquifer associated with Barton Springs in the Austin area, Texas. U.S. Geological Survey Water Resources Investigations Report 86-4036, Austin, Texas, 123 pp.
- Solar Pathfinder™, 2017, Solar Pathfinder™ website. <<http://www.solarpathfinder.com/PF?id=TaBkNLSW#sunpath>> *Last accessed 27 July, 2017.*
- SonTek. 2007. FlowTracker® Handheld ADV® Technical Manual. SonTek/YSI Inc., San Diego, CA. 126 pp.
- Sorman, A.U., and M.J. Abdulrazzak, 1993, Infiltration-recharge through wadi beds in arid regions. *Hydrological Sciences Journal*, 38(3): 173-186.
- Springer, A.E., and L.E. Stevens, 2009, Spheres of discharge of springs. *Hydrogeology Journal*, 17:83-93. DOI 10.1007/s10040-008-0341-y
- Springer, A.E., L.E. Stevens, D.E. Anderson, R.A. Parnell, D.K. Kreamer, L. Levin, and S. Flora, 2008, A comprehensive springs classification system: integrating geomorphic, hydrogeochemical, and ecological criteria. *In* Aridland springs in North America: ecology and conservation, Stevens, L.E. and V.J. Meretsky (Eds.). University of Arizona Press, Tucson, Arizona.
- Springs Stewardship Institute, 2014, SIP and SEAP Field Sheets. <<http://docs.springstewardship.org/PDF/FieldFormOct2014.pdf>> *Last accessed 7 December, 2016.*
- Stevens, L.E., A.E. Springer, J.D. Ledbetter, 2011, Inventory and monitoring protocols for springs ecosystems, Version: 1 June 2011. 64 pp. <[http://docs.springstewardship.org/PDF/Springs\\_Inventory\\_Protocols\\_110602.pdf](http://docs.springstewardship.org/PDF/Springs_Inventory_Protocols_110602.pdf)> *Last accessed 7 December 2016.*
- Texas Natural Resources Information System (TNRIS), 2017, StratMap2011 50cm Bell, Burnet, McLennan. <<https://tnris.org/data-catalog/entry/stratmap-2011-50cm-bell-burnet-mclennan/>> *Last accessed 13 April 2017.*
- Turnipseed, D.P., and V.B. Sauer, 2010, Discharge measurements at gaging stations: U.S. Geological Survey Techniques and Methods book 3, chap. A8, 87p.
- Zhang, Y.K., and K.E. Schilling, 2006, Effects of land cover on water table, soil moisture, evapotranspiration, and groundwater recharge: A field observation and analysis. *Journal of Hydrology*, 319(1-4): 328-338.

Appendix A  
Dissolved nitrate/nitrite concentrations for Salado Springs

Table A1. Dissolved nitrate/nitrite content in groundwater and surface water at Salado Springs on February 11-16, 2016 (low-traffic weekend). Concentrations are reported in mg/L.

Site	Pre-weekend	Weekend	Post-weekend
Main Street Bridge ( <i>upstream</i> )	2.84	2.70	2.70
Stagecoach Inn Cave Well	4.09	4.10	4.26
Big Boiling Spring	4.31	4.28	4.25
Little Bubbly Spring	4.07	4.25	4.14
Side Spring	4.25	4.27	4.21
Critchfield Spring	4.05	3.87	4.07
Doc Benedict Spring	3.82	3.65	3.75
Anderson Spring	4.09	4.00	3.81
Inn on the Creek ( <i>downstream</i> )	3.12	3.04	3.07

Table A2. Dissolved nitrate/nitrite content in groundwater and surface water at Salado Springs on March 23-30, 2016 (Easter long-weekend). Concentrations are reported in mg/L.

Site	Pre-weekend	Weekend	Post-weekend
Main Street Bridge ( <i>upstream</i> )	1.73	1.4	1.27
Stagecoach Inn Cave Well	2.87	2.44	2.92
Big Boiling Spring	2.87	2.76	2.69
Little Bubbly Spring	2.91	3.02	2.81
Side Spring	2.78	3.04	2.87
Critchfield Spring	3.21	2.73	2.84
Doc Benedict Spring	2.38	2.38	2.43
Anderson Spring	2.62	2.38	2.52
Inn on the Creek ( <i>downstream</i> )	1.69	1.66	1.60

Table A3. Dissolved nitrate/nitrite content in groundwater and surface water at Salado Springs on September 1-7, 2016 (Labor Day long-weekend). Concentrations are reported in mg/L.

Site	Pre-weekend	Weekend	Post-weekend
Main Street Bridge ( <i>upstream</i> )	1.62	1.41	1.68
Stagecoach Inn Cave Well	2.40	3.31	1.88
Big Boiling Spring	2.48	2.68	3.31
Little Bubbly Spring	3.11	3.77	3.84
Side Spring	2.66	3.02	2.85
Critchfield Spring	3.65	2.38	3.43
Doc Benedict Spring	2.58	3.41	3.09
Anderson Spring	2.89	3.44	2.64
Inn on the Creek ( <i>downstream</i> )	2.00	1.72	2.28

Table A4. Dissolved nitrate/nitrite content in groundwater and surface water at Salado Springs on September 14-21, 2016 (Salado Chocolate and Wine event-weekend). Concentrations are reported in mg/L. Several samples were collected but not analyzed due to an error in sample identification. Unanalyzed samples are denoted by N/A.

Site	Pre-weekend	Weekend	Post-weekend
Main Street Bridge ( <i>upstream</i> )	1.54	N/A	2.37
Stagecoach Inn Cave Well	N/A	N/A	3.67
Big Boiling Spring	3.57	N/A	3.69
Little Bubbly Spring	2.61	N/A	3.68
Side Spring	3.02	N/A	3.69
Critchfield Spring	3.72	N/A	3.67
Doc Benedict Spring	3.45	2.71	3.53
Anderson Spring	N/A	N/A	3.59
Inn on the Creek ( <i>downstream</i> )	2.05	2.4	2.73

Appendix B  
Spring Assessment: SIP and SEAP datasheets  
(Springs Stewardship Institute, 2014)



**1 Discharge Sphere (Spring Type)**

Anthropogenic  
 Cave  
 Exposure  
 Fountain  
 Geyser  
 Gushet  
 Hanging Garden  
 Helocrene  
 Hillslope  
 Hypocrene  
 Limnocrene  
 Mound-form  
 Rheocrene

**2 Sensitivity**

None  
 Location  
 Survey  
 Both

**3 Land Unit**

BLM  
 DOE  
 NPS  
 Private  
 State  
 Tribal  
 USFS  
 Other

**4 Georeference Source**

GPS  
 Map  
 Other

**5 Surface Type**

BW Backwall  
 C Cave  
 CH Channel  
 CS Colluvial slope  
 HGC High Grad. Cienega  
 LGC Low Grad Cienega  
 Mad Unfocused Madiculous  
 O Organic Ooze  
 P Pool  
 PP Plunge Pool  
 SB Sloping Bedrock  
 SM Spring Mound  
 TE Terrace  
 TU Tunnel  
 Upl Adjacent Uplands  
 WH Wet Hillslope  
 Oth Other

**6 Surface Subtype**

CH Riffle, Run, Margin, Eph  
 TE LRZ, MRZ, URZ, HRZ  
 UPL,LRZMRZ,LRZURZ,  
 MRZURZ, HRZMRZ  
 All Anthro

**7 Slope Variability**

Low, Medium, High

**8 Soil Moisture**

1 - Dry  
 2 - Dry-Moist  
 3 - Moist-Dry  
 4 - Wet-Dry  
 5 - Moist  
 6 - Saturated-Dry  
 7 - Wet  
 8 - Saturated-Moist  
 9 - Wet-Saturated  
 10 - Saturated  
 11 - Inundated

**9 Substrate**

1 clay  
 2 silt  
 3 sand  
 4 fine gravel  
 5 coarse gravel  
 6 cobble  
 7 boulder  
 8 bedrock  
 Organic Soil/Matter  
 Other/anthropogenic

**10 Lifestage**

Adult  
 Egg  
 Exuvia  
 Immature  
 Larvae  
 Mixed  
 Other  
 Pupae  
 Shell

**11 Habitat**

AQ - Aquatic  
 T - Terrestrial

**12 Method (Invertebrates)**

Spot  
 Benthic

**13 Detection Type (Vertebrates)**

Call  
 Observed  
 Sign  
 Reported (by others)  
 Other

**14 Cover Codes**

GC Ground Cover  
 SC Shrub Cover  
 MC Midcanopy Cover  
 TC Tall Canopy Cover  
 AQ Aquatic Cover  
 NV Nonvascular (moss, etc)  
 BC Basal Cover

**15 Emergence Environ/Detail**

Cave  
 Subaerial  
 Subglacial  
 Subaqueous-lentic freshwater

Subaqueous-lentic freshwater  
 Subaqueous-estuarine  
 Subaqueous-marine

**16 Source Geomorphology**

Contact Spring  
 Fracture Spring  
 Seepage or filtration  
 Tubular Spring

**17 Flow Force Mechanism**

Anthropogenic  
 Artesian  
 Geothermal  
 Gravity  
 Other

**18/19 Parent Rock Type/Subtype**

Igneous  
 andesite  
 basalt  
 dacite  
 diorite  
 gabbro  
 grandodiorite  
 granite  
 peridotite  
 rhyolite  
 Metamorphic  
 gneiss  
 marble  
 quartzite  
 slate  
 schist  
 Sedimentary  
 coal  
 conglomerate  
 dolomite  
 evaporates  
 limestone  
 mudstone  
 sandstone  
 shale  
 siltstone  
 Unconsolidated

**20 Channel Dynamics**

Mixed runoff/spring dominated  
 Runoff dominated  
 Spring dominated  
 Subaqueous

**21 Flow Consistency**

Dry intermittent  
 Erratic intermittent  
 Perennial  
 Regular intermittent

**22 Measurement Technique**

Current meter  
 Weir  
 Cutthroat flume  
 Other

©Springs Stewardship Institute rev 10/14

Spring Name \_\_\_\_\_ Page \_\_\_\_\_ of \_\_\_\_\_ OBS \_\_\_\_\_

Invertebrates	Species Name	Qty	<sup>10</sup> Stage	<sup>11</sup> Habitat	<sup>12</sup> Method	Rep #	Comments	
	Benthic Rep	Rep #	Location	Velocity m/sec	Depth cm	Substrate	Area Sq M	Time Sec

Entered by \_\_\_\_\_ Date \_\_\_\_\_ Checked by \_\_\_\_\_ Date \_\_\_\_\_







Spring Name \_\_\_\_\_ Page \_\_\_\_\_ of \_\_\_\_\_ OBS \_\_\_\_\_

Measurement Device(s) \_\_\_\_\_ Date Last Calibrated \_\_\_\_\_ Air Temp \_\_\_\_\_

Collection Location/Comments \_\_\_\_\_

**Field Measurements**

Depth (cm)	pH	Conductivity	Dissolved O <sup>2</sup>	Water Temp. (°C)	Turbidity	Alkalinity	Other	Device
Average								

**Collected for Analysis**

Sample Type	Sample Taken?	Duplicate Taken?	Container	Filtered (Y/N)	Treatment	
Anions						
Cations						
Nutrients						
<sup>2</sup> H and <sup>18</sup> O Isotopes						

Water Quality

Entered by \_\_\_\_\_ Date \_\_\_\_\_ Checked by \_\_\_\_\_ Date \_\_\_\_\_

Spring Name \_\_\_\_\_ Date \_\_\_\_\_ Page \_\_\_\_ of \_\_\_\_ Obs \_\_\_\_\_

Information Source \_\_\_\_\_

Aquifer/WQ	Cond	Risk	Habitat	Cond	Risk	Human Influence	Cond	Risk	Administrative Context	Cond	Risk
Spring dewatered (Y/N)	<input type="checkbox"/>	<input type="checkbox"/>	Isolation	<input type="checkbox"/>	<input type="checkbox"/>	Surface water quality	<input type="checkbox"/>	<input type="checkbox"/>	Information quality/quantity	<input type="checkbox"/>	<input type="checkbox"/>
Aquifer functionality	<input type="checkbox"/>	<input type="checkbox"/>	Habitat patch size	<input type="checkbox"/>	<input type="checkbox"/>	Flow regulation	<input type="checkbox"/>	<input type="checkbox"/>	Cultural significance	<input type="checkbox"/>	<input type="checkbox"/>
Spring discharge	<input type="checkbox"/>	<input type="checkbox"/>	Microhabitat quality	<input type="checkbox"/>	<input type="checkbox"/>	Road/trail/railroad	<input type="checkbox"/>	<input type="checkbox"/>	Historical significance	<input type="checkbox"/>	<input type="checkbox"/>
Flow naturalness	<input type="checkbox"/>	<input type="checkbox"/>	Native plant ecological role	<input type="checkbox"/>	<input type="checkbox"/>	Fencing	<input type="checkbox"/>	<input type="checkbox"/>	Recreational significance	<input type="checkbox"/>	<input type="checkbox"/>
Flow persistence	<input type="checkbox"/>	<input type="checkbox"/>	Trophic dynamics	<input type="checkbox"/>	<input type="checkbox"/>	Construction	<input type="checkbox"/>	<input type="checkbox"/>	Economic value	<input type="checkbox"/>	<input type="checkbox"/>
Water quality	<input type="checkbox"/>	<input type="checkbox"/>	<b>Score</b>			Herbivory	<input type="checkbox"/>	<input type="checkbox"/>	Conformance to mgmt plan	<input type="checkbox"/>	<input type="checkbox"/>
Algal and periphyton cover	<input type="checkbox"/>	<input type="checkbox"/>	<b>Biotic Integrity</b>			Recreational	<input type="checkbox"/>	<input type="checkbox"/>	Scientific/educational value	<input type="checkbox"/>	<input type="checkbox"/>
			Native plant richness/diversity	<input type="checkbox"/>	<input type="checkbox"/>	Adjacent conditions	<input type="checkbox"/>	<input type="checkbox"/>	Environmental compliance	<input type="checkbox"/>	<input type="checkbox"/>
			Native faunal diversity	<input type="checkbox"/>	<input type="checkbox"/>	Fire influence	<input type="checkbox"/>	<input type="checkbox"/>	Legal status	<input type="checkbox"/>	<input type="checkbox"/>
			Sensitive plant richness	<input type="checkbox"/>	<input type="checkbox"/>						
			Sensitive faunal richness	<input type="checkbox"/>	<input type="checkbox"/>						
			Nonnative plant rarity	<input type="checkbox"/>	<input type="checkbox"/>						
			Nonnative faunal rarity	<input type="checkbox"/>	<input type="checkbox"/>						
			Native plant demography	<input type="checkbox"/>	<input type="checkbox"/>						
			Native faunal demography	<input type="checkbox"/>	<input type="checkbox"/>						

Notes:

---

---

---

---

---

---

---

---

---

---

Recommendations:

---

---

---

---

---

Entered by \_\_\_\_\_ Date \_\_\_\_\_ Checked by \_\_\_\_\_ Date \_\_\_\_\_

Appendix C  
Sunpath diagrams for Salado Springs

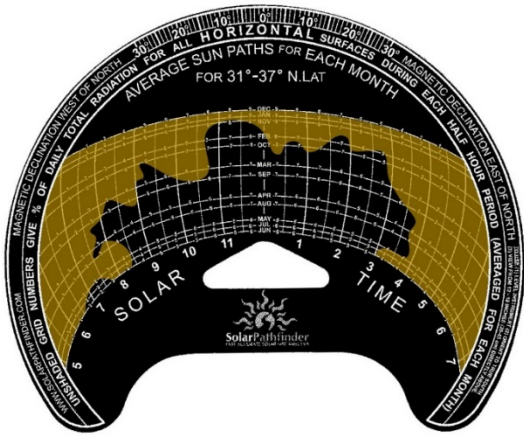


Figure C-1. Sun path diagram for Robertson (Ludwigia) Spring, October 27, 2016.

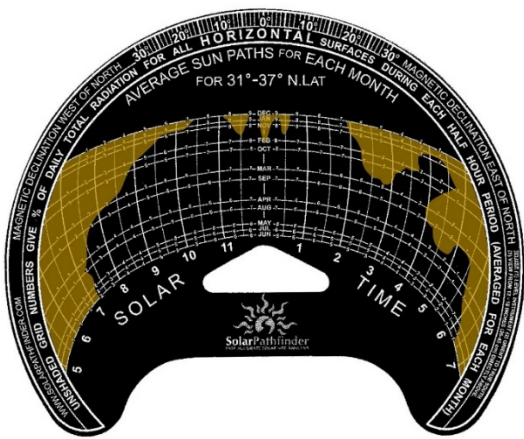


Figure C-2. Sun path diagram for Big Boiling Spring, September 22, 2016.

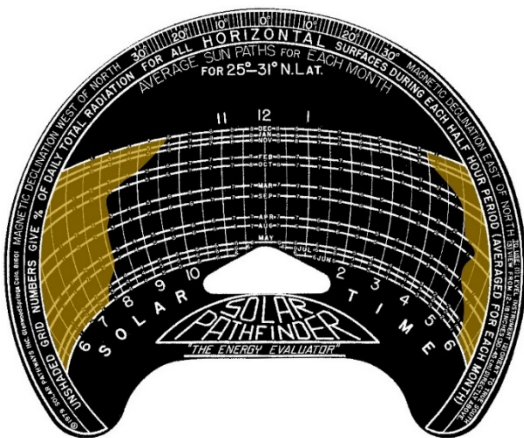


Figure C-3. Sun path diagram for Little Bubbly Spring, September 22, 2016.

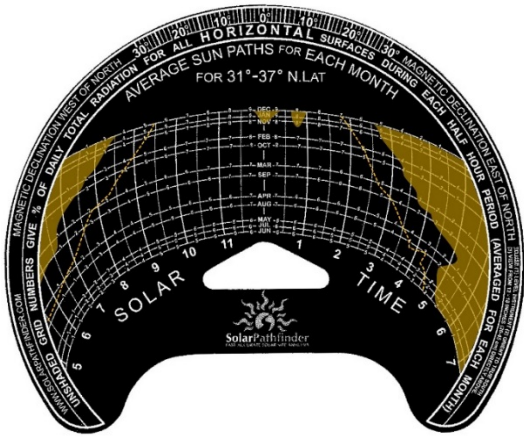


Figure C-4. Sun path diagram for Side Spring, September 22, 2016.

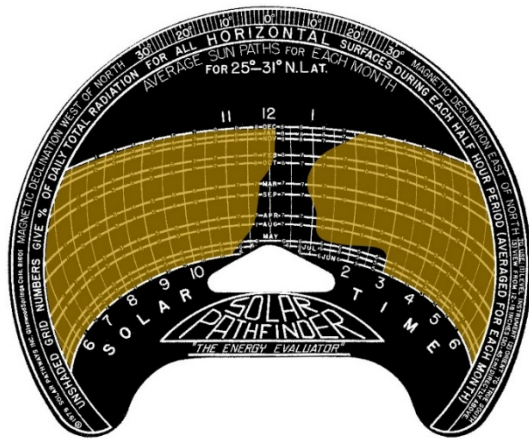


Figure C-5. Sun path diagram for Critchfield Spring, September 22, 2016.

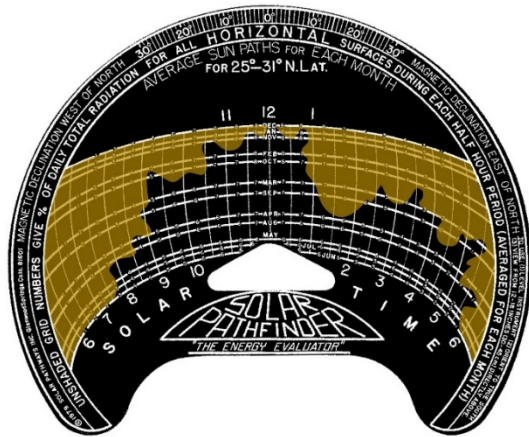


Figure C-6. Sun path diagram for Doc Benedict Spring, September 22, 2016.

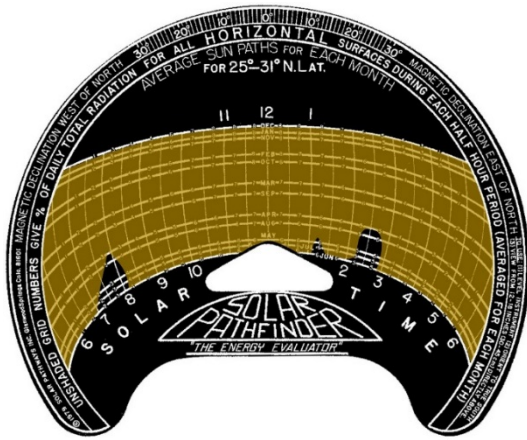


Figure C-7. Sun path diagram for Anderson Spring, September 22, 2016.

**Phase III**

# Phase 3: Assessing groundwater recharge in Salado Creek basin with WSR- 88D and datalogger data



*A research report submitted to the Bell County Adaptive Management Coalition c/o  
Clearwater Underground Water Conservation District,  
Bell County, Texas*

Final Report, December 2017

Submitted By:

Stephanie S. Wong, graduate student

Dr. Joe C. Yelderman Jr., Ph.D., P.G.

Baylor University, Department of Geosciences



# Contents

Contents .....	2
Project Overview .....	3
Introduction .....	3
Data and Methods .....	5
Land Cover .....	7
Precipitation Over the Northern Segment .....	9
Effects of rain location and magnitude	
WSR-88D and weather station comparison	
Continuation of Monitoring .....	13
Future Work .....	13
Summary & Project Conclusions .....	13
References .....	14

## Project Overview

Baylor University (“Baylor”), in collaboration with the Bell County Adaptive Management Coalition and the Clearwater Underground Water Conservation District (CUWCD), undertook a study to gain a deeper understanding of recharge over the Northern Segment of the Edwards Balcones Fault Zone (BFZ) Aquifer (the “Northern Segment”) for the purposes of providing insight for groundwater resource management and supporting collaboration between the CUWCD and community stakeholders. This study follows two previous phases of work related to the Northern Segment; phase 1 began in 2013 and focused on instrumentation, field tests, and feasibility studies to build knowledge of how much recharge occurs and the pathways that recharge takes to the aquifer. Phase 2 research, which spanned spring and summer 2016, focused on continuing monitoring activities while adding new monitoring parameters, refining field tests and samples, as well as analysis and interpretation of data gathered during phase 1.

Although this report serves as a final summary of the research efforts completed under the 2017 contract, there is still much to learn about the Northern Segment system. Collaborative efforts, monitoring, and data gathering are on-going.

## Introduction

The study area for this project was the outcrop portion of the Northern Segment of the Edwards BFZ aquifer in Bell County (Figure 1). Research focused on the Salado Creek basin, which overlies outcropping geologic units of the Edwards aquifer and is important for their connection to the Salado Springs complex in downtown Salado. The springs are critical habitat for the Salado salamander and a measure of CUWCD’s DFC. The total area of the Salado Creek basin is 173 square miles (10 814 acres).

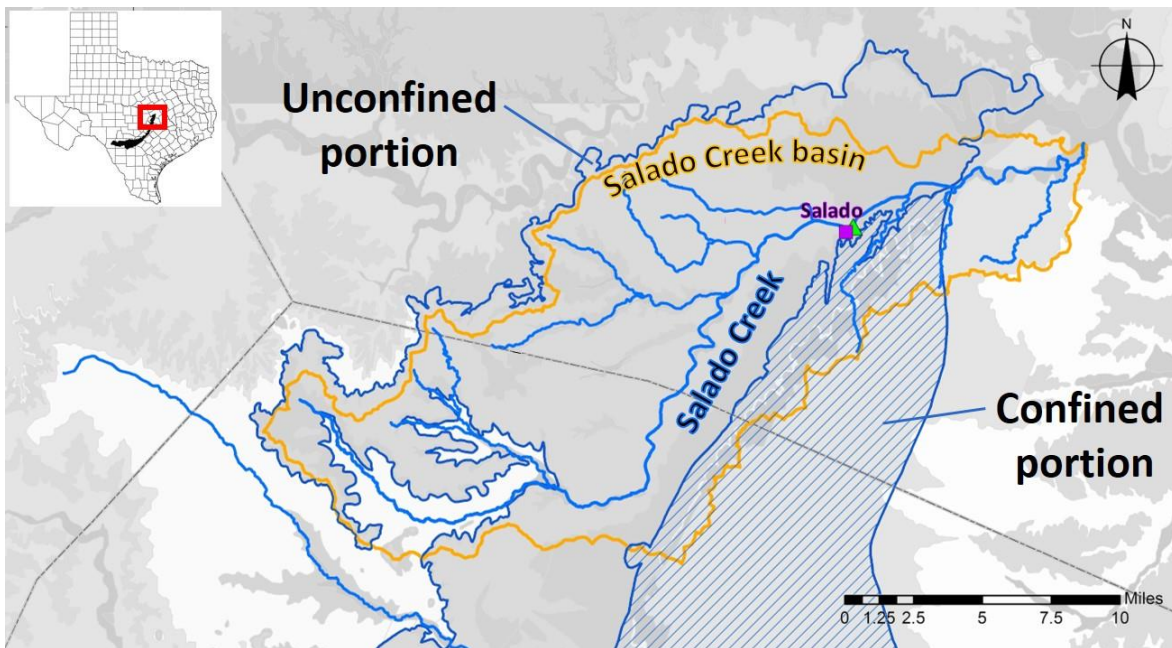


Figure 1. Project setting is the outcrop (unconfined) portion of the Northern Segment of the Edwards BFZ aquifer.

When working in nature, generalizations are often needed to simplify complex systems. Traditionally in hydrologic studies, the geology is treated as homogeneous, or the stratigraphy is simplified. Recharge is also often estimated as an annual average over the entire aquifer when making water budget calculations. At times, both geology and recharge are generalized. However, precipitation can be spatially heterogeneous. Since karst also is heterogeneous,

it is even more important to consider precipitation variability over karst systems like the Edwards aquifer to better understand recharge. The main objective of this study was to investigate the spatial variability of recharge of the Northern Segment using WSR-88D data to better understand recharge in the aquifer. Specific objectives of this study were to:

- Investigate and describe, qualitatively and quantitatively, the relationship between precipitation and changes in groundwater level and chemistry in the Northern Segment of the Edwards BFZ Aquifer
- Evaluate land use in the basin
- Maintain groundwater monitoring at the Stagecoach Inn Cave well
- Build a logistical foundation for data and future work in the regional aquifer encompassing Salado Creek basin

There are generally two types of precipitation: convective and stratiform. Convective precipitation occurs when parcels of air rise vertically through the mechanism of convection or temperature – and therefore density – differences (Figure 2, A). Clouds are constrained to a small area and build upwards, forming deep columns. The resulting rain falls at various intensities and is often concentrated in one area. Thunderstorms that are typical in Texas are examples of convective precipitation. Stratiform precipitation occurs when large air masses move across each other diagonally (Figure 2, B). Associated clouds are low and shallow, forming continuous cloud cover. Resulting rain events are low-intensity. The light showers or drizzle that occur throughout the Pacific Northwest are examples of stratiform precipitation.

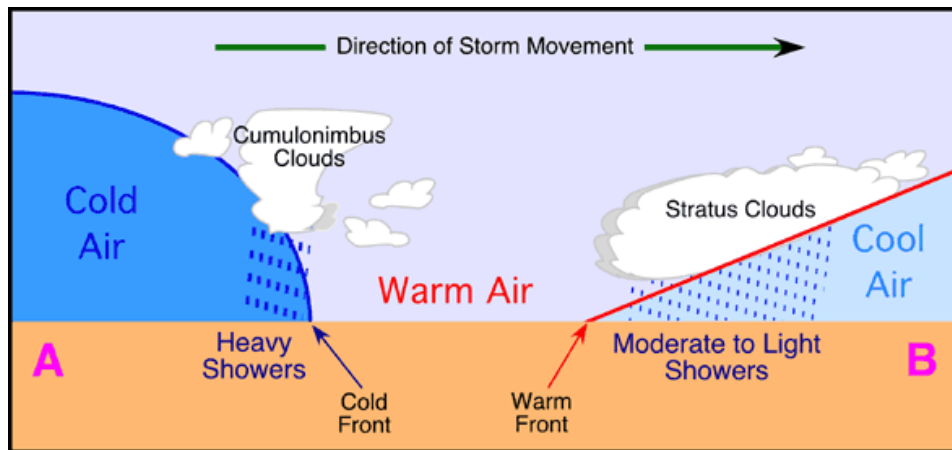


Figure 2. Schematic diagram showing how different cloud types form, leading to different precipitation styles. A is convective precipitation, and B is stratiform precipitation.

Precipitation in Texas is mostly convective, resulting in locally-intense and short-duration events (Ward and Valdes, 1995). Stable, stratiform weather systems that produce sustained and moderate-intensity rain are not common. Therefore, most recharge to the Edwards aquifer in the Salado Creek basin should be a result of convective rain events. The variability of the rainfall creates a problem requiring a dense network of dependable rain gages. Unfortunately, rain gages are usually few and far between.

In contrast to sparsely distributed rain gauges, WSR-88D data facilitates closer examination of the spatial variability of rain events. The WSR-88D dataset is a National Weather Service product, collected as part of the NEXRAD program. The data are collected using Doppler radar; there are 156 Doppler radar stations located across the United States, 13 in Texas. Raw data are processed in-house using National Weather Service PPS (Precipitation Processing System) algorithms and validated with field data. This process estimates rainfall in a 4-km grid at hourly intervals, and greatly increases the ability to capture precipitation variability. Figure 3 contrasts the spatial coverage of 64

selected WSR-88D stations in the study area with three weather stations deployed across the outcrop of the Northern Segment in Bell County and maintained by CUWCD and Baylor.

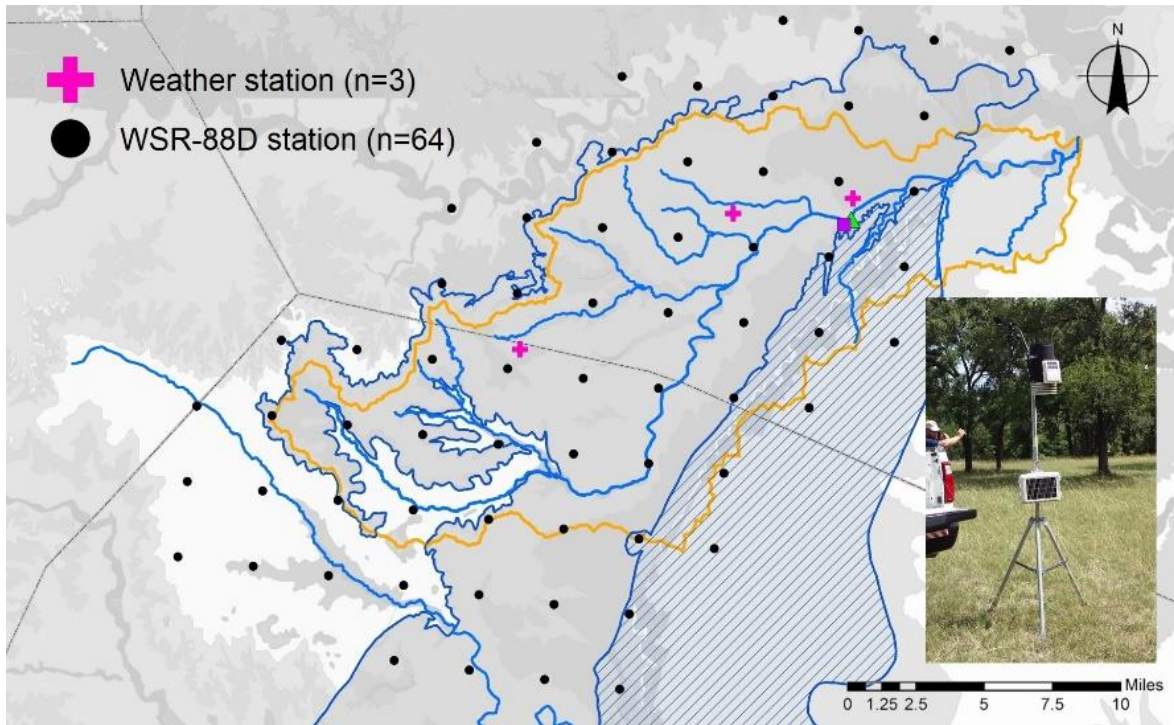


Figure 3. Map comparing the spatial distribution of WSR-88D stations and deployed weather stations. The inset photo is of deployed Vantage Pro weather stations.

## Data and Methods

Geospatial datasets for visualizing surface geology and land cover were obtained from TNRIS (the Texas Natural Resources Information System) and processed using ArcMap 10.0. The surface geology dataset is part of the Geologic Atlas of Texas (GAT), created by the U.S. Geological Survey in cooperation with the Texas Water Development Board. The most recent update of this dataset was in 2007. The land use / land cover datasets are part of the National Land Cover Database and were created through the collaboration of several federal agencies. Two datasets, 2001 and 2011, were obtained for temporal comparison, as these represent the oldest and most-recently available datasets utilizing common land cover categories.

A critical dataset for this project was WSR-88D data. WSR-88D data were accessed through the CUWCD data management dashboard. Daily precipitation totals were compiled for WSR-88D stations that are within the outcrop portion of the Northern Segment in Bell County and northern Williamson County, as well as stations adjacent to the basin boundary to interpolate between points and account for the effects of boundary conditions (Figure 3). Sixty-four WSR-88D stations were included in this data compilation and analysis for the period of December 2016 to November 2017. Data from the CUWCD database were exported to Microsoft Excel and formatted for import into a geographic information system (ArcMap 10.0) for analysis.

An overview of the workflow in ArcMap 10.0 is shown in Figure 4. ArcMap 10.0 was used to convert numerical rain totals to maps to visualize the spatial variability of precipitation events. Once events were mapped, precipitation patterns could be compared. Weather station and WSR-88D data for compared for June to November 2017.

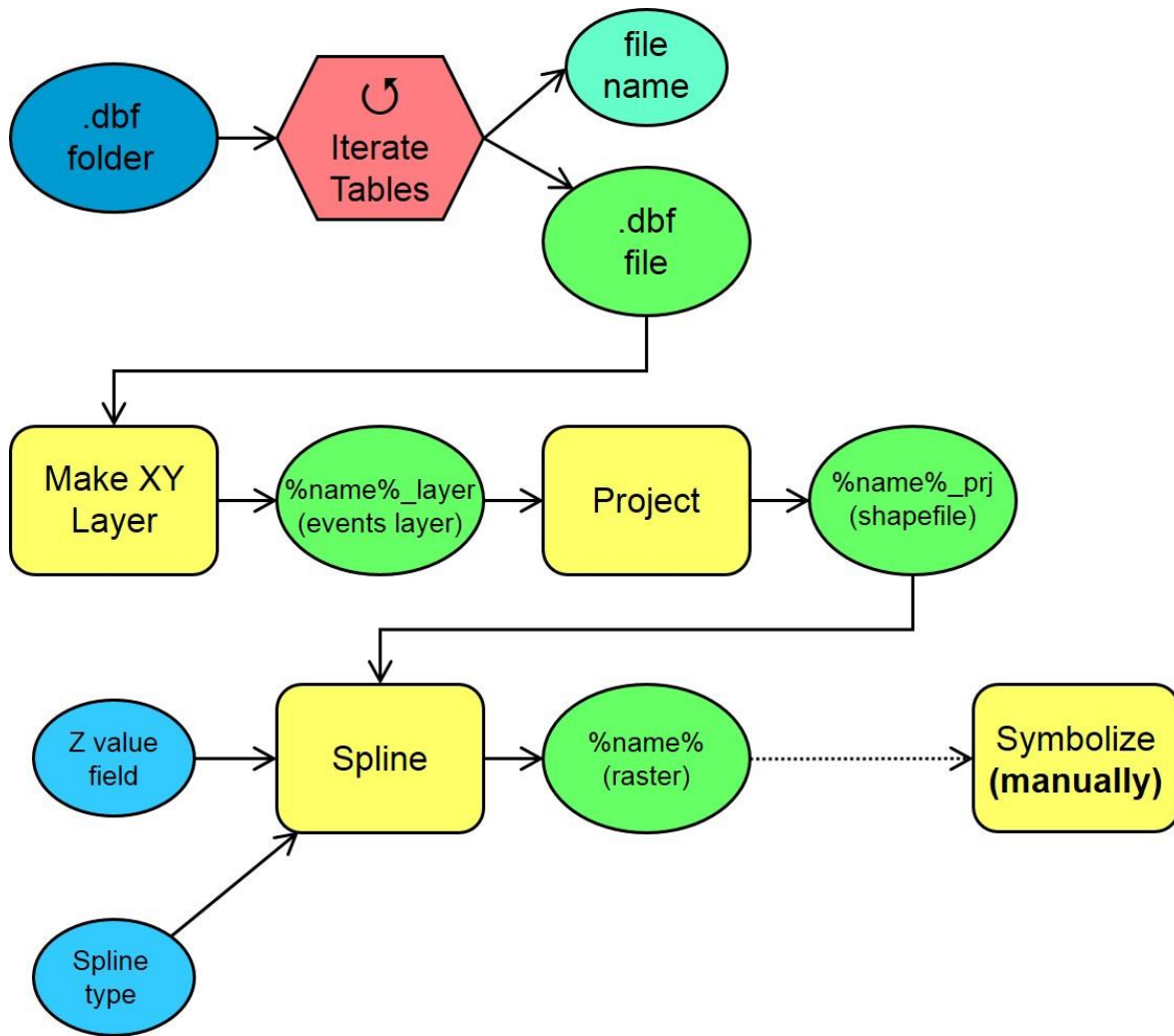


Figure 4. ArcMap 10.0 workflow for converting rain data to rain maps.

## Land Cover

The Northern Segment of the Edwards BFZ aquifer is comprised of three hydraulically-connected formations in the study area: the Comanche Peak Formation, the Edwards Formation, and the Georgetown Formation (Figure 5). All these units are Cretaceous in age and composed mainly of carbonate (limestones). The Edwards and Comanche Peak formations are part of the Fredericksburg Group, and the Georgetown is part of the Washita Group. Compared to the Comanche Peak and Georgetown formations, the Edwards is more karsted.

The underlying confining unit is the uppermost member of the Walnut Formation, the Keys Valley member. It is comprised of carbonaceous clay referred to as a marl. The overlying confining unit is the Del Rio Formation (Sometimes referred to as the Grayson Formation). The Del Rio is a carbonaceous clay-rich unit and often referred to as the Del Rio Clay. Upper Cretaceous units overlying the Del Rio Formation that crop out in the Salado Creek basin include the Buda Formation, Eagle Ford Group, and the Austin Chalk. None of these are considered aquifers in the study area.

Due to the heterogeneity in the geology underlying Salado Creek basin, recharge response in the Northern Segment will be variable depending on where rain falls, especially during convective events.

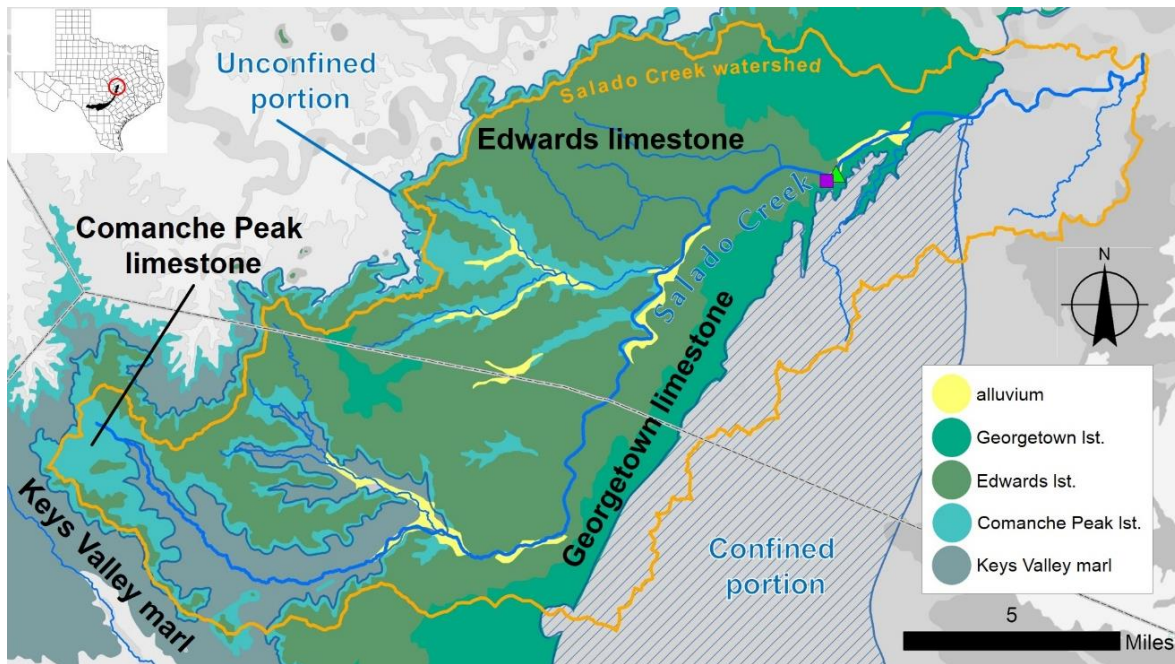


Figure 5. Surface geology in the outcrop portion of the Northern Segment. The major geologic formations are the Keys Valley marl, Comanche Peak limestone, Edwards limestone, and Georgetown limestone.

Land cover maps for 2001 and 2011 are shown in Figures 6 and 7 respectively. Most of the study area is comprised of vegetated cover types (forest, herbaceous, cultivated categories). Overall, no drastic change was observed between 2001 and 2011. However, there may be local changes in land cover that may be significant for recharge. More detailed analysis may be necessary if change in recharge potential at a specific site needs to be investigated.

Recharge potential in the study area can be said to be largely driven by precipitation and differences in surface geology, since soils in the study area are generally thin and land cover has not changed significantly at the basin-scale. As development along the Interstate-35 corridor continues, recharge potential may become increasingly determined by land use and cover, as opposed to geology. The surface geology and land cover maps in this report serve as documentation of baseline conditions, and may be used for future comparisons.

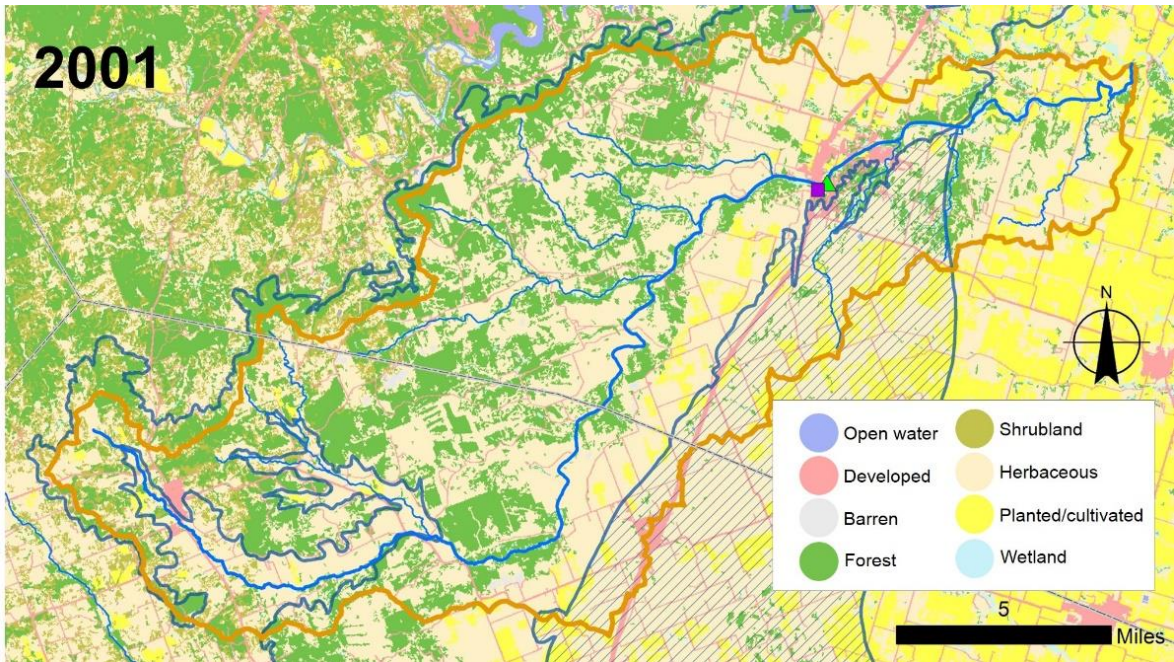


Figure 6. Land use and cover types in the study area in 2001.

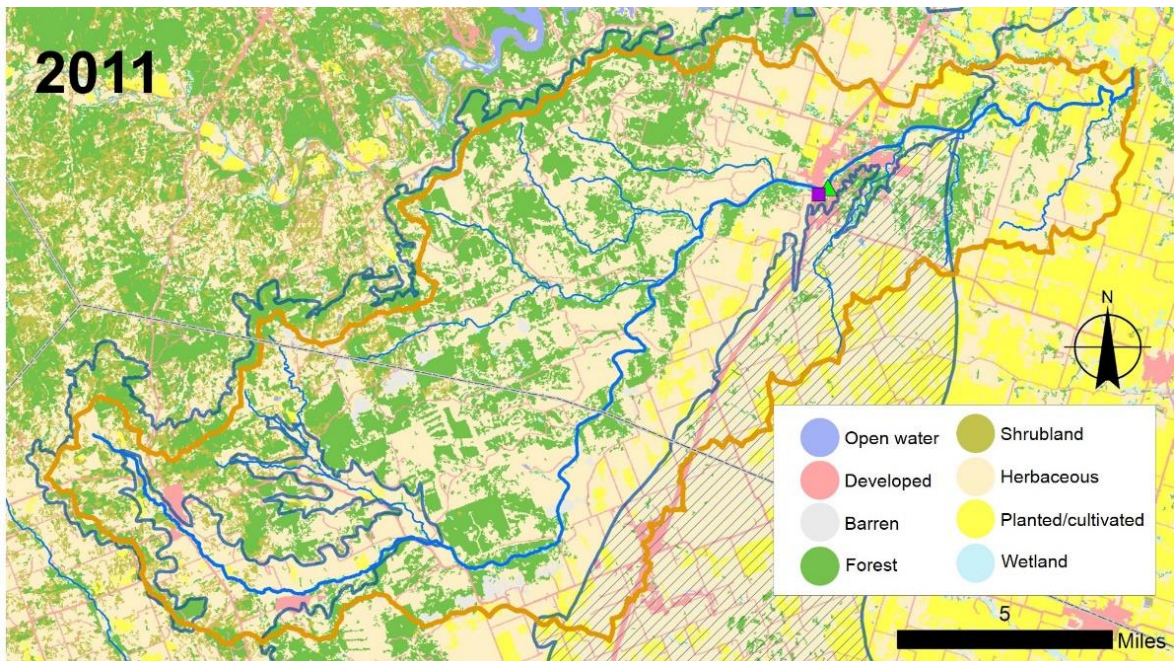


Figure 7. Land use and cover types in the study area in 2011.

## Precipitation Over the Northern Segment

Visualization of WSR-88D as maps revealed several patterns (Figure 8). Many events were observed to be convective, which agrees with documentation of Texas precipitation being mostly convective (Ward and Valdes, 1995). Fronts moving through the Northern Segment could also be observed. Some events were also observed to be stratiform. Varying rain location and magnitude had different recharge responses in the Northern Segment, as observed at the Stagecoach Inn cave.

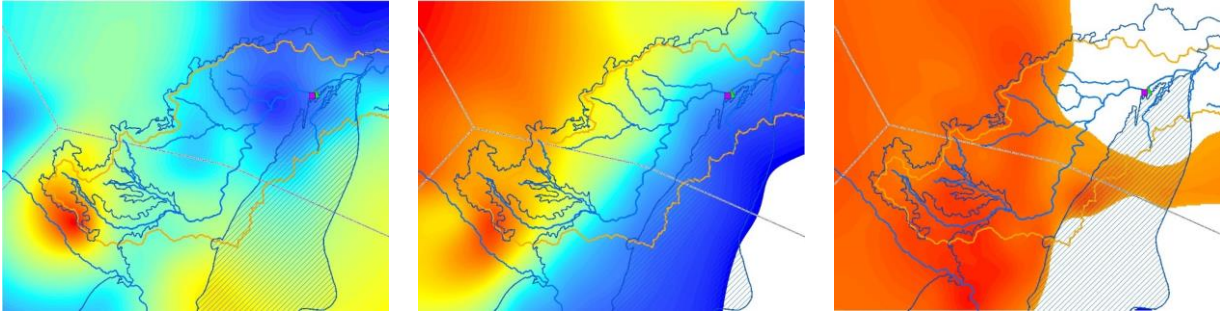


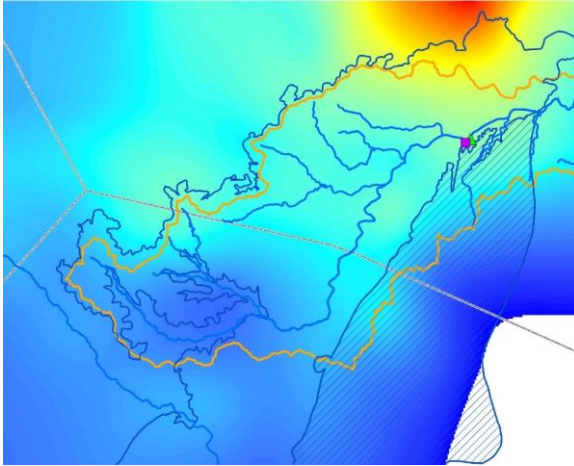
Figure 8. Examples of precipitation patterns in the Northern Segment. Cooler colors represent less rain, while warmer colors represent more rain. *Left*, an example of a convective event where rain was concentrated in the upper basin; *middle*, a stratiform event spread out over the upper and middle of the basin; *right*, a front extending southwest-northeast is moving across the basin.

### *Effects of rain location and magnitude*

Rain maps for March 12 and April 3, 2017 are compared in Figure 9. While both convective events are similar in magnitude. The March 12 event had rainfall ranging from 0.67 to 1.09 inches in the basin, with an average rainfall of 0.88 inches; total rainfall over the Salado Creek basin was 793 acre-feet. The April 3 event had rainfall ranging from 0.64 to 1.12 inches in the basin, with an average of 0.78 inches; total rainfall over the Salado Creek basin was 685 acre-feet. However, the events are concentrated in different areas of the study area. The March 12 event is concentrated in just outside of the lower part of the basin, not considered to be in the same flow system as the Stagecoach Inn cave. The April 3 event is concentrated in the middle part of the basin, over the Edwards and Georgetown Limestone formations and upgradient from the cave well. Both formations are more hydraulically-conductive than the Keys Valley Marl and Comanche Peak Limestone in the upper basin; the Edwards especially is more karsted compared to the other geological formations in the basin. Comparing these rain maps to the groundwater hydrograph at Stagecoach Inn cave well (Figure 10), the slightly larger March 12 event produced a smaller (about 0.05 foot) rise in groundwater level, while the April 3 event produced a rise in groundwater level of twice as much (about 0.1 foot). Since these similar-magnitude events produced different magnitudes of response, they highlight the importance of capturing the spatial variability of rain and how the location of rainfall concentration results in differing recharge amounts.

Rain maps for April 3 and 12, 2017 are compared in Figure 11. Both convective events are concentrated in the middle part of Salado Creek basin, over the Edwards and Georgetown Limestone formations, but are of different magnitudes. The April 3 event had rainfall ranging from 0.64 to 1.12 inches in the basin, with an average of 0.78 inches; total rainfall over the Salado Creek basin was 685 acre-feet. The April 12 event had rainfall ranging from 0.84 to 2.28 inches, with an average of 1.38 inches; total rainfall over the Salado Creek basin was 1244 acre-feet. Comparing the rain maps to the groundwater hydrograph at Stagecoach Inn cave well (Figure 12), the smaller event on April 3 produced about 0.1 foot rise in groundwater level, while the larger event on April 12 produced about 0.8 foot rise in groundwater level. Intuitively, the magnitude of a rain event impacts the resulting recharge. More analyses may be possible as more storms and their locations are compared to spring responses.

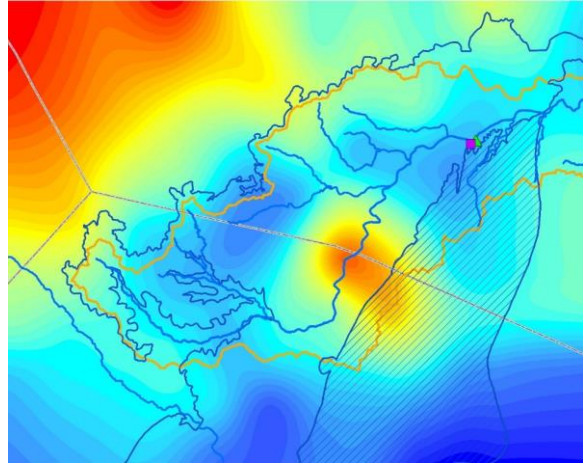
March 12, 2017:



Min. rain = 0.67 inches  
Max. rain = 1.09 inches  
Avg. rain = 0.88 inches

**Total rain over basin: 793 acre-feet**

April 3, 2017:



Min. rain = 0.64 inches  
Max. rain = 1.12 inches  
Avg. rain = 0.78 inches

**Total rain over basin: 685 acre-feet**

Figure 9. Two convective events were similar in magnitude, but rainfall was concentrated in different parts of the study area.

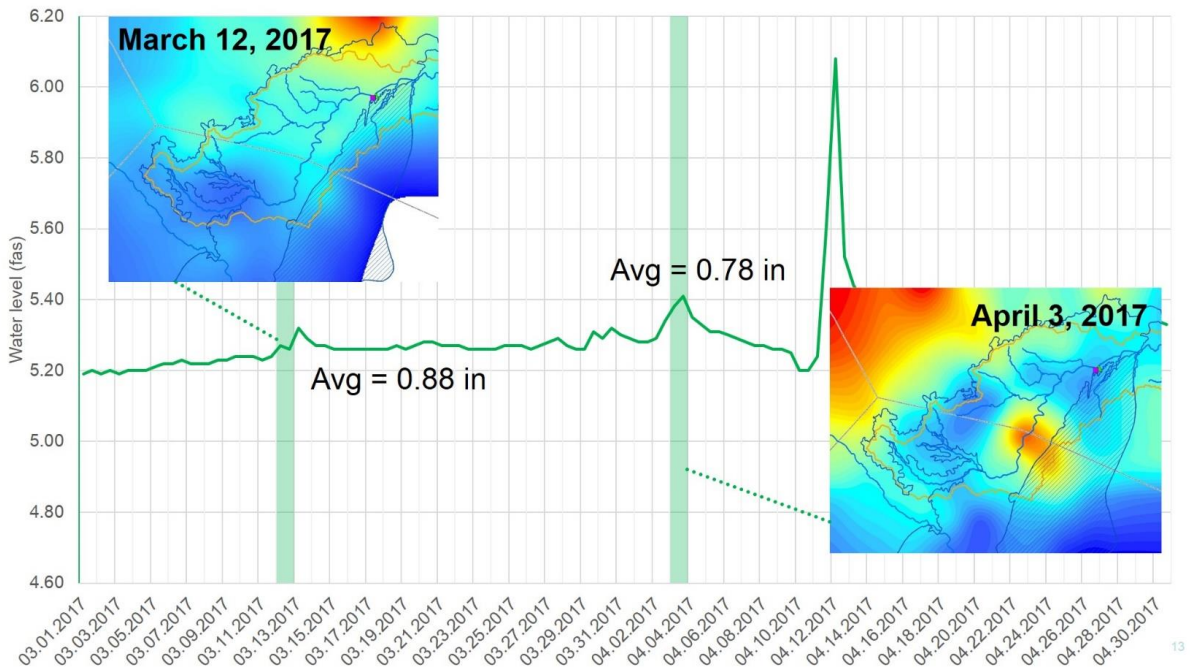
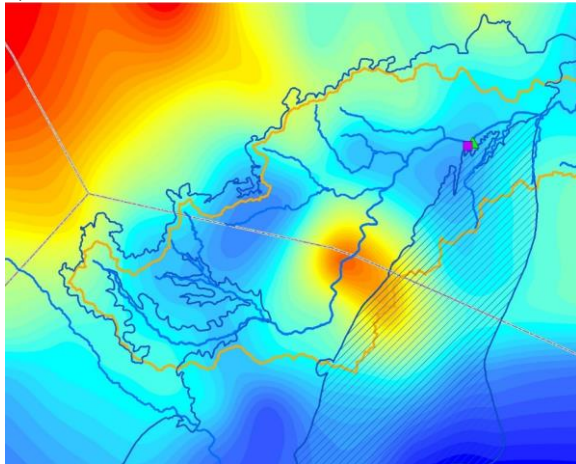


Figure 10. The March 12 and April 3 rain events were similar in magnitude but produced different groundwater level responses due to where rainfall was concentrated in the study area. The numerical labels near each hydrograph peak is the average rainfall from each event.

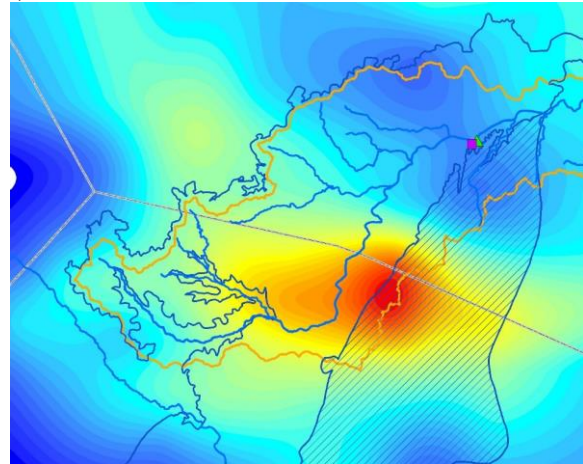
April 3, 2017:



Min. rain = 0.64 inches  
 Max. rain = 1.12 inches  
 Avg. rain = 0.78 inches

**Total rain over basin: 685 acre-feet**

April 12, 2017:



Min. rain = 0.84 inches  
 Max. rain = 2.28 inches  
 Avg. rain = 1.38 inches

**Total rain over basin: 1244 acre-feet**

Figure 11. Two convective events were concentrated in similar areas, but were of different magnitude.

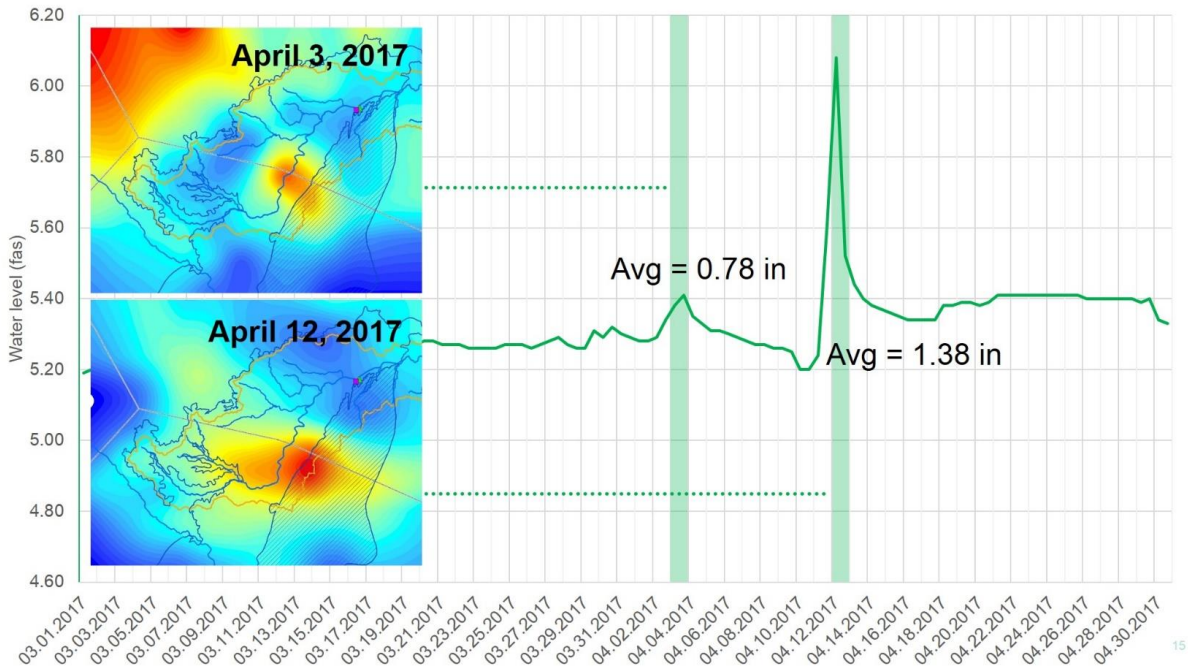


Figure 12. The April 3 and 12 rain events were both concentrated in the middle part of Salado Creek basin, and produced different groundwater level responses due to different magnitude rainfalls. The numerical labels near each hydrograph peak is the average rainfall from each event.

*WSR-88D and weather station comparison*

Fifty-four rain days were documented using WSR-88D data from June to November 2017. Daily rain totals for all three weather stations were compared to the WSR-88D grid value in the same spatial location; the summary statistics are shown in Table 1. The maximum WSR-88D grid values are greater than documented values at all three weather stations, while average WSR-88D grid values are less than those at the weather stations. Both sets of numbers appear to be statistically significantly different from each other although similar in magnitude. The statistics suggest that WSR-88D may be better at estimating small rains. The WSR-88D's dual band polarized beam produces a spatial point dataset suitable for interpolation by surface generation algorithms. The base data are quality control checked using a Multi-Sensor Precipitation Estimation approach that utilizes both satellite derived estimates and ground truth control points in the form of rain gauges to produce a field corrected precipitation estimate for a gridded dataset with a 4km x 4km nominal resolution (Lawrence and others, 2003). The dataset is constructed of points that represent the center of the 4km grid. Surface generation is used to produce gridded data in a resolution suitable for individual applications.

Perhaps the rain gages do not collect enough water to tip the bucket because it is adhering to the sides or evaporation is great enough to prevent the collection. In contrast, the weather stations may be better at capturing isolated, big events that might get smoothed over in the mapping process. However, it is also possible the interpolation process fills in spaces with small amounts of data where it may not have rained. When utilizing validation points for spatial precipitation distribution, it should be noted that unless the gauge location directly corresponds with the WSR-88D generated grid, the measured versus interpolated data may not match the gridded amount. Studies have shown that algorithms which combine sensor inputs - radar, gauge, satellite - yield more accurate precipitation estimates than those which rely on a single sensor (Seo, 1999; Seo and others, 1999; Seo and Breidenbach, 2002).

Table 1. Summary statistics comparing daily rain totals in inches for WSR-88D data and weather stations.

	Maximum Value	Minimum Value	Average Value
<u>Gault site</u>			
WSR-88D	1.95	0	0.234
Weather station	3.1	0	0.221
<u>Salado</u>			
WSR-88D	2.00	0	0.240
Weather station	2.05	0	0.165
<u>Hidden Springs</u>			
WSR-88D	1.91	0	0.216
Weather station	2.51	0	0.193

## Continuation of Monitoring

### *Stagecoach Inn Cave*

Monitoring of groundwater conditions in the Northern Segment continue at Stagecoach Inn Cave. Monitoring at the Cave has supported several research projects and was essential to the research in this Phase 3 effort. Monitoring has continued with no major datalogger issues or data gaps, and the OTT CTD sensor plus datalogger has functioned well. Annual maintenance on the datalogger was performed in early June, where the datalogger was brought back to Baylor University for calibration and replacement of batteries and desiccant. Moving forward, plans are to repeat this maintenance routine annually, in addition to downloading data and checking battery status throughout the year.

### *Weather stations*

There are currently still three Vantage Pro II weather stations deployed on the outcrop portion of the Northern Segment. Station one is located at the Gault Archaeological School, station two is located in the village of Salado, and station three is located in the Hidden Springs housing development.

The main adjustment with the weather stations in 2017 is the implementation of routine site visits to download data about once every seven weeks. Routine visits started in June, and have helped minimize data gaps due to limited data storage on the weather stations.

## Future Work

Future work will continue to focus on understanding groundwater flow and aquifer characteristics the Northern Segment and associated springs in Bell County, but extend to the aquifer's northernmost extent near Stillhouse Hollow Lake and Tahuaya Springs. Preliminary work characterizing the aquifer in this area started in fall of 2017 at Spring Creek; where the top of the Walnut, the entire Comanche Peak, and bottom of the Edwards Formations are exposed.

Plans for future work also include working more closely with US Fish and Wildlife biologist, Pete Diaz, to relate aquifer characteristics and groundwater conditions to salamander habitat by incorporating infrared imagery.

## Summary & Project Conclusions

- WSR-88D data allow for greater correlation of recharge events with surface water and groundwater monitoring data.
- Especially in karst systems,
  - Similar magnitude storms can have different groundwater responses depending on where rain falls
  - Small, evenly distributed rains may not result in recharge
- Weather stations vs. NEXRAD WSR-88D data – **Both are important!**
  - Weather stations – event details and totals (numerical)
  - NEXRAD WSR-88D data – basin-wide event perspective (visuals, maps)
- Land cover and recharge:
  - Historically, geologically-controlled
  - Future, changing land use may have more impact
  - Documentation of land use / land cover serves as baseline to detect future change
- Improved management schedule helps maintain instruments and data continuity
- Future work to expand outside of Salado Creek basin

## References

Lawrence, B.A., M.I. Shebsovich, M.J. Glaudemans, and P.S. Tilles, 2003, ENHANCING PRECIPITATION ESTIMATION CAPABILITIES AT NATIONAL WEATHER SERVICE FIELD OFFICES USING MULTI-SENSOR PRECIPITATION DATA MOSAICS: Office of Hydrologic Development, National Weather Service, NOAA, Silver Spring, Maryland.

Seo, D.J., 1999: Real-time estimation of rainfall fields using radar rainfall and rain gauge data: *J. Hydrol.*, 208, 37-52.

Seo, D.J., J. Breidenbach, and E. Johnson, 1999: Real-time estimation of mean field bias in radar rainfall data: *J. Hydrol.*, 223, 131-147.

Seo, D.J. and J. Breidenbach, 2002: Real-time correction of spatially nonuniform bias in radar rainfall data using rain gauge measurements: *J. Hydrometeor.*, 3, 93-111.

Ward, G. and Valdes, J.B., 1995, "Water Resources" in *The Impact of Global Warming on Texas: A Report of the Task Force on Climate Change in Texas*. North, G.R.; Schmandt, J.; Clarkson, J. (eds.). University of Texas Press, Austin. 251 pp.